The Dimension of Causal Sets

by

David A. Meyer
B.A., M.A., Mathematics
The Johns Hopkins University (1979)

Submitted to the Department of Mathematics
in partial fulfillment of the requirements for the degree of

Doctor of Philosophy

at the
Massachusetts Institute of Technology
20 October 1988

Signature of author_____
Department of Mathematics
20 October 1988

Certified by_____
Professor Daniel Z. Freedman
Thesis Supervisor

Certified by_____
Professor Daniel J. Kleitman, Chairman
Mathematics Committee

Accepted by_____
Professor Sigurdur Helgason, Chairman
Departmental Graduate Committee

Contents

Acknowledgements

There are many people without whom the completion of this thesis would have been impossible; I thank all of them: My advisor, Daniel Z. Freedman, for his guidance and patience throughout my graduate career. Douglas Eardley, who introduced me to general relativity and started me doing research. Rafael Sorkin, whose breadth of interests and depth of understanding I hope some day to approach, who has been the source and inspiration for my research over the last two years. Joohan Lee and, especially, Luca Bombelli, for the many discussions out of which the four of us developed the causal set program. Carl Brown, whose assistance with the intricacies of the SUHEP computer system was invaluable. The Department of Mathematics at Syracuse University, which took the chance of hiring me with an incomplete degree. The Relativity Group and, most recently, the High Energy Theory Group in the Physics Department at Syracuse University, for their interest in and support of my work, as well as for providing a most stimulating environment for research. I am also grateful for the support and encouragement of many friends during the time it took to complete my degree, especially Bob Bieri and Peter Monta who constituted the audience at my thesis defense. Finally I would like to thank my brothers, sisters and parents for their support, academic, financial and emotional; without them, my efforts would be meaningless.

The Dimension of Causal Sets

by

David A. Meyer

Submitted to the Department of Mathematics
in partial fulfillment of the requirements
for the degree of

Doctor of Philosophy

Massachusetts Institute of Technology
20 October 1988

Abstract

A radical approach to quantum gravity has recently been proposed by Bombelli, Lee, Meyer and Sorkin along lines similar to earlier proposals by 't Hooft and Myrheim. This proposal, that the fundamental structure underlying spacetime is a causal set—a locally finite partially ordered set, and its motivations are described in the Introduction and the mathematical and physical background is developed. The connection between causal sets and the Lorentzian manifolds of general relativity is made by way of an *embedding* of a causal set into a Lorentzian manifold: a mapping f such that $f(p)$ lies to the past of $f(q)$ in the manifold iff $p \prec q$ in the causal set. The Minkowski dimension of a causal set is the dimension of the minimal Minkowski space into which the causal set can be embedded. This concept of dimension is examined in the second chapter and is compared to the combinatorial dimension of partially ordered sets. If a Lorentzian manifold is to approximate the causal set one must require more than that the embedding preserve the causal relations: the points should also be distributed uniformly in the manifold. In the third chapter, starting from the model of points distributed according to the Poisson process, the expectation values of various causal set parameters (the number of relations among the elements of an interval, for example) are found in terms of the dimension and curvature of the manifold. These formulae can be inverted (exactly, in the case of Minkowski space) to *define* a Hausdorff or fractal (since it need not be an integer) dimension and local curvature for an arbitrary causal set. These analytic results are also verified by computer simulation. In the Conclusion the implications for the quantum dynamics of causal sets are examined and directions for further work are discussed.

I. Introduction

The work described in the following chapters concerns some mathematical questions which have arisen in a program initiated recently as an approach to quantizing gravity. To place it in context this chapter outlines the program (for additional discussion see [Bombelli, Lee, Meyer and Sorkin 1987, 1988, Bombelli 1987 and Moore 1988]) and its motivation, includes a brief review of the relevant physical and mathematical background, and introduces the particular aspect of this approach—namely, how spacetime dimension appears—which is investigated in the following chapters.

Quantum gravity

There are many reasons to believe a quantum theory of gravity is either necessary or desirable. (See, for example, the essays in [Christenson 1984].) At the level of classical general relativity, the singularity theorems of Hawking and Penrose [Hawking and Ellis 1973] show that under various sets of conditions on the matter stress-energy tensor, conditions which obtain in physically reasonable situations, Einstein's equation predicts the formation of spacetime singularities. Thus general relativity is incomplete; it does not provide for boundary conditions to be imposed at these singularities. On the other hand, our most complete theories describing

matter are quantum field theories: $\lambda\phi^4$ theory, QCD, the Weinberg-Salam model, etc. (for a complete exposition see, *e.g.*, [Itzykson and Zuber 1980]). Since Einstein's equation relates the metric of spacetime as a dynamical variable to the matter stress-energy tensor, a completely consistent theory of gravity seems to necessitate quantizing the gravitational field. The Einstein-Hilbert action, however, leads to a perturbatively non-renormalizable theory. (See [Weinberg 1979] and references therein.) The coupling constant in the theory is not dimensionless, rather it is the square of the Planck length $\sqrt{G\hbar/c^3} \approx 1.616 \times 10^{-33}$cm, the fundamental length scale in the theory. At much larger scales problems can be approximated semiclassically by quantum field theory on a curved background spacetime [Birrell and Davies 1982]. Perhaps the most significant result obtained this way is Hawking's discovery of the thermal emission of quantum black holes [Hawking 1975]. This result, however, also indicates the need for a complete quantum theory: the black hole evaporates as it emits particles and is driven toward the domain in which the semiclassical approximation can be expected to fail.

Thus it appears that a quantum theory of gravity is necessary but that the familiar techniques of quantum field theory do not suffice. Moreover, attempts to obtain a renormalizable theory by modifying the Lagrangian, as in supergravity [Freedman, van Nieuwenhuizen and Ferrara 1976, Deser and Zumino 1976, for reviews see Jacob, ed. 1986] and higher derivative [Utiyama and DeWitt 1962, Stelle 1977, Boulware, Horowitz and Strominger 1983] theories, have not been entirely successful. In fact, quantum gravity is in a difficult, and peculiar, situation with respect to other scientific theories. The development of most physical theories can be understood in terms of Taketani's schematic evolution [Taketani 1936] wherein a process of cognition of nature proceeds through three stages: phenomenological, substantialistic, and essentialistic. To illustrate this process, consider strong in-

teraction physics (for a detailed history see [Green, Schwarz and Witten 1987]): The phenomenological stage began with the observation of large numbers of hadron resonances, including some with relatively high spin. Experiments on scattering amplitudes in what came to be called the Regge region, small angle scattering at high energy, led to the duality hypothesis and the Veneziano amplitude which implemented it. These developments and their exploration, leading to the recognition that the Veneziano model was really that of a relativistic string, comprised a substantialistic stage ... but not for the theory of hadrons! For at about the same time as Veneziano's proposal, in 1968, new phenomena were found in the region of high energy scattering at fixed angles. The observed scattering amplitudes were inconsistent with the Veneziano model but were explained in a distinct substantialistic stage as being evidence for a quark model. Finally, with the formulation of quantum chromodynamics, the theory of strong interactions reached the essentialistic stage.

For quantum gravity theories, by contrast, it is unclear what the phenomena are; thus Taketani's second and third stages are developed first and often simultaneously. In modifying the Lagrangian to be supersymmetric or contain higher derivative terms, it is the condition of renormalizability (and agreement with general relativity at large scales) which is playing the role of the phenomena; the substance and dynamics are variants of familiar quantum field theories. Similarly, note that with the formulation of QCD, string theory was left with neither a phenomenological nor an essentialistic stage; although more recent developments in string theory indicate that rather than explaining strong interactions, it may provide a generalization of Yang-Mills theory and general relativity leading to a quantum theory of gravity, the phenomena are still lacking and no essential understanding of the underlying concepts yet exists. Another recent example is the canonical approach using Ashtekar's new variables [Ashtekar 1988]; again the substance has changed:

the basic variables are different and the states satisfying the quantum constraints are found in a loop space representation.

There are, however, as yet unexplained physical phenomena which might be addressed by a quantum theory of gravity. The smallness of the cosmological constant is an immediate example; in fact, one difficulty with supergravity theories is that they typically have an anti-de Sitter space ground state with cosmological constant of order one [Freund and Rubin 1980, Brietenlohner and Freedman 1982; for an example, see also Meyer 1986, reprinted in Appendix D]. It has also been suggested that the ultraviolet divergences in quantum field theories might be regulated by gravity (see [Isham 1984] and references therein). This has led to many proposals for fundamentally discrete structures underlying spacetime: regular lattices in Minkowski space [Schild 1949, Coish 1959] and random lattices based on the ideas of Regge calculus [Itzykson 1984, Lee 1985, Lehto, Nielson and Ninomiya 1986], for example. The number of spacetime dimensions might also be predictable: Kaluza-Klein theories introduced the idea that four is only the effective dimension of spacetime [Appelquist, Chodos and Freund, eds. 1987] and investigations into topology change in general relativity [Geroch 1967, Tipler 1977, Yodzis 1972, 1973, Sorkin 1986a], geons [Sorkin 1986b], and quantum geometry (spacetime foam) [Wheeler 1964, Hawking 1978] have pushed this idea even further. Finally, the most ambitious proposals aim to develop spacetime from some more fundamental substance; these include the intrinsically quantum mechanical spin lattice [Penrose 1972b] and twistor [Penrose 1975] programs of Penrose and Finkelstein's quantum causal space [Finkelstein 1969, 1972, Finkelstein, Frye and Susskind 1974], the potentially quantum mechanical Einstein algebras suggested by Geroch [Geroch 1972, Yodzis 1975], and, most recently, string theory without background geometry [Witten 1986, Horowitz, Lykkan, Rohm and Strominger 1986, Horowitz and Witt 1987]

as well as p-adic string theory [Freund and Olson 1987, 1988, Freund and Witten 1987, Volovich 1987].

The concerns of these latter proposals are concisely summarized by Riemann's query [Riemann 1854], "Why is there a spatial metric?" Given the subsequent developments in physics and differential geometry, this should be amended to 'spacetime' rather than 'spatial' and augmented by the supplementary questions: "Why is the metric of Lorentzian signature?" and "Why does spacetime have the topological and differentiable structures that allow the definition of a metric field?" Our approach is guided by these questions and informed by the mathematical results discussed next.

Causal structure

Recall that in general relativity a spacetime is a Lorentzian manifold $(M, \mathbf{g})$ [Hawking and Ellis 1973, Penrose 1972a]: a connected C^∞ Hausdorff manifold M with a globally defined nondegenerate C^∞ tensor field $\mathbf{g} : T_pM \times T_pM \to \mathbf{R}$ of signature $(- + \cdots +)$. Such a Lorentzian metric divides the non-zero tangent vectors at each point $P \in M$ into three classes: $\mathbf{X} \in T_pM$ is timelike, null, or spacelike when $\mathbf{g}(\mathbf{X}, \mathbf{X})$ is negative, zero, or positive, respectively. The set of null vectors in T_pM is called the null cone at p; it disconnects the set of timelike vectors into two components. If there is a consistent continuous choice of one of these two components (the future-pointing timelike vectors, say) at each point $p \in M$, the spacetime is time-orientable. A curve in M is a smooth map from some interval of $\mathbf{R}$ into M, and is called future or past directed timelike or null, or spacelike, if its tangent vector is everywhere in the corresponding class. Two points in M are said to be timelike related if there is a timelike curve connecting them, null related if there is not but there is such a null curve, and spacelike related otherewise. Two points are causally

related if they are either timelike or null related; write $x \in J^-(y)$ and $y \in J^+(x)$ if there is a future directed causal (again, timelike or null) curve from x to y (write $x \in I^-(y)$ and $y \in I^+(x)$ if the curve is timelike; also $I^+(x) \cap I^-(y)$ is called the Alexandroff neighborhood determined by x and y). By the causal structure of a spacetime one means the specification of all these relations. The remarkable fact is that the causal structure of a spacetime alone comes very close to determining not only the metric but also the topology and differentiable structure. More precisely, we have the following two theorems:

Theorem (Hawking): Let $(\mathcal{M}, \mathbf{g})$ and $(\mathcal{M}', \mathbf{g}')$ be spacetimes and suppose there is a homeomorphism $f : \mathcal{M} \to \mathcal{M}'$ such that both f and f^{-1} preserve future directed continuous null geodesics. Then f is a smooth conformal isometry [Hawking, King and McCarthy 1976].

Theorem (Malament): If $(\mathcal{M}, \mathbf{g})$ and $(\mathcal{M}', \mathbf{g}')$ are past and future distinguishing (*i.e.*, $I^-(x) = I^-(y) \Rightarrow x = y$ and $I^+(x) = I^+(y) \Rightarrow x = y$) and $f : \mathcal{M} \to \mathcal{M}'$ is a causal isomorphism then f is a homeomorphism [Malament 1977].

Putting these two theorems together we see that if the two spacetimes have the same causal structure (*i.e.*, there is a causal isomorphism between them) then the manifolds are homeomorphic and (since the homeomorphism preserves, in particular, the future directed continuous null geodesics) hence conformally isometric: $\mathbf{g}' = \Omega^2 \mathbf{g}$ for some local conformal factor Ω^2. Thus the causal structure determines the topology, differentiable structure, and conformal metric $\mathbf{g}/|\det \mathbf{g}|^{1/n}$.

Now, a causal structure is nothing more than a partial ordering P on the points of $\mathcal{M}$. As such, it is conceptually much simpler than the tower of constructions supporting the definition of a metric field, and it is natural to suppose that the metric $\mathbf{g}$ should be derived from P rather than the reverse. Hawking and Malament's

theorems show that P contains almost all the information needed to determine the metric; it lacks only the conformal factor $|\det \mathbf{g}|^{1/n}$ or local volume element. To solve this problem, recall some of the possible phenomenology discussed in the previous section: both the singularities of general relativity and the infinities of quantum field theory suggest that spacetime may not be truly continuous. So we implement the suggestion of [Riemann 1854] that "the reality underlying space may be a discrete manifold;" then a finite volume of spacetime contains only a finite number of elements, the volume being defined by the number of 'point-events' it contains.

Thus the proposal is that the substance, or structure, underlying spacetime is what Riemann might have called an ordered discrete manifold; we will refer to it as a causal set. Macroscopic causality should arise from the confluence of order relations and the volume, or conformal factor, obtain from the number of elements; in fact all the topological, differentiable, and geometric structures of spacetime should derive their ultimate expression from these characteristics of causal sets. This proposal has been made previously without being developed to any great extent: ['t Hooft 1979] proceeded to assume that there was a four dimensional continuum limit and thence derived conditions on its metric, while [Myrheim 1978] gave a heuristic derivation of the results of Hawking and Malament and suggested that spacetime geometry arise statistically. The work described here is concerned with different issues than those emphasized by these authors (developing further, in particular, the origin of spacetime dimension) but the fundamental proposal is essentially the same.

Partially ordered sets

The mathematical object which we will use to implement this program is a partially ordered set (poset): a set P with an order relation $\prec$ which is reflexive ($x \prec x$),

antisymmetric ($x \prec y$, $y \prec x \Rightarrow x = y$) and transitive ($x \prec y$, $y \prec z \Rightarrow x \prec z$). If $x \prec y$ or $y \prec x$ then x and y are comparable (related); otherwise they are incomparable (unrelated). Posets occur widely in mathematics: A typical example is the set $2^{[n]}$ of all subsets of $[n]$ (the set of integers $\{1, \ldots, n\}$) ordered by inclusion, *i.e.*, $A \prec B \iff A \subset B$ as sets; this is called the binomial poset B_n. Another familiar example is the set of positive integers with the order relation $i \prec j \iff i \mid j$ (i divides j). There is a vast modern literature on posets (see [Rival, ed. 1981, 1985, Fishburn 1985, Stanley 1986] and references therein); here we will recall only the immediately relevant definitions and results, for the most part following the notation and vocabulary of [Stanley 1986].

An (induced) subposet of P is a poset obtained by restricting the relation on P to some subset of P. In particular, an interval $[x, y]$ of P is the subposet whose elements are $\{z \in P : x \prec z \prec y\}$. Posets which have only finite intervals, as in the two examples, are called locally finite posets. If an interval $[x, y]$ contains only the two elements x and y then y is said to cover x. The covering relations generate the entire partial ordering under transitive closure; thus a poset is unambiguously defined by the directed graph with vertices the elements in the poset and which has a directed edge from x to y iff x is covered by y (we will sometimes refer to such an edge, or the relation it represents, as a link). Such a graph, with the directions indicated by drawing the vertex y above the vertex x iff $x \prec y$, is called a Hasse diagram. Figure I.1 shows the Hasse diagrams for B_4 and for the positive integers ordered by divisibility. Both of these posets have a unique minimal element, denoted by $\hat{0}$; the binomial posets also have a unique maximal element, denoted by $\hat{1}$. In general, any element with no predecessors is a minimal element and any one with no successors is a maximal element.

A subposet $C \subset P$ is a chain if every pair of elements in C is comparable (such

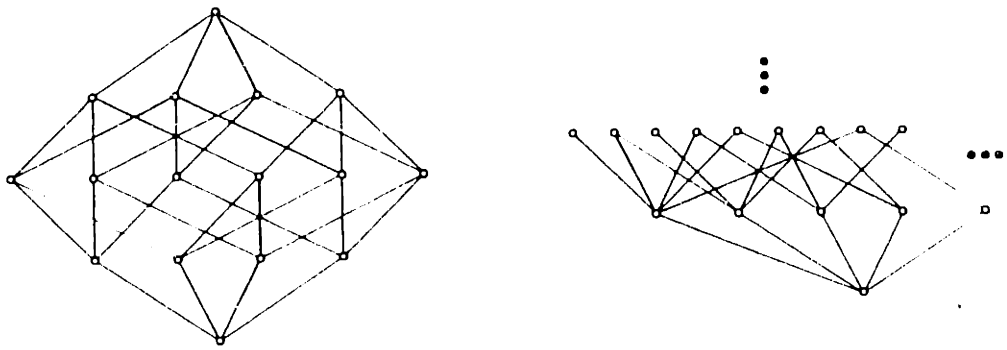

Figure I.1: The Hasse diagram for the binomial poset B_4 is shown on the left; on the right is (a portion of) the Hasse diagram for the integers ordered by divisibility. For the integers, the minimal element is 1, the rank one elements are the primes, the rank two elements are composites with two factors, etc.

a poset is totally ordered). The length of a finite chain is $|C| - 1$; the length (rank) of P is the maximum of the lengths of the chains in P. A subposet $A \subset P$ is an antichain if every pair of elements in A is incomparable. The width of P is the maximum cardinality of antichains in P. An order ideal is a subposet $I \subset P$ with the property that $x \in I$, $y \prec x \Rightarrow y \in I$. A dual order ideal is a subposet $I \subset P$ with the property that $x \in I$, $x \prec y \Rightarrow y \in I$. In finite posets every (dual) order ideal I is generated by an antichain, namely the (minimal) maximal elements of I.

Most of these substructures of posets will aquire a physical interpretation when the association between posets and the spacetime manifold of general relativity is defined in the next section. Additional (more specialized) definitions will be delayed until needed in the next chapter.

Causal sets

Using the language developed in the preceding section we may now make precise the notion of a causal set: it is, by definition, a locally finite partially ordered set. To relate this conception of spacetime with the classical spacetime manifold of general relativity we impose a physical interpretation on the causal set: its elements

are 'events' and the relations among them are causal relations. More precisely, we define:

Definition: An *embedding* of a causal set P into a Lorentzian manifold $(\mathcal{M}, \mathbf{g})$ is a map $f : P \to \mathcal{M}$ which preserves relations, *i.e.*, $f(x) \in J^-\big(f(y)\big) \iff x \prec y$.

Thus a causal set can be embedded into a spacetime manifold iff it can be realized as a set of points with the causal relations induced by the metric. In some sense then, the causal set is a finite approximation to the causal structure of $(\mathcal{M}, \mathbf{g})$.

The theorems of Hawking and Malament quoted earlier imply, however, that embedding a causal set into a Lorentzian manifold approximately determines, at most, the conformal metric; the following additional conditions must be imposed to constrain the local conformal factor:

Definition: An embedding of P into $(\mathcal{M}, \mathbf{g})$ is *faithful* if the images of the elements of P are distributed uniformly with respect to the volume form on $(\mathcal{M}, \mathbf{g})$ with density 1 and, moreover, the characteristic volume scale on which the geometry changes is much greater than 1.

These conditions will be made more explicit later; for the moment it is sufficient to observe that the first allows the interpretation of number as volume while the second precludes the presence of large conformal factors introduced on small scales to adjust the density. Thus it seems reasonable to expect that the existence of a faithful embedding of P into $\mathcal{M}$ determines the metric almost uniquely: if there are two manifolds with metric into which P can be faithfully embedded, they should be 'approximately isometric.' This is our main conjecture, the *Hauptvermutung*; although it will not be proved here, or even stated precisely, from a mathematical viewpoint the results on the dimension of causal sets described in the next two

chapters may be taken as evidence supporting this conjecture (but most likely are not steps directly toward a proof). It is worth noting that this is not an unfamiliar situation: By studying the ring of functions on a manifold, as in the Einstein algebra [Geroch 1972, Yodzis 1975], much of the structure can be determined; in particular the points of the manifold can be identified as the maximal ideals in the ring. More generally, spaces of maps from one space to another contain much of the information about the two spaces; this is why one is interested in homotopy theory. In a related example, as has been noted recently in connection with string theory [Bowick and Rajeev 1987], the elements of a loop space ΩX which are reparametrization invariant (*i.e.*, the fixed points under the action of *Diff* S^1) are isomorphic to the point set of X. From this point of view our goal is to determine the geometric structure of $\mathcal{M}$ by studying the maps which are faithful embeddings of causal sets.

Having established this association between causal sets and spacetime manifolds we may assign a physical interpretation to several of the substructures defined for posets. By definition, two elements are comparable if their embedded images are causally related; incomparable elements have spacelike related images. An interval corresponds to an Alexandroff neighborhood; restricting causal sets to be locally finite means that all the Alexandroff neighborhoods have finite volume—none contains an asymptotic region. If two elements are linked in a causal set then their images under an embedding will be nearest neighbors: the Alexandroff neighborhood they determine will contain the image of no other element in the causal set. Further, a chain in P is embedded as a sequence of causally related events—there is a causal curve passing through them. On the other hand, an antichain is embedded as a set of spacelike related points. Finally, an order ideal corresponds to a past set, a dual order ideal to a future set.

To this point the discussion has been purely classical, a physical interpretation

being assigned to causal sets through faithful embeddings into spacetime manifolds. But recall that the program is an approach to quantum gravity. As such, we expect the description of spacetime as a causal set to be valid even in situations where the manifold description breaks down: inside a black hole, in the very early universe, or in topology changing processes. In general, causal sets should describe spacetime at the Planck scale; hence the density in the definition of faithful embedding should be 1 in natural, *i.e.*, Planck, units. In fact, the causal set is to be thought of as the fundamental structure to which the spacetime manifold of general relativity is only a large scale approximation. In a quantum 'sum over histories' approach a quantum amplitude would be defined for every causal set and the spacetime manifold should arise as the classical limit from the condition of constructive interference among these amplitudes. Implementing such an approach requires a quantum dynamics of causal sets, Taketani's third stage, possibly by way of an action assigned to any causal set. The investigation of Hausdorff dimension of causal sets leads to one proposal for such an action; this is discussed in the concluding chapter.

From this point of view, where the causal set is the underlying structure of spacetime, subject to quantum fluctuations, it is clear that not every causal set which must be considered is faithfully embeddable in the four dimensional spacetime manifold we observe. Nevertheless, at large scales the causal sets whose contributions dominate the amplitude in the sum over histories should be well approximated by a Lorentzian manifold. In this context, consider 'coarse graining' a causal set to obtain one which provides a larger scale view. Specifically, a subposet P' is a coarse-graining of P if there is some parameter $p \in [0,1]$ such that the elements of P' are obtained by retaining each element of P with probability p. This requirement should be interpreted as leading (most often) to coarse-grainings preserving only those features of P which have characteristic volume scale larger than $1/p$. Thus

it might happen that a causal set which could not be faithfully embedded in any manifold would become embeddable when coarse grained. Alternatively, even if a causal set can be embedded faithfully in some manifold, for example a Kaluza-Klein spacetime, coarse graining will erase the small scale structure and leave behind, in this example at least, a causal set embeddable in a manifold of simpler effective topology and lower dimension.

Thus we have several motivations for studying the dimension of causal sets as defined by embeddings into Lorentzian manifolds. Aesthetically, it is desirable to have a theory which predicts the dimension of spacetime; possibly a quantum theory of gravity can do so. Further, we have the physical idea that a coarse-graining of the causal sets whose contributions dominate the sum over histories should be faithfully embeddable in a spacetime manifold. Moreover, determining the dimension of the manifold from an embedded causal set provides evidence in support of the mathematical *Hauptvermutung* that a faithful embedding determines the metric almost uniquely. In Chapter II we begin by studying the Minkowski dimension of causal sets, keeping in mind the idea that an arbitrary Lorentzian manifold can be formed by patching together small (almost) flat open neighborhoods. In Chapter III we consider the problem more globally and define a Hausdorff dimension for causal sets. Finally, in the Conclusion we compile the results on dimension, propose a possible action for causal sets, and outline the directions for further research. Appendices A, B and C contain listings of the computer code used to obtain the results in Chapter III. Appendix D contains a reprint of my paper "On the stability of a non-supersymmetric ground state," *Class. Quantum Grav.* **3** (1986) 881–887 which describes the results of some earlier graduate work.

II. Minkowski Dimension

Locally, a Lorentzian manifold is approximately flat. Also, in a small volume, statistical fluctuations in a uniform distribution are such that the few points contained in the volume need not be recognizably uniformly distributed. Thus we will begin our investigation into how dimensional information is encoded in causal sets by considering the simplest possible case: embedding causal sets into Minkowski space, namely the manifold $\mathbf{R}^d$ with the flat Lorentz metric η of signature $(- + \cdots +)$, without requiring faithfullness.

Definition

It is easy to see how to embed many causal sets in Minkowski space this way. The simple example in Figure II.1 shows how to embed a 'diamond' poset into two dimensional Minkowski space. Also, although the 'crown' poset of Figure II.2

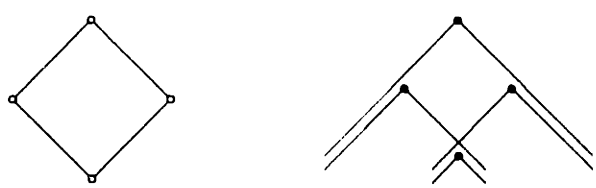

Figure II.1

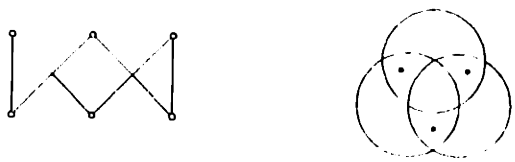

Figure II.2: An embedding of the 'crown' poset into three dimensional Minkowski space is indicated by the intersections of the past lightcones of the images of the elements with a spacelike plane.

cannot be embedded in two dimensions, it can be embedded in three dimensional Minkowski space as shown. Notice that both of these examples come from binomial posets: the 'diamond' is B_2 and the 'crown' is the middle two layers of B_3. This leads us to make the following conjecture.

Conjecture: The binomial poset B_n can be embedded in n dimensional Minkowski space.

But the binomial poset bears a special relation to all other posets, as expressed by the following well known result.

Lemma II.1: A poset P with no more than n elements can always be realized as a subposet of B_n.

Proof: Label the elements in P from 1 to n. Then define a map $f : P \to B_n$ by $f(i) := \{j \in P : j \prec i\}$, where we are identifying the elements of B_n with subsets of $[n]$. This is clearly an order preserving injection, so P is a subposet of B_n. ∎

The importance of this result is that it guarantees that if the conjecture is true then all causal sets can be embedded in a Minkowski space of some dimension; thus we may make the following definition.

Definition: The *Minkowski dimension* of a causal set is the dimension of the lowest dimensional Minkowski space into which it can be embedded (not necessarily

faithfully).

The validity of this definition for all causal sets depends on the truth of the conjecture above. Although for our immediate purposes it would suffice to accept it as applying to exactly those causal sets which can be embedded in some Minkowski space, the next section discusses an attempt to prove the conjecture; as it is only partially successful the following sections take another tack, investigating the connection with the combinatorial definition of poset dimension.

Embedding the binomial poset

The most natural approach to embedding B_n in n dimensional Minkowski space is to exploit the symmetries of B_n: Consider a regular $n-1$ simplex. Let $e_1, \ldots, e_n$ be vectors from its barycenter to the n vertices, normalized by $e_i \cdot e_i = n-1$. For use in the following calculations we note that

$$\begin{aligned} &e_1 + \cdots + e_n = 0 \\ &e_1 \cdot (e_1 + \cdots + e_n) = 0 \quad \Rightarrow \quad e_i \cdot e_j = -1, \quad i \neq j \\ &\|e_1 + \cdots + e_k\|^2 = k(n-k). \end{aligned}$$

As before, since the elements of B_n may be thought of as the subsets of $[n]$, there is a natural bijection between them and subsets of $\{e_1, \ldots, e_n\}$; thus we shall embed the element corresponding to the subset $A \subset [n]$ at $t_{|A|}$, $r_{|A|} \cdot \sum_{i \in A} e_i$.

Set $t_1 := 0$, $r_1 := 1$. Then we may define the time coordinates recursively by

$$\begin{aligned} (t_{k+1} - t_k)^2 &:= \|r_{k+1}(e_1 + \cdots + e_{k+1}) - r_k(e_1 + \cdots + e_k)\|^2 \\ &= r_{k+1}^2(k+1)\big(n-(k+1)\big) + r_k^2 k(n-k) - 2r_k r_{k+1} k\big(n-(k+1)\big) \end{aligned}$$

and ensure embedding by requiring

$$\begin{aligned} t_{k+1}^2 &< \|r_{k+1}(e_1 + \cdots + e_{k+1}) - e_n\|^2 \\ &= r_{k+1}^2(k+1)\big(n-(k+1)\big) + (n-1) + 2r_{k+1}(k+1). \end{aligned}$$

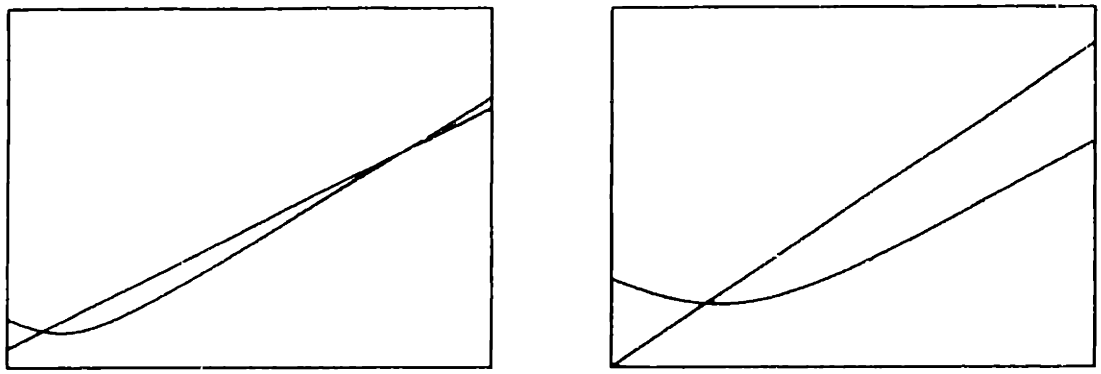

Figure II.3: When the slope of the line is less than that of the hyperbola's asymptote the solution region is bounded; when it is greater the solution region is unbounded. These graphs are for $n = 6$, $r_2 = 0.25$ and 0.50, respectively, with r_3 running from 0 to 1.5 along the horizontal axis.

Note that for $k = 1$ these conditions become

$$t_2^2 := r_2^2 \cdot 2(n-2) + (n-1) - 2r_2(n-2)$$

$$t_2^2 < r_2^2 \cdot 2(n-2) + (n-1) + 2r_2 \cdot 2,$$

and will hold for any positive choice of r_2.

In general, solving the defining equation for t_{k+1}^2, combining with the inequality and simplifying, we find that there will be solutions iff

$$2r_{k+1}\left[(k+1) + r_k k\big(n-(k+1)\big)\right] + (n-1) - t_k^2 - r_k^2 k(n-k)$$
$$> 2t_k\left[r_{k+1}^2(k+1)\big(n-(k+1)\big) + r_k^2 k(n-k) - 2r_k r_{k+1} k\big(n-(k+1)\big)\right]^{1/2}.$$

Graphing the left hand side of this inequality as a function of r_{k+1} gives a line; similarly, the right hand side gives a hyperbola. Since the hyperbola is symmetric with respect to the horizontal axis (and does not intersect it), there will be solutions iff the curves intersect in the first or second quadrants. Figure II.3 shows the types of intersection that can occur.

Replacing the inequality with equality, squaring and simplifying, we obtain a

quadratic equation for r_{k+1}:

$$\begin{aligned}
&4r_{k+1}^2\Big\{\big[(k+1)+r_k k\big(n-(k+1)\big)\big]^2 - t_k^2(k+1)\big(n-(k+1)\big)\Big\} \\
&\quad + 4r_{k+1}\Big\{\big[(k+1)+r_k k\big(n-(k+1)\big)\big]\big[(n-1)-t_k^2-r_k^2 k(n-k)\big] \\
&\qquad\qquad + 2r_k k\big(n-(k+1)\big)t_k^2\Big\} \\
&\quad + \Big\{\big[(n-1)-t_k^2-r_k^2 k(n-k)\big]^2 - 4r_k^2 k(n-k)t_k^2\Big\} = 0.
\end{aligned}$$

This equation has real solutions iff the discriminant D is non-negative. After some algebra we find

$$\begin{aligned}
D/16t_k^2 &= (k+1)\big(n-(k+1)\big)\big[(n-1)-t_k^2\big]^2 \\
&\quad + 4k(k+1)\big(n-(k+1)\big)\big[(n-1)-t_k^2\big]r_k \\
&\quad + 2k\Big\{2k\big(n-(k+1)\big)^2(n-1) + 2(k+1)^2(n-k) \\
&\qquad - (k+1)(n-k)\big(n-(k+1)\big)\big[(n-1)+t_k^2\big]\Big\}r_k^2 \\
&\quad + 4k^2(k+1)(n-k)\big(n-(k+1)\big)r_k^3 \\
&\quad + k^2(k+1)(n-k)^2\big(n-(k+1)\big)r_k^4.
\end{aligned}$$

This expression may be simplified by defining

$$\epsilon := r_k^2 k(n-k) + (n-1) + 2r_k k - t_k^2 > 0.$$

Expressing t_k^2 in terms of ϵ, we obtain

$$D/16t_k^2 = -4kn^2\big(n-(k+2)\big)r_k^2 + (k+1)\big(n-(k+1)\big)\epsilon^2.$$

For $k=2$, $\epsilon = 2r_2 n$, so $D = 64t_2^2 r_2^2(n-1)n^2$ which is positive definite. Thus we can solve the quadratic equation, which becomes, after expressing t_2^2 in terms of r_2:

$$-r_3^2\big\{3(n-4)-2r_2\cdot 3(n-3)+r_2^2\cdot 2(n-3)\big\}+2r_3 r_2\big\{(2n-5)-r_2\cdot 2(n-2)\big\}-r_2^2(n-2)=0.$$

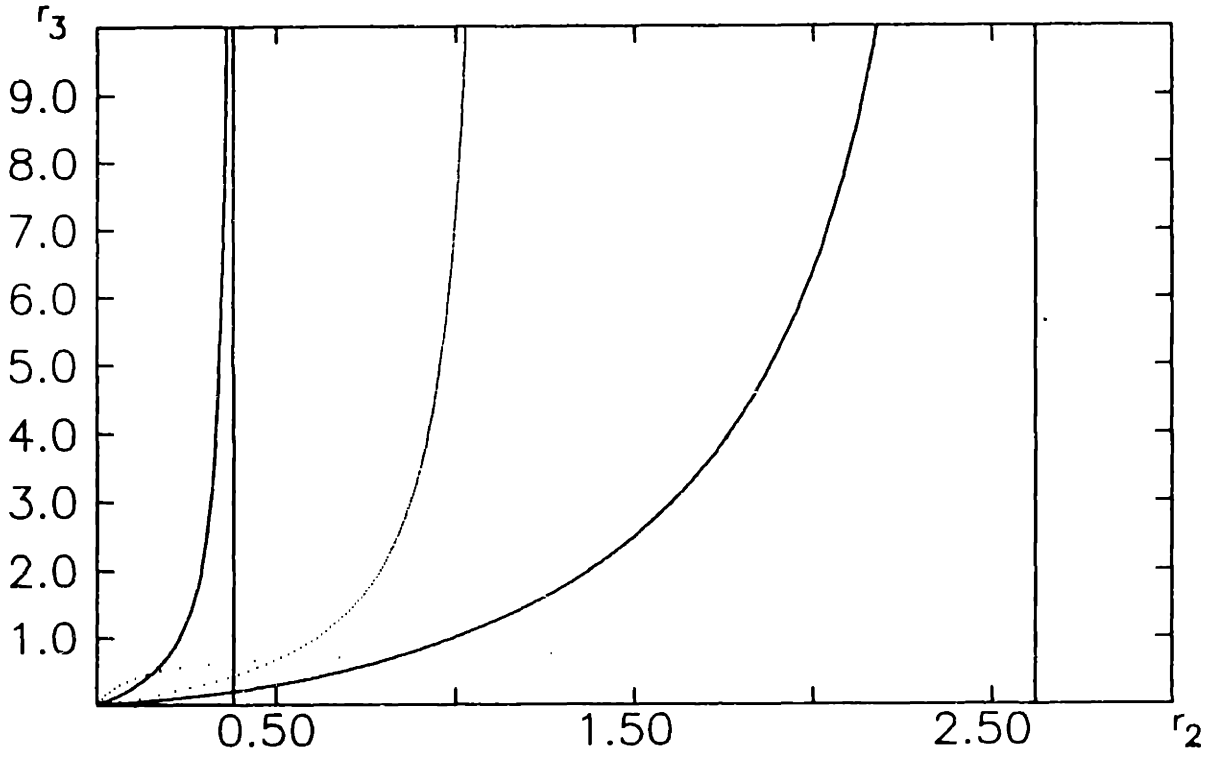

Figure II.4: The values of r_2 and r_3 which satisfy the embedding condition lie inside the region bounded by the solid curves with asymptotes at r_2^- and r_2^+. Inside this region the discriminant in the solution for r_4 attains its local maximum for each value of r_3 along the ridge line indicated by the dotted curve. The second dotted curve, with the horizontal asymptote, is the locus of the extraneous solutions mentioned in the text. These curves are again plotted for $n = 6$.

Note that when the coefficient of r_3^2 is positive, it means that the line shown in Figure II.3 is steeper than the asymptote of the hyperbola, while when it is negative the opposite is true. This coefficient when

$$r_2^{\pm} = \frac{3(n-3) \pm \sqrt{3(n-3)(n-1)}}{2(n-3)}$$

so denoting the solutions to the quadratic equation in r_3 by $r_3^+(r_2)$ and $r_3^-(r_2)$ we see that for $r_2 \in (0, r_2^-)$ the original inequality has solutions for $r_3 \in (r_3^-(r_2), r_3^+(r_2))$, while for $r_2 \in [r_2^-, r_2^+)$ the solutions are $r_3 \in (r_3^-(r_2), \infty)$. Figure II.4 shows the allowed range of r_3 for each value of r_2; the vertical asymptotes are at r_2^- and r_2^+.

Can we continue to $k = 3$? In this case

$$D/64t_3^2 = -3n^2(n-5)r_3^2 + (n-4)\epsilon^2$$

which is positive definite only for $n \leq 5$; for $n > 5$ we must determine its sign in the region shown in Figure II.4. At a fixed value of r_3 we may extremize with respect to r_2:

$$\frac{\partial}{\partial r_2}\left(\frac{D}{64t_3^2}\right) = \frac{\partial}{\partial r_2}(n-4)\epsilon^2 = -2(n-4)\epsilon\frac{\partial}{\partial r_2}t_3^2 = -4(n-4)\epsilon t_3\frac{\partial}{\partial r_2}t_3.$$

This vanishes if $\epsilon = 0$ or $\partial t_3/\partial r_2 = 0$. ($t_3$ cannot vanish.) $\epsilon = 0$ at the boundary of the allowed region; by inspection $D < 0$ here and these are local minima for fixed r_3. Between them D attains a local maximum when $\partial t_3/\partial r_2 = 0$, namely when

$$\frac{(n-2)(r_2\cdot 2-1)}{\sqrt{r_2^2\cdot 2(n-2)+(n-1)-2r_2(n-2)}} + \frac{2\big(r_2(n-2)-r_3(n-3)\big)}{\sqrt{r_3^2\cdot 3(n-3)+r_2^2\cdot 2(n-2)-2r_2r_3\cdot 2(n-3)}} = 0.$$

Moving the second term to the left hand side, multiplying by the common denominator, squaring (Note that this introduces an extraneous solution.) and simplifying, we obtain a quadratic expression for r_2 in terms of r_3:

$$r_2^2\cdot 2(n-2)\big[2r_3^2(n-3)-(n-2)\big] - r_2\cdot 4r_3(n-2)(n-3)(r_3-1) - r_3^2(n-3)(n-4) = 0.$$

If we solve this equation for r_2 in terms of r_3 we obtain the dotted curves in Figure II.4; the curve running along the middle of the allowed region indicates the loci of the local maxima for fixed r_3. (The other dotted curve is the locus of the extraneous solutions introduced when we squared the equation.) Plugging this solution for r_2 back into the discriminant and verifying that it is negative would prove that the discriminant is negative throughout the allowed region. This is difficult to do analytically, but easy numerically. Figure II.5 shows the graph of $D/64t_3^2$ as a function of r_2 for various fixed values of r_3; the values at the local maxima are negative and decreasing away from the origin.

Inasmuch as one trusts numerical results, then, for $n \geq 6$ the discriminant which occurs in the solution for r_4 is negative throughout the region of allowed r_2

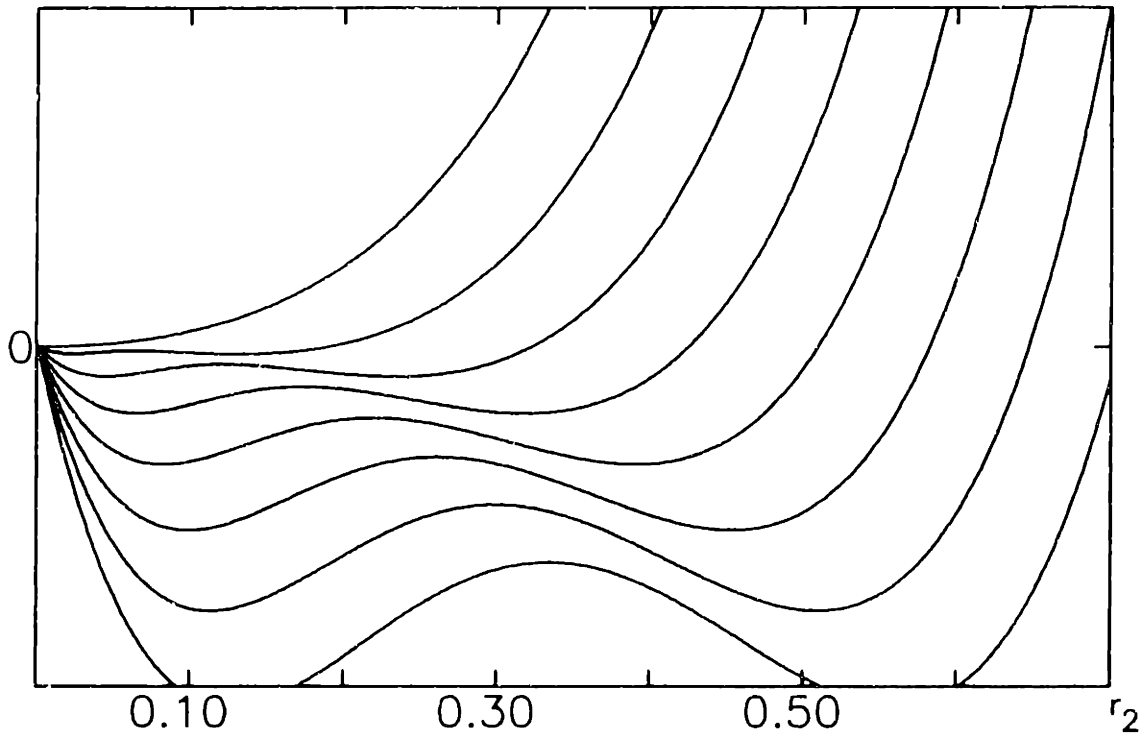

Figure II.5: $D/64t_3^2$ as a function of r_2 for $r_3 = 0, 0.05, 0.1, 0.15, 0.2, 0.25, 0.3$ and 0.35. As r_3 increases the descriminant becomes more negative in the allowed region (between the local minima). These curves are plotted for $n = 6$; the vertical scale runs from -50 to 50.

and r_3; hence there is no real solution and B_n cannot be embedded symmetrically in n dimensional Minkowski space.

For $n < 6$ it is easy to obtain embeddings. Table II.1 contains a representative solution:

k	r_k	t_k	bound
1	1.00000	0.00000	3.16228
2	1.00000×10^{-5}	1.99998	2.00001
3	1.33252×10^{-5}	2.00001	2.00002
4	3.33217×10^{-5}	2.00006	2.00007
5	6.18356×10^{-5}	2.00013	2.00015

Table I.1: A representative embedding of B_5 into Minkowski space. The bounds on the times are the ones from the embedding condition given the choices of r_k.

The conclusion of this section, therefore, is that the observation that B_2 and B_3 can be embedded in two and three dimensional Minkowski space, respectively, can only be extended up to dimension five *via* symmetrical embeddings. While it is possible that asymmetrical embeddings exist, these results at least indicate that the conjecture of the previous section will be difficult to prove directly. Instead, in the next section we consider the standard definition of poset dimension and determine its relation with the Minkowski dimension.

Combinatorial dimension I

We begin with some definitions.

Definition: A *total ordering* of a set is a partial ordering for which the trichotomy principle holds, *i.e.*, every two elements are related. A total order is a *(linear) extension* of a partial order if $x \prec y$ in the partial order implies $x < y$ in the total order (for $x \neq y$).

The basic result, first proved by [Szpilrajn 1930], is that every partial order admits an extension and, moreover, if x and y are unrelated in the partial order, there is an extension in which $x < y$ and one in which $y < x$.

Definition: The *intersection* of a collection of total orders (of a given set) is the partial order consisting of the relations on which all the total orders agree.

An example of this is shown in Figure II.6 where the 'diamond' poset is realized as the intersection of two total orders. Dushnik and Miller used these ideas to define poset dimension [Dushnik and Miller 1941]:

Definition: The *combinatorial dimension* of a partial order is the cardinality of the smallest collection of total orders whose intersection is the partial order.

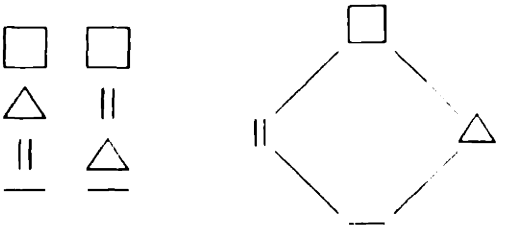

Figure II.6

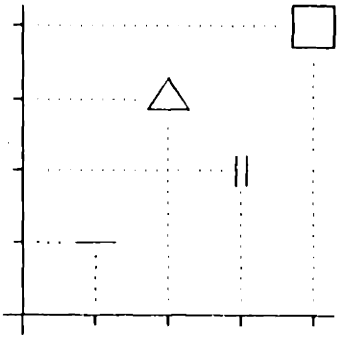

Figure II.7

Although this definition of dimension is purely combinatorial, it is nevertheless related to the Minkowski dimension:

Proposition II.2: A causal set can be embedded in two dimensional Minkowski space iff it has combinatorial dimension at most two.

Proof: There is a geometrical interpretation of the combinatorial dimension: if the dimension is d, choose a system of orthogonal coordinates in $\mathbf{R}^d$ and identify the position of an element in each total order as its corresponding coordinate. Figure II.7 shows the 'diamond' poset in $\mathbf{R}^2$. With this interpretation an element in the poset precedes another element iff all of its coordinates are smaller. Thus, cross sections of the region in which an element must lie to precede another are $d-1$ simplices; so let us call the regions past lightpyramids. In two dimensions, however, these lightpyramids are congruent to past lightcones in Minkowski space; we need only interpret the coordinates as the null coordinates $u := t - x$ and $v := t + x$ to obtain a Minkowski embedding from a combinatorial one. Conversely, given a two dimensional Minkowski embedding of any finite poset, we can adjust the images slightly if necessary to ensure that no two have the same null coordinate (or else widen the lightcones slightly); then the ordering in u and the ordering in v provide the desired combinatorial realization. ∎

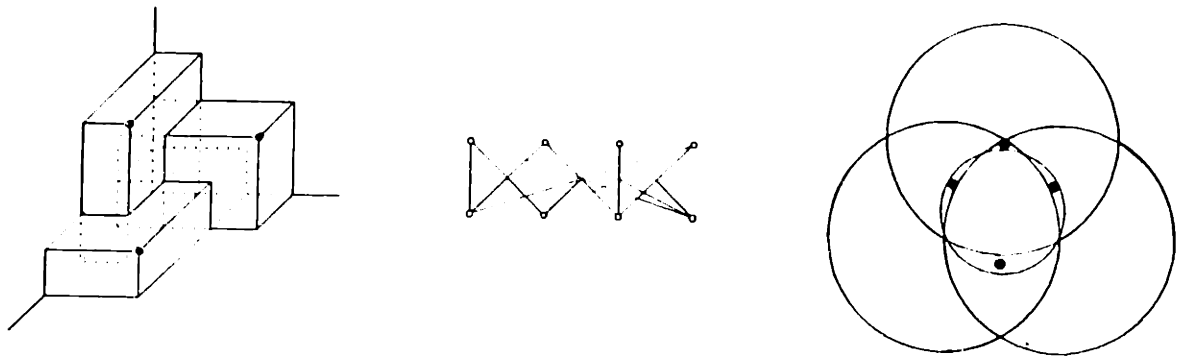

Figure II.8: The poset S_2^2 with a diagram demonstrating the impossibility of its having combinatorial dimension three on the left and an explicit embedding into three dimensional Minkowski space indicated by the intersections of the past lightcones of the images of the elements with a spacelike plane on the right.

It is the geometrical interpretation of the combinatorial dimension which allows us to make this simple connection to the Minkowski dimension. But it also indicates how to construct a counterexample to the hypothesis that this result holds in higher dimensions. Consider a poset with three unrelated elements: the geometrical realization of their past lightpyramids in the first octant of $\mathbf{R}^3$ will form three rectangular parallelepipeds intersecting to form a fourth. An additional element in the poset, unrelated to the first three but succeeding elements in each of the regions where two but not all three of them intersect, must succeed every element in the fourth parallelepiped which is their triple intersection. But this is not the case in three dimensional Minkowski space: see Figure II.8 for a diagram and the simple poset (S_2^2 in the notation of [Kelly and Trotter 1982]) which realizes this situation, having combinatorial dimension four and Minkowski dimension three.

It is natural to conjecture at this stage that the Minkowski dimension is always less than or equal to the combinatorial dimension. Now, the combinatorial dimension of posets has been extensively studied. (Recent surveys may be found in [Kelly and Trotter 1982, Fishburn 1985].) For example, the binomial poset B_n has combinatorial dimension n [Komm 1948]. Moreover, many upper bounds for the

combinatorial dimension of a poset have been found:

- cdim $P \leq$ cdim $P' + 1$ where P' is obtained from P by removing a single element [Hiraguchi 1951].
- cdim $P \leq 2 +$ cdim $(P \setminus C)$ where C is a chain in P [Hiraguchi 1951].
- cdim $P \leq$ width P [Hiraguchi 1955].
- cdim $P \leq \max\{2, |P \setminus A|\}$ where A is an antichain in P [Kimble 1973, Trotter 1975].
- cdim $P \leq |P|/2$ for $|P| \geq 4$ [Hiraguchi 1951].
- cdim $P \leq 1 +$ width $(P \setminus M)$ where M is the set of maximal elements of P [Trotter 1975].
- cdim $P \leq 1 + 2$ width $(P \setminus A)$ where $A \neq P$ is an antichain in P [Trotter 1974].

If it could be shown that the Minkowski dimension did not exceed the combinatorial dimension, each of these results would imply an upper bound on the Minkowski dimension. Alternatively, notice that the first result in this list gives an upper bound very similar to the one we would obtain following the argument of the first section in this chapter should the conjecture there be true: neither dimension would be greater than the number of elements in the poset. Of course, this is a vanishingly weak upper bound: since N points can span only $N-1$ dimensions in a linear space, if a causal set can be embedded in any Minkowski space, it can be embedded in an $N-1$ dimensional one. Although our primary motivation in obtaining an upper bound should be to show that the Minkowski dimension is well defined, one might hope that these other upper bounds on the combinatorial dimension have analogues as well. After all, with a 10^{240} Planck volume universe, this would give what is probably the largest number of dimensions ever considered for spacetime!

As yet we have no indication that this (large) upper bound is at all relevant: we have seen examples of causal sets of Minkowski dimension two and three (Figures II.3, II.4 and II.8), but have not shown that any causal set has dimension greater than three. It would be unfortunate if, in fact, all causal sets which were not planar could be embedded in three dimensions, as is the case with graphs in Euclidean space, for example.

There are also, however, lower bounds on the combinatorial dimension. Recall the first upper bound on the list in the preceding section: cdim $P \leq$ cdim $P' + 1$ where P' is obtained from P by removing a single element. This is often called the One-point Removal Theorem: removing a single element from a poset decreases its dimension by at most one. (It is easy to see that a weaker version of this is true for the Minkowski dimension: removing a single element cannot increase the dimension since if a causal set is embedded, it remains embedded upon the removal.) Thus one is led to define [Kelly and Trotter 1982]:

Definition: A poset is *d–irreducible* if it has combinatorial dimension d and the removal of any element reduces its dimension.

Examples: B_2 is not 2–irreducible, but the 'crown' poset is 3–irreducible.

It is clear that any poset with combinatorial dimension at least d contains a d–irreducible subposet: By the One-point Removal Theorem, if the elements are removed one at a time, the dimension either decreases by one or remains the same; removing elements until the dimension is d, then removing all elements which do not reduce the dimension further, one obtains a d–irreducible poset. The d–irreducible posets are thus *obstructions* to embedding a poset in fewer than d total orders.

They are similar to the Kuratowski subgraphs K_5 and $K_{3,3}$ which prevent a graph from being planar [Kuratowski 1930].

More generally, this phenomenon is related to what [Kelly and Rota 1973] have termed the *critical problem* of combinatorial geometry: given a set S in a projective space P_n over a finite field, find the linear subspaces $V \subseteq P_n$ of maximum dimension d such that $V \cap S = \emptyset$. They conjecture that the *critical exponent* $c := n - d$ is determined by the nonexistence of certain obstructions and indicate the parallel between this problem and the problem in algebraic geometry of determining the minimum number of conditions on a hypersurface necessary to ensure that it contains a given algebraic variety. Similarly, in a problem closer to physics, extending a cross section over a subspace of the base space of a fibre bundle to a cross section over the entire base space requires the vanishing of obstruction cocycles in the homotopy groups of the fibre [Steenrod 1951]. The Gribov ambiguity [Singer 1978] and the determination of the connected components of the configuration space of a gauged nonlinear sigma model [Percacci 1986] are instances of this problem, as are the orientability and existence of a spin structure on a manifold [Borel and Hirzebruch 1959, Milnor 1963]. In all these problems there is some algebraic object which is related to the obstructions: the Birkhoff (or characteristic, or chromatic) polynomial for a combinatorial geometry, the Hilbert polynomial in algebraic geometry, and a cohomology class in $H^n\big(M; \mathcal{B}(\pi_{n-1})\big)$ for extensions of fibre bundle cross sections (specifically, the second Steifel-Whitney class in the case of spin structure).

Ideally one would develop such algebraic machinery in the case of posets. Lacking that, one at least would like to be able to list exhaustively the d–irreducible posets. We shall see a hint in the next section that some algebraic formulation may exist for the problem of determining the Minkowski dimension of a causal set. In the meantime, we can compile a partial list of irreducible posets. There is only one

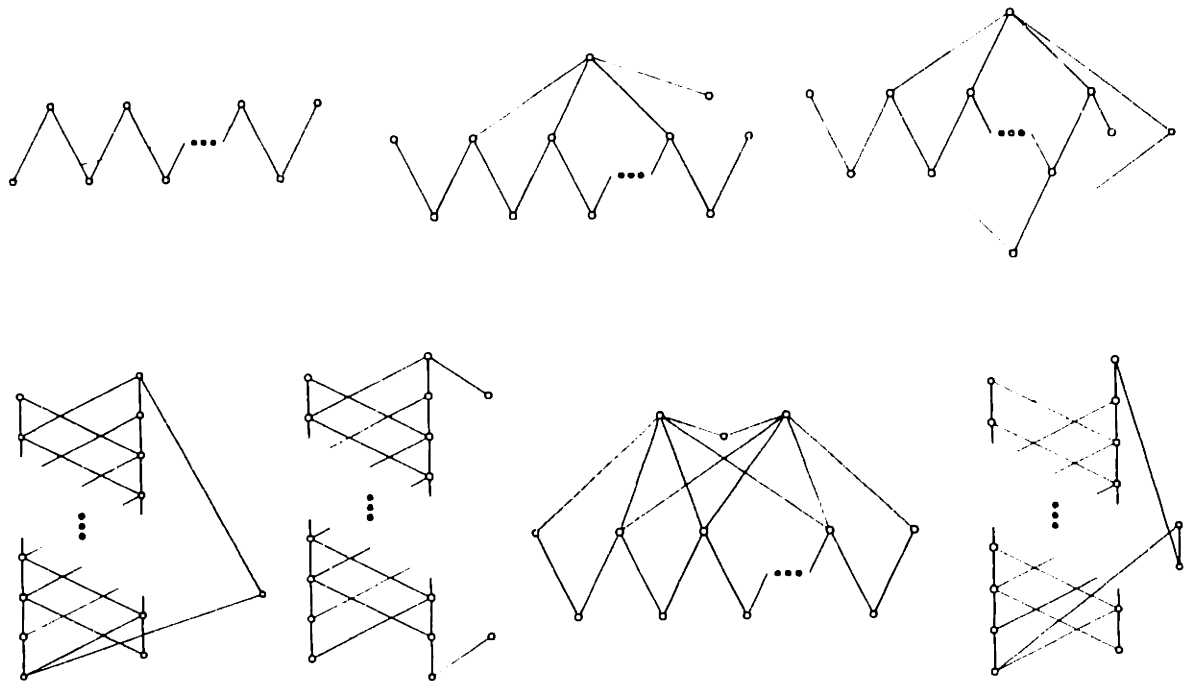

Figure II.9: The seven infinite families of 3–irreducible posets: A_n, E_n, F_n, G_n, H_n, I_n and J_n.

2–irreducible poset: two unrelated elements. 3–irreducible posets were discovered by [Harzheim 1970, Baker, Fishburn and Roberts 1971, Kelly and Rival 1975]; and the list was finally completed independently by [Kelly 1977] and by [Trotter and Moore 1976]. The results, summarized in [Kelly and Trotter 1982], are that there are seven infinite families and ten exceptional 3–irreducible posets (up to duality and isomorphism); these are shown in Figures II.9 and II.10.

Since we have seen that the combinatorial and Minkowski dimensions are related to some extent, the natural step now is to define:

Definition: A causal set is *d–irreducible* if it has Minkowski dimension d and the removal of any element reduces its dimension.

We have not proved a One-point Removal Theorem for causal sets; nevertheless if we have a causal set with Minkowski dimension d, we know that removing an

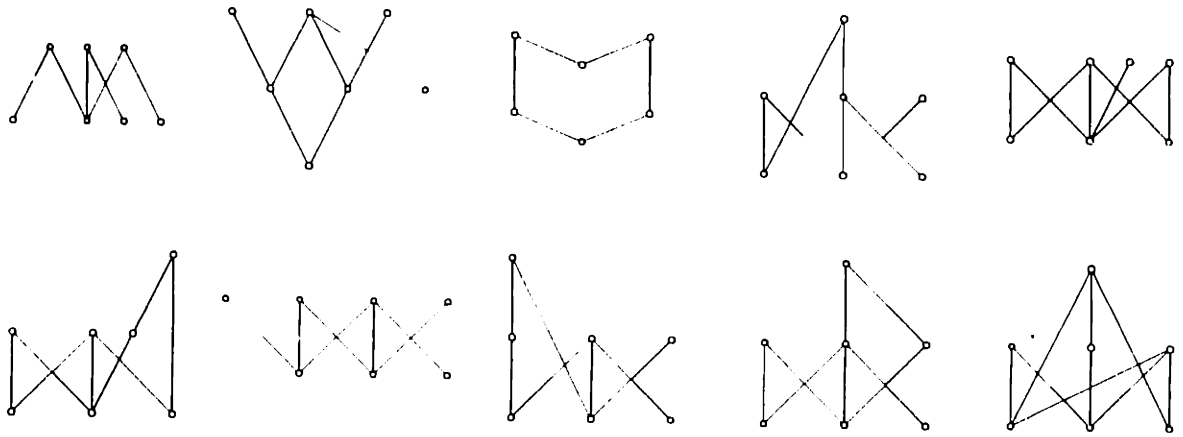

Figure II.10: The ten exceptional 3–irreducible posets: B, C, D, CX_1, CX_2, CX_3, EX_1, EX_2, FX_1 and FX_2.

element cannot increase the dimension. So we can remove, one at a time, the elements whose removal does not reduce the Minkowski dimension of the causal set. When no such elements remain the causal set is d–irreducible. This proves the following proposition:

Proposition II.3: A causal set with Minkowski dimension d must contain a d–irreducible causal set.

So which are the d–irreducible causal sets? By our earlier result that Minkowski and combinatorial dimension two are the same, there is only the same single 2–irreducible causal set. For dimension three we have the following result:

Theorem II.4: Every 3–irreducible causal set is a 3–irreducible poset and conversely.

Proof: Consider such a causal set. Removing any element reduces it to Minkowski dimension two, and hence by Proposition II.2, to combinatorial dimension two. But the One-point Removal Theorem tells us that the combinatorial dimension cannot decrease by more than one when a single element is removed. Since the original

causal set could not have had combinatorial dimension two (else its Minkowski dimension would also have been two), it must have had combinatorial dimension three. Thus it was a 3–irreducible poset.

Conversely, consider a 3–irreducible poset. Since we do not have a One-point Removal Theorem to tell us that the Minkowski dimension decreases by at most one upon removal of a single element, it is conceivable, *a priori*, that this poset has Minkowski dimension greater than three. We have, however, a complete list of the 3–irreducible posets so we can look for an explicit embedding of each in three dimensional Minkowski space. Inspecting Figures II.9 and II.10 we find that such embeddings do exist. Thus the 3–irreducible causal sets are exactly the 3–irreducible posets. ∎

This result justifies the assertion made in the first section of this chapter that the 'crown' poset could not be embedded in two dimensional Minkowski space: since it is a 3–irreducible poset it is also a 3–irreducible causal set.

The situation for d–irreducible posets is considerably more complex when $d \geq 4$ [Paoli, Trotter and Walker 1985]. Since there are posets of each possible dimension (the binomial posets, for example) there must be d–irreducible posets for every dimension. [Trotter and Ross 1982] have shown, however, that for any poset P having combinatorial dimension $d \geq 3$ there exists a $(d+1)$–irreducible poset containing P as a subposet. Thus d–irreducible posets for $d \geq 4$ can be arbitrarily complicated and a proof based on examination of cases, as above, cannot be extended to higher dimensions.

Recall that our motivation for examining d–irreducible causal sets is to obtain a lower bound on the Minkowski dimension of a causal set: if it contains a d–irreducible causal set then it must have Minkowski dimension at least d. In par-

ticular, we would like to know that not all causal sets have dimension less than or equal to three (four, or ten, or twenty-six would be fine!). Now, although the set of all d-irreducible posets for $d \geq 4$ is complicated, there are simple families of d–irreducible posets for all d. The standard example of such a family is the set of posets $S_d \subset B_d$ consisting of the elements corresponding to the subsets of $[d]$ of sizes 1 and $d-1$. S_d is a d–irreducible poset [Paoli, Trotter and Walker 1985]. In the following section we apply some geometric and topological methods to deduce that B_n also contains d–irreducible causal sets.

Irreducible causal sets

The binomial poset B_n has n rank 1 elements (elements covering the minimal element). Suppose these elements are embedded in d dimensional Minkowski space. Then their future lightcones will divide the spacetime into regions in which the other elements must be embedded by virtue of their relations to these elements. In the following discussion we will enumerate the regions formed and infer a lower bound on the Minkowski dimension of B_n. (The argument is closely related to computing the Euler characteristic of a CW complex; pursuing this connection further might lead to the purely algebraic computation of Minkowski dimension suggested in the previous section.)

Definition: By an arrangement of n (future) lightcones *in general position* in $d \geq 2$ dimensional Minkowski space we mean that every $k \leq d$ lightcones intersect to form a $d-k$ dimensional variety, which we will call a *conic* variety, and any larger number of lightcones has no common intersection.

What is this variety? The equations of the lightcones can be written out explicitly in the form

$$(t-t_1)^2 = \sum_{i=1}^{d-1}(x^i - x_1^i)^2$$

$$\vdots$$

$$(t-t_k)^2 = \sum_{i=1}^{d-1}(x^i - x_k^i)^2.$$

Differences of pairs of equations produce $k-1$ independent linear equations which intersect to form a $d-k+1$ dimensional hyperplane, *which may be spacelike*; call it H. The intersection of H with any one of these k lightcones is their common intersection, a $d-k$ dimensional conic variety Q lying in H (and, of course, in each of the lightcones). For $k=1$, Q is a lightcone, while for $k>1$, Q is a hyperboloid, paraboloid or ellipsoid.

With this in mind, consider an arrangement of n (future) lightcones C_i in general position in d dimensions. Define $M_d(n)$ to be the maximum number of d–cells (*i.e.*, regions homeomorphic to the interior of an S^{d-1}) formed in d dimensional Minkowski space by any n (future) lightcones. The number of d–cells formed by $C_1,\ldots,C_n$ is no more than the number of d–cells formed by $C_1,\ldots,C_{n-1}$ plus the number of $(d-1)$–cells C_n is divided into by its intersections with $C_1,\ldots,C_{n-1}$; define $C_{d-1}(n-1)$ to be the maximum number of $(d-1)$–cells formed on a $d-1$ dimensional conic variety by its intersection with $n-1$ other $d-1$ dimensional conics, *i.e.*, (future) lightcones. Then

$$M_d(n) \leq M_d(n-1) + C_{d-1}(n-1).$$

In general, a $d-k$ dimensional variety Q lying in the $d-k+1$ dimensional hyperplane H determined by k of the lightcones as described above is cut into $(d-k)$–cells by its intersection with the $n-k$ conic varieties Q_i formed by the intersection of each of the remaining $n-k$ lightcones with H (all of which are

therefore translations and scalings of each other). Thus, the number of $(d-k)$-cells formed on Q by $Q_1, \ldots, Q_{n-k}$ is no more than the number of $(d-k)$-cells formed on Q by $Q_1, \ldots, Q_{n-k-1}$ plus the number of $(d-k-1)$-cells on Q_{n-k} formed by its intersections with $Q_1, \ldots, Q_{n-k-1}$, so

$$C_{d-k}(n-k) \leq C_{d-k}(n-k-1) + C_{d-k-1}(n-k-1).$$

The initial conditions for this recursion are

$$C_d(1) = 2 \qquad d \geq 2$$

$$C_1(n) = 2n+1.$$

So we obtain the numbers in the following table:

$C_d(n)$	number of lightcones n							
dim d	1	2	3	4	5	6	7	8
1	3	5	7	9	11	13	15	17
2	2	5	10	17	26	37	50	65
3	2	4	9	19	36	62	99	149
4	2	4	8	17	36	72	134	233
5	2	4	8	16	33	69	141	275
6	2	4	8	16	32	65	134	275
7	2	4	8	16	32	64	129	263

Table II.2

which are given by

$$C_d(n) \leq \binom{n}{d} + \sum_{i=0}^{d} \binom{n}{i}.$$

Before solving the recursion relation for $M_d(n)$ we must note that the case $d=2$ is special, for the intersections of lightcones here are simply single points, not

the more general S^0 consisting of two points used to obtain the initial condition $C_1(n) = 2n + 1$. So for $d = 2$ we have

$$M_2(n) = M_2(n-1) + n.$$

Applying the initial condition $M_d(1) = 2$ we may easily solve this to obtain

$$M_2(n) = 1 + \frac{n(n+1)}{2}.$$

For $d \geq 3$, since the initial condition $M_d(1) = 2$ is the same as for $C_d(1)$, and since lower dimensional Minkowski space bounds do not occur in the recursion relation, we obtain simply

$$M_d(n) \leq C_d(n).$$

Thus the bounds on $M_d(n)$ are as shown in Table II.3:

$M_d(n)$	number of lightcones n							
dim d	1	2	3	4	5	6	7	8
2	2*	4*	7	11	16	22	29	37
3	2	4	9*	19*	36*	62	99	149
4	2	4	8	17	36	72*	134*	233
5	2	4	8	16	33	69	141	275*
6	2	4	8	16	32	65	134	275
7	2	4	8	16	32	64	129	263

Table II.3

Hence we may deduce the following:

Theorem II.5: The Minkowski dimension of B_n is at least as large as the minimal d satisfying

$$\binom{n}{d} \geq \sum_{i=d+1}^{n} \binom{n}{i}.$$

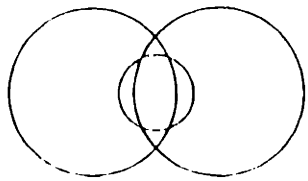

Figure II.11: Three future lightcones can cut three dimensional Minkowski space into nine distinct pieces: eight pieces are clearly present in this diagram showing the intersections of the lightcones with a spacelike plane; the ninth is the region of spacetime interior to the middle lightcone but exterior to the other two. That this region exists is indicated by the fact that the small circle is not entirely contained in either of the larger ones.

Proof: The n rank 1 elements in B_n, when embedded in d dimensional Minkowski space, divide it into at most $M_d(n)$ regions. Since B_n requires at least 2^n regions to embed, we obtain this inequality. ∎

The bounds on $M_d(n)$ which imply these values for d are indicated by astrices in Table II.3.

It may seem peculiar that n future lightcones can ever cut a spacetime into more than 2^n regions. For example, can the bound of $M_3(3) = 9 > 2^3$ be attained? The answer, in fact, is yes: this phenomenon is the effect of the boundary condition $C_1(n) = 2n + 1$ and can be realized even in this simple case as shown in Figure II.11 where three future lightcones cut three dimensional Minkowski space into nine distinct pieces. Of course, only the number of regions bearing different relations to the future lightcones is relevant and this can be no more than 2^n.

More relevantly, from this table we can recognize the first example we have seen of a causal set with Minkowski dimension greater than three: B_6. In fact, there are binomial posets which have arbitrarily large Minkowski dimension and therefore, by Proposition II.3, there are d–irreducible causal sets for arbitrarily large d. Since d must be greater than $n/2$ to solve the inequality in Theorem II.5, the number of elements in these d–irreducible causal sets is less than $2^{2d} = 4^d$. A volume grows as the d^{th} power of a length so we conclude that the Minkowski dimension

of a causal set is a reasonable local characterization of the dimension. In the next chapter we will examine what can be determined about the dimension when the global condition of faithfullness is imposed on the embedding.

III. Hausdorff Dimension

Recalling the discussion in the Introduction, we expect that while the fact that a given causal set can be embedded in a Lorentzian manifold may put a lower bound on the dimension of the manifold as described in the last section of Chapter II, a faithful embedding should be required to determine the geometrical structure. So in this chapter we investigate how to extract the dimension of a manifold (and some of its geometry) from a causal set which can be faithfully embedded therein.

Uniform distribution

The definition of a faithful embedding requires that the images of the elements in the causal set be uniformly distributed in the manifold. To implement this condition we take them to be the outcome of a stochastic process: points sprinkled uniformly (so that the probability of finding a point in a region of finite volume depends only on the volume of the region) and independently (so that for two disjoint regions the probability of a finding a point in one region is independent of the the probability of finding a point in the other) in the manifold.

If the volume of a manifold $\mathcal{M}$ is finite, this is just the uniform process: a sequence of independent random variables $X_1, \ldots, X_n$ each uniformly distributed

in the manifold. Although most of the discussion and terminology in this section follows [Baclawski and Rota 1979], this use of 'independent random variables' differs slightly from the standard definition: A (continuous) random variable is usually taken to be a function from a sample space Ω of possible outcomes, with a probability measure defined on events, to $\mathbf{R}^d$ such that the sets $\{\omega \in \Omega : X^i(\omega) \leq x^i; i \in [d]\}$ are events, denoted $(X \leq \mathbf{x})$, for all choices of $\mathbf{x} := (x^i)$. Two such random variables X_1 and X_2 are independent if the events $(X_1 \leq \mathbf{x}_1)$ and $(X_2 \leq \mathbf{x}_2)$ are independent, *i.e.*, $P\big((X_1 \leq \mathbf{x}_1) \cap (X_2 \leq \mathbf{x}_2)\big) = P(X_1 \leq \mathbf{x}_1)P(X_2 \leq \mathbf{x}_2)$, where $P(A)$ denotes the probability of the event $A \subset \Omega$. If we took the X_i to be the coordinates of points in the manifold for some coordinatization then these definitions would apply; as this is artificial and unnecessary we simply take the range of the X_i to be the possible sample points themselves. Then each X_i is distributed independently according to the same probability density function $f_X(\mathbf{x})$ which is uniform in the sense that for any measurable region (event) $A \subset \mathcal{M}$,

$$\int_A f_X(\mathbf{x})\sqrt{-g}\, d\mathbf{x} = \frac{\mathrm{vol}[A]}{\mathrm{vol}[\mathcal{M}]},$$

which implies that $f_X(\mathbf{x}) = 1/\mathrm{vol}[\mathcal{M}]$. Note that this definition would fail for a manifold of infinite volume.

Alternatively, consider the random variables obtained by transforming the X_i by the characteristic function for a region $A \subset \mathcal{M}$:

$$\chi_A(X_i) := \begin{cases} 1 & \text{if } X_i \in A \\ 0 & \text{otherwise.} \end{cases}$$

From these we obtain a collection of random variables

$$N_n(A) := \sum_{i=1}^{n} \chi_A(X_i)$$

which simply count the number of the X_i which fall into each region A; this collection is a generalization of the usual notion of a random function—a collection of

random variables parametrized by a single continuous parameter. Since the manifold has finite volume it is easy to find the probability density function for each (discrete) random variable $N_n(A)$:

$$P\big(N_n(A) = k\big) = \binom{n}{k} \left(\frac{\mathrm{vol}[A]}{\mathrm{vol}[\mathcal{M}]}\right)^k \left(1 - \frac{\mathrm{vol}[A]}{\mathrm{vol}[\mathcal{M}]}\right)^{n-k}.$$

These random variables $N_n(A)$ are *estimators* for the volume of A. In fact, if we compute the expectation value of $N_n(A)$ we obtain

$$\begin{aligned}\langle N_n(A)\rangle &:= \sum_{k=0}^{n} k \binom{n}{k} \left(\frac{\mathrm{vol}[A]}{\mathrm{vol}[\mathcal{M}]}\right)^k \left(1 - \frac{\mathrm{vol}[A]}{\mathrm{vol}[\mathcal{M}]}\right)^{n-k} \\ &= n\frac{\mathrm{vol}[A]}{\mathrm{vol}[\mathcal{M}]},\end{aligned}$$

so $N_n(A)\,\mathrm{vol}[\mathcal{M}]/n$ is an *unbiased* estimator for the volume of A, *i.e.*, it is a random variable whose expectation value is the parameter being estimated.

It is this alternate approach which generalizes to manifolds of infinite volume. Let $\rho := n/\mathrm{vol}[\mathcal{M}]$ and consider the limit $N_\rho(A)$ of $N_n(A)$ as n and $\mathrm{vol}[\mathcal{M}]$ become infinite while ρ stays constant. A familiar computation shows that

$$\lim_{\substack{n,\mathrm{vol}[\mathcal{M}]\to\infty \\ n/\mathrm{vol}[\mathcal{M}]=\rho}} P\big(N_n(A) = k\big) = \frac{\big(\rho\,\mathrm{vol}[A]\big)^k}{k!} e^{-\rho\,\mathrm{vol}[A]},$$

which is the Poisson distribution. Thus in the infinite volume case we should properly speak of a Poisson process with density (intensity) ρ and take the integer random variables $N_\rho(A)$ to be fundamental. From now on we will set the density to one: the points are sprinkled with unit Planck density. Then $N(A) := N_1(A)$ is an unbiased estimator for the volume of A:

$$\begin{aligned}\langle N(A)\rangle &:= \sum_{k=0}^{\infty} k \frac{\big(\mathrm{vol}[A]\big)^k}{k!} e^{-\mathrm{vol}[A]} \\ &= \mathrm{vol}[A].\end{aligned}$$

(In fact, it is also an *efficient*, or minimum variance, estimator.) Thus the desired identification of volume with number is achieved by this model of points distributed uniformly in the manifold.

A natural question to ask at this point is how to determine that a given embedding is faithful. Although in this chapter we are primarily concerned with exactly those causal sets which are obtained by sprinkling points uniformly in a Lorentzian manifold (and which are thus faithfully embedded by definition), when we take a causal set to be fundamental and ask whether a given manifold approximates it *via* a faithful embedding, it is necessary to be able to test whether the distribution of images is uniform. Such a test must, perforce, be statistical. Similar questions arise in diverse contexts: testing random number generators for computers [Knuth 1969], analyzing aggregation in biological systems (*e.g.*, locations of trees in a forest) [Diggle 1983 and references therein], and investigating the distribution of galaxies [Neyman and Scott 1958, Blackman and Tukey 1959, Peebles 1974, 1980, Raine 1981, Hewett, Burbidge and Fang, eds. 1986]. The general procedure is to develop some test statistic which compares a set of observations with that predicted by a uniform distribution.

For example, along the lines of the preceding discussion, we might partition a finite volume manifold M into regions of volume V, count the number of points in each region to obtain a collection of observations $Y_k :=$ the number of regions containing k points for $k = 0, \ldots, n := \mathrm{vol}[M]$, and form the statistic

$$\sum_{k=0}^{n} \frac{(Y_k - np_k/V)^2}{np_k/V},$$

where p_k denotes the probability that a region of volume V contains k points: $\binom{n}{k}(\frac{V}{n})^k(1 - \frac{V}{n})^{n-k}$. This is a chi-square statistic with n degrees of freedom (in practice we would expect the Y_k for $k \gg V$ or $k \ll V$ to be very small and might

therefore choose to group some of the Y_k together—the recommended practice is to make the expected values at least 5—reducing the number of degrees of freedom). For a given set of observations we could check tables of the chi-square distribution to determine the likelihood of its computed value; if this probability were too low we would reject the hypothesis that the distribution was uniform.

Clearly, there are an infinite number of such tests. Each partition of the manifold, for example, gives a different statistic; one might also generalize the Kolmogorov-Smirnov test for continuous random variables [Knuth 1969] in various ways: the standard in biological applications seems to be to compute distributions of distances between points [Diggle 1983] while in observational cosmology the correlation function and its Fourier transform, the power spectrum, are preferred [Blackman and Tukey 1959, Raine 1981]. In fact, even the results we derive later in this chapter on dimension and geometry could be turned into statistical tests of uniformity. The important thing to remember, however, is that no statistical test can *prove* that a distribution is uniform—it can only assign a probability to the observations under the assumption of uniformity; if this probability is small we may conclude that the distribution is unlikely to be uniform, but no more. Thus a precise formulation of the *Hauptvermutung* in this model must be probabilistic.

Minkowski space: uniform distributions

So let us begin by considering causal sets which arise from uniform distributions of points in Minkowski space. These causal sets are quite different from those we saw in Chapter II: Figures III.1 and III.2 show the Hasse diagrams for causal sets of 50, 100 and 200 points distributed uniformly in two dimensional Minkowski space. (Incidentally, note that each is a coarse graining of those succeeding it.) These causal sets were produced by the Pascal program which appears in Appendix A;

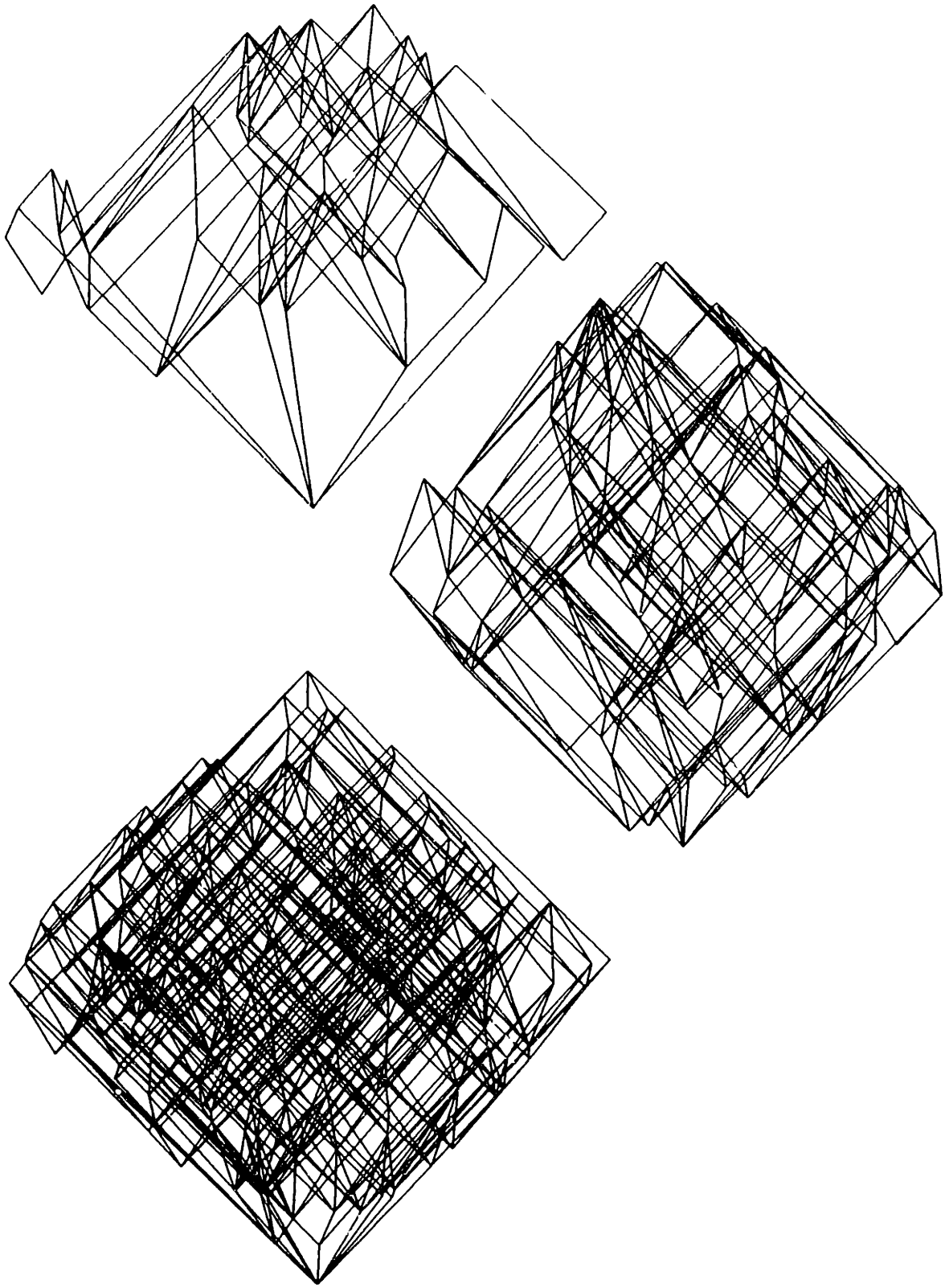

Figure III.1: Hasse diagrams for causal sets with 50, 100 and 200 elements embedded faithfully in two dimensional Minkowski space using the system random number generator.

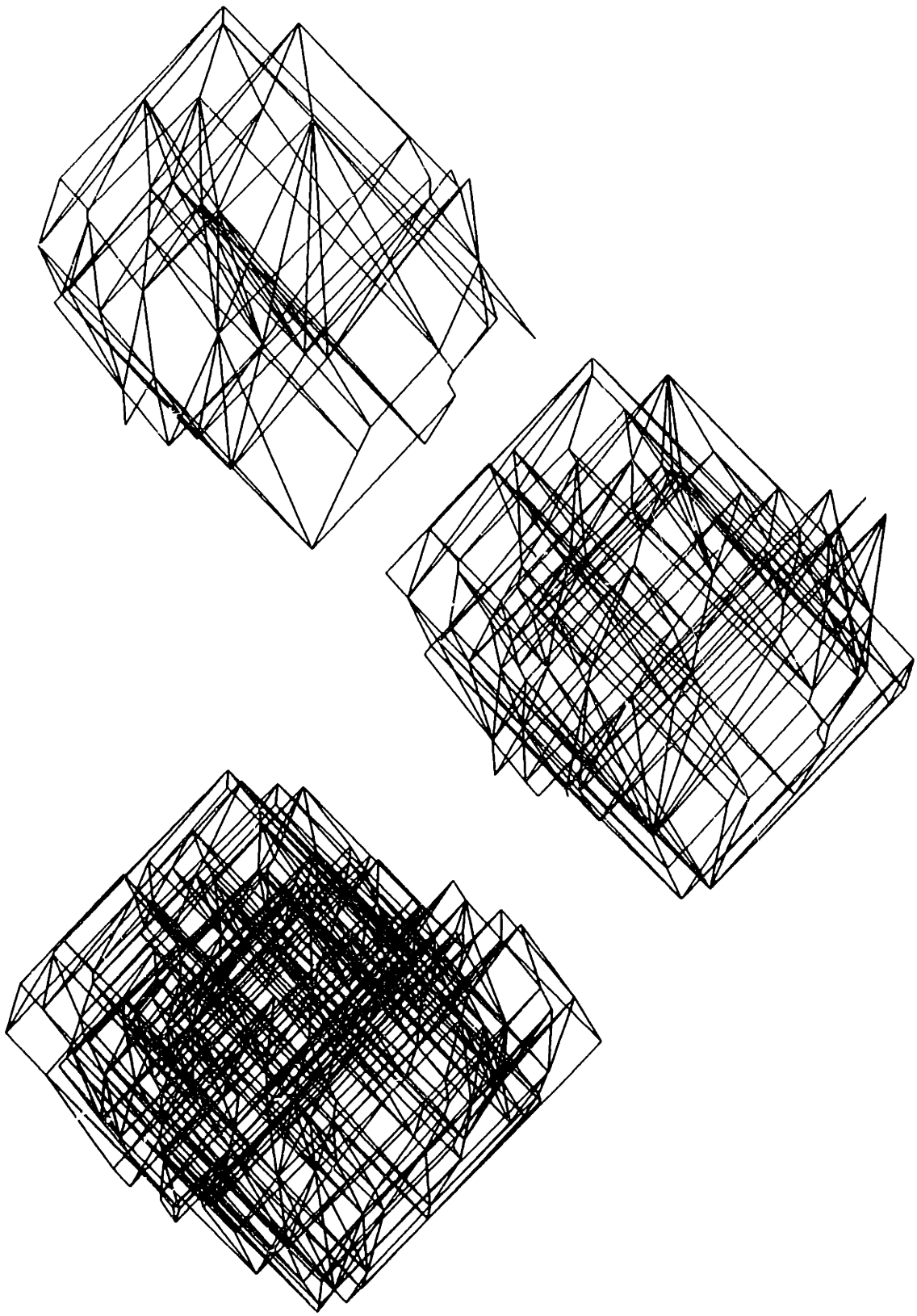

Figure III.2: Hasse diagrams for causal sets with 50, 100 and 200 elements embedded faithfully in two dimensional Minkowski space using procedure *random*.

the points in Figure III.1 were distributed using the computer system supplied random number generator, while those in Figure III.2 were distributed using the procedure *random* listed in the program.

The chi-square test described in the previous section can be applied here to check that these causal sets are faithfully embedded. Of course, in this case it is really a test of the random number generator used to produce the points. But this is worth checking as we perform computer experiments to illustrate the analytic results described later in this chapter and random number generators are notoriously nonrandom [Knuth 1969, Press, Flannery, Teukolsky and Vetterling 1986]. The one used in this program is a slight modification of the one given by Press, *et al.* implementing Knuth's recommendation. To apply the chi-square test the Alexandroff neighborhood was partitioned into B^2 smaller Alexandroff neighborhoods similar to the original (*i.e.*, 'square'). Typical data are contained in Table III.1: this is the case with $N = 50$ points and $B^2 = 25$ regions; recall that $Y_k :=$ the number of regions containing k points.

k	Y_k	expect
0	4	⎤ 10.0
1	6	⎦
2	7	6.9
3	4	⎡
4	3	⎢ 8.1
5	0	⎢
6	1	⎣

Table III.1

Notice that the Y_k have been combined so that each set has an expected value of at least 5. The chi-square statistic computed for this data has two degrees of freedom: $\nu = 2$ and $\chi^2_2 \approx 0.00213$. Thus the results are extremely uniform; in fact, almost

too uniform: $P(\chi^2_2 < 0.00201) \approx 0.01$ and $P(\chi^2_2 < 0.1026) \approx 0.05$ [Abramowitz and Stegun 1964]. For comparison, causal sets were also produced using the system supplied random number generator. The results are shown in Table III.2.

	B^2	ν	program χ^2_ν	system χ^2_ν
$N = 50$	25	2	0.00213*	4.83
	49	2	1.72	1.28
	100	2	0.0146*	3.24
$N = 100$	49	4	4.44	3.86
	100	3	2.84	1.43
	196	2	0.939	0.0137*
$N = 200$	49	5	1.07*	2.45
	100	5	4.66	2.49
	196	3	0.693	0.224*
	400	3	1.56	0.714

Table III.2

None of the χ^2 values lies outside of the 0.01 to 0.99 probability range; those indicated by an asterisk lie outside the 0.05 to 0.95 probability range [Abramowitz and Stegun 1964]. Thus both random number generators seem to be producing uniform distributions (for further verification 20 independent runs were made in the case $N = 200$, $B^2 = 100$; for each generator exactly 10% (*i.e.*, 2) of the resulting χ^2_5 values lay outside the 0.05 to 0.95 probability range); thus we may take the resulting causal sets to be faithfully embedded. For the rest of this chapter we use the portable random number generator in the program of Appendix A.

Minkowski space: dimension

It is natural to continue to consider causal sets arising from uniform distributions of points inside Alexandroff neighborhoods in higher dimensional Minkowski space. As the simplest example of the sort of calculations we will be doing, let us derive

the following well known, but useful, result.

Lemma III.1: In $d+1$ dimensional Minkowski space the volume of an Alexandroff neighborhood A of height T is

$$\text{vol}[A] = \frac{2V_{d-1}}{d+1}\left(\frac{T}{2}\right)^{d+1}$$

where V_{d-1} is the volume bounded by a unit S^{n-1}.

Proof: The volume is given by

$$\text{vol}[A] := \int_A \sqrt{-g}\, d\mathbf{x}.$$

Since we are in Minkowski space, $\sqrt{-g} = 1$; choosing spherical polar coordinates such that the vertices of A lie on the $r = 0$ axis at $t = 0$ and $t = T$, the integral becomes:

$$\begin{aligned}\text{vol}[A] &= 2\int_0^{T/2} dt \int_0^t dr\, A_{d-1} r^{d-1} \\ &= \frac{2V_{d-1}}{d+1}\left(\frac{T}{2}\right)^{d+1}\end{aligned}$$

where A_{d-1} is the area of a unit S^{d-1} and we have also used the fact that $A_{d-1} = dV_{d-1}$. ∎

Thus, if points are distributed according to a Poisson process in a manifold $\mathcal{M} \supset A$ we have

$$\langle N(A)\rangle = \frac{2V_{d-1}}{d+1}\left(\frac{T}{2}\right)^{d+1},$$

so if we knew T we could estimate the dimension of the manifold by counting the points which fall in A and then inverting this formula to find $d+1$. That is, we would determine the exponent of length with which the volume scales. This is a familiar way to measure dimension: The *d-dimensional outer measure* of a set A in some metric space is defined to be [Hurewicz and Wallman 1941, Billingsley 1965]

$$m_d(A) := \lim_{\epsilon \to 0} \inf \sum_i (\text{diam } S_i)^d,$$

where the infimum extends over all countable coverings of A by closed spheres S_i of diameter less than ϵ. It is clear that this limit (although it may be infinite) exists since as the infimum is taken over more restricted coverings its value must increase. Now consider how this measure of A changes with the exponent d: if $m_d(A)$ is finite there is an ϵ–covering $\{s_i\}$ for which

$$\sum(\text{diam } s_i)^d \leq \inf \sum(\text{diam } S_i)^d + 1 \leq m_d(A) + 1$$

so for $d' > d$

$$\inf \sum(\text{diam } S_i)^{d'} \leq \sum(\text{diam } s_i)^{d'} \leq \epsilon^{d'-d} \sum(\text{diam } s_i)^d \leq \epsilon^{d'-d}(m_d(A) + 1)$$

which goes to 0 as $\epsilon \to 0$. Thus if $m_d(A)$ is finite, $m_{d'}(A)$ vanishes for all $d' > d$. But at $d = 0$ the limit is infinite so there must be a critical point—an exponent d at which the measure changes from ∞ to 0. This exponent, which need not be an integer, is the *Hausdorff dimension* of the set A:

$$\text{Hdim } A := \sup\{d : m_d(A) = \infty\} = \inf\{d : m_d(A) = 0\}.$$

In his original paper [Hausdorff 1919] showed that the dimension of the Cantor set was $\log 2/\log 3$; Besicovitch was responsible for many subsequent developments, particularly those related to sets of points in the plane (see, for example [Besicovitch 1934, 1935, Besicovitch and Ursell 1937, Besicovitch and Taylor 1954]; most recently [Mandelbrot 1983] has applied these ideas in the context of fractals.

It is with this definition in mind that we choose to call the dimension estimated by solving the volume-height relation for the exponent $d+1$ the Hausdorff dimension of a causal set (strictly, in the way we apply it, of an interval of a causal set). But to do this we need to measure the height T of the Alexandroff neighborhood. The lengths of (longest) chains in the causal set whose points lie in A are the most

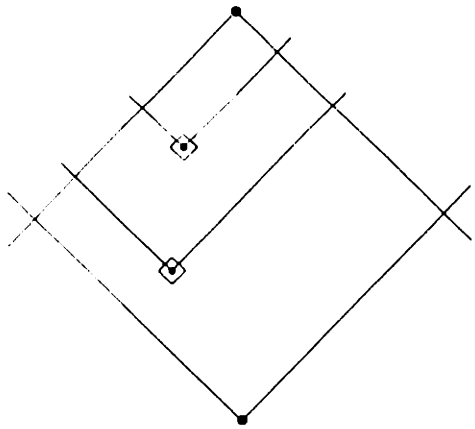

Figure III.3

obvious measure of the height of A, so consider a chain consisting of k points. For any k differential volume elements $d\mathbf{x}_1, \ldots, d\mathbf{x}_k$ satisfying $d\mathbf{x}_j \subset J^+(d\mathbf{x}_i)$ for $i < j$, as shown in Figure III.3, we may define a random variable

$$\chi_{[d\mathbf{x}_1,\ldots,d\mathbf{x}_k]} := \begin{cases} 1 & \text{if } \exists! \text{ chain with points in } d\mathbf{x}_1, \ldots, d\mathbf{x}_k \\ 0 & \text{otherwise.} \end{cases}$$

Then

$$\begin{aligned} P(\chi_{[d\mathbf{x}_1,\ldots,d\mathbf{x}_k]} = 1) &= P(\exists! \text{ point in } d\mathbf{x}_1) \ldots P(\exists! \text{ point in } d\mathbf{x}_k) \\ &= d\mathbf{x}_1 e^{-d\mathbf{x}_1} \ldots d\mathbf{x}_k e^{-d\mathbf{x}_k} \\ &= d\mathbf{x}_1 \ldots d\mathbf{x}_k + \text{ higher order terms} \end{aligned}$$

(abusing notation slightly) since the points are independently distributed according to the Poisson process. Now, let C_k be the random variable counting the number of chains of length $k-1$:

$$C_k := \sum_{d\mathbf{x}_1,\ldots,d\mathbf{x}_k} \chi_{[d\mathbf{x}_1,\ldots,d\mathbf{x}_k]}.$$

Because the χs are not independent it is difficult to write down the probability density function for C_k; however, their expectation values still add, so

$$\begin{aligned} \langle C_k \rangle &= \sum_{d\mathbf{x}_1,\ldots,d\mathbf{x}_k} \langle \chi_{[d\mathbf{x}_1,\ldots,d\mathbf{x}_k]} \rangle \\ &= \sum_{d\mathbf{x}_1,\ldots,d\mathbf{x}_k} P(\chi_{[d\mathbf{x}_1,\ldots,d\mathbf{x}_k]} = 1) \\ &= \int_A d\mathbf{x}_1 \int_{J^+(\mathbf{x}_1)} d\mathbf{x}_2 \ldots \int_{J^+(\mathbf{x}_{k-1})} d\mathbf{x}_k \end{aligned}$$

since $\langle \chi_{[dx_1,\ldots,dx_k]} \rangle = P(\chi_{[dx_1,\ldots,dx_k]} = 1) = dx_1 \ldots dx_k$. (We have written $J^+(x_i)$ to mean $J^+(x_i) \cap A$.)

Theorem III.2: Letting $\omega = (d+1)/2$ we have

$$\langle C_k \rangle = \frac{(\mathrm{vol}[A])^k}{k} \left(\frac{\Gamma(d+2)}{2} \right)^{k-1} \frac{\Gamma(\omega)\Gamma(2\omega)}{\Gamma(k\omega)\Gamma\big((k+1)\omega\big)}.$$

Proof: By induction. We have already proved the result for $k = 1$ in the preceding lemma. For $k = l + 1$,

$$\langle C_{l+1} \rangle = \int_A dx_1 \int_{J^+(x_1)} dx_2 \ldots \int_{J^+(x_l)} dx_{l+1}.$$

Since $J^+(x_1) \cap A$ is an Alexandroff neighborhood itself, the induction hypothesis gives

$$\langle C_{l+1} \rangle = \int_A dx_1 \frac{(\mathrm{vol}[J^+(x_1)])^l}{l} \left(\frac{\Gamma(d+2)}{2} \right)^{l-1} \frac{\Gamma(\omega)\Gamma(2\omega)}{\Gamma(l\omega)\Gamma\big((l+1)\omega\big)}.$$

Using the same coordinate system as in the proof of the lemma, if x_1 has coordinates (t, r, Ω) then the height of $J^+(x_1)$ is $\sqrt{(T-t)^2 - r^2}$, so

$$\begin{aligned} \mathrm{vol}[J^+(x_1)] &= \frac{2V_{d-1}}{(d+1)2^{d+1}} \left[(T-t)^2 - r^2\right]^\omega \\ &= \frac{2V_{d-1}}{(d+1)2^{d+1}} \left[(T-v)(T-u)\right]^\omega, \end{aligned}$$

where $u := t - r$ and $v := t + r$ are lightcone coordinates. Thus

$$\int_A dx_1 \left(\mathrm{vol}[J^+(x_1)]\right)^l = \left(\frac{2V_{d-1}}{(d+1)2^{d+1}} \right)^l \frac{A_{d-1}}{2} \times \\ \times \int_0^T dv \int_0^v du \left[(T-u)(T-v)\right]^{l\omega} r^{d-1}.$$

Replacing r by $\left[(T-u) - (T-v)\right]/2$ and using the binomial expansion gives

$$\int_A dx_1 \left(\mathrm{vol}[J^+(x_1)]\right)^l = \left(\frac{2V_{d-1}}{(d+1)2^{d+1}} \right)^l \frac{A_{d-1}}{2^d} \sum_{j=0}^{d-1} (-1)^{d-j-1} \binom{d-1}{j} \times$$

$$\times \int_0^T dv(T-v)^{l\omega+d-j-1} \int_0^v du(T-u)^{l\omega+j}$$

$$= \left(\frac{2V_{d-1}}{(d+1)2^{d+1}}\right)^l \frac{A_{d-1}}{2^d} \frac{T^{(l+1)(d+1)}}{(l+1)(d+1)} \times$$

$$\times \sum_{j=0}^{d-1} (-1)^{d-j-1} \binom{d-1}{j} \frac{1}{l\omega+d-j}$$

$$= \frac{d\,(\mathrm{vol}[A])^{l+1}}{l+1} \frac{(-1)^{d-1}}{l\omega+d} \sum_{j=0}^{d-1} (-1)^j \binom{d-1}{j} \frac{-(l\omega+d)}{-(l\omega+d)+j}$$

where we have multiplied and divided by $l\omega + d$ in order to apply Vandermonde's Theorem in the form (see, *e.g.*, [Knuth 1973a]):

$$\sum_k (-1)^k \frac{a}{a+k} \binom{n}{k} = \binom{a+n}{n}^{-1}.$$

Doing so, then applying the identity

$$(-1)^{d-1} \binom{-l\omega-1}{d-1} = \binom{l\omega+d-1}{d-1}$$

and writing the binomial coefficients in terms of gamma functions gives

$$\int_A d\mathbf{x}_1 \left(\mathrm{vol}[J^+(x_1)]\right)^l = \frac{l\,(\mathrm{vol}[A])^{l+1}}{l+1} \frac{\Gamma(d+2)}{2} \frac{\Gamma(l\omega)}{\Gamma\big((l+2)\omega\big)}.$$

Plugging this back into the expression for $\langle C_{l+1} \rangle$ produces

$$\langle C_{l+1} \rangle = \frac{(\mathrm{vol}[A])^{l+1}}{l+1} \left(\frac{\Gamma(d+2)}{2}\right)^l \frac{\Gamma(\omega)\Gamma(2\omega)}{\Gamma\big((l+1)\omega\big)\Gamma\big((l+2)\omega\big)}$$

as desired. ∎

It may seem surprising that the expression for $\langle C_k \rangle$ does not depend on the height of the Alexandroff neighborhood explicitly, but only in the precise combination that appears in the volume. Of course, since k volume integrals were performed in the derivation, it is clear whence the volume dependence arises. (The apparent discrepancy between the pure number $\langle C_k \rangle$ and the $[L]^{k(d+1)}$ units on the right

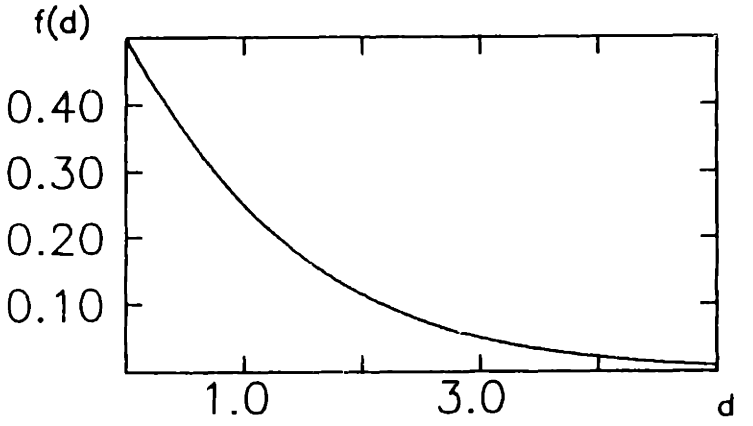

Figure III.4

hand side of the expression is resolved by recalling that $\rho \equiv 1$.) In fact, since the volume, height and dimension are related by the result of Lemma III.1, even had the height appeared we could have replaced it by its expression in terms of the other two parameters.

Even without a random variable with explicit T dependence we may now approximate the dimension of the Minkowski space. (Since a dependence on T is there implicitly, and also motivated our choice of random variable—the numbers of chains of given length, we will continue to refer to this as a Hausdorff dimension.) The simplest way to use the result of the theorem is to specialize to $k = 2$, in which case C_k is simply the number of relations among the elements of the causal set whose images lie in A:

$$\langle \text{relations} \rangle = (\text{vol}[A]) \, {}_2\frac{\Gamma(d+2)\Gamma(\omega)}{4\Gamma(3\omega)}.$$

The coefficient multiplying $(\text{vol}[A])^2$ depends only on the dimension; we denote it by $f(d)$ and graph this function in Figure III.4 ($f(d)$ is half the 'ordering fraction' of [Myrheim 1978]). Since $\langle N(A) \rangle = \text{vol}[A]$, given a causal set embedded in an Alexandroff neighborhood (*i.e.*, any interval of a causal set) we may count the number of elements to approximate the volume, count the number of relations to approximate the right hand side of this relation, plug them in and invert $f(d)$ to

obtain an approximation for the dimension of the Minkowski space in which the causal set can be faithfully embedded.

To check how good an approximation this procedure gives we must calculate the variance of the measured quantity, namely $C_2/(\mathrm{vol}[A])^2$. Recall that $\mathrm{Var}(C_2) := \langle C_2^2 \rangle - \langle C_2 \rangle^2$. The second term is just the square of the result already found; to evaluate the first term we use the definition of C_2 in terms of the χs:

$$\begin{aligned}
\langle C_2^2 \rangle &= \Big\langle \Big(\sum_{d\mathbf{x}_i, d\mathbf{x}_j} \chi_{[d\mathbf{x}_i, d\mathbf{x}_j]} \Big)^2 \Big\rangle \\
&= \Big\langle \sum_{\substack{d\mathbf{x}_i, d\mathbf{x}_j \\ d\mathbf{x}_k, d\mathbf{x}_l}} \chi_{[d\mathbf{x}_i, d\mathbf{x}_j]} \chi_{[d\mathbf{x}_k, d\mathbf{x}_l]} \Big\rangle \\
&= \sum_{\substack{d\mathbf{x}_i, d\mathbf{x}_j \\ d\mathbf{x}_k, d\mathbf{x}_l}} \langle \chi_{[d\mathbf{x}_i, d\mathbf{x}_j]} \chi_{[d\mathbf{x}_k, d\mathbf{x}_l]} \rangle \\
&= \sum_{\substack{d\mathbf{x}_i, d\mathbf{x}_j \\ d\mathbf{x}_k, d\mathbf{x}_l}} P(\chi_{[d\mathbf{x}_i, d\mathbf{x}_j]} = 1 \text{ and } \chi_{[d\mathbf{x}_k, d\mathbf{x}_l]} = 1).
\end{aligned}$$

Now, the χs are not independent, but the probabilities of points lying in the $d$xs are, so the sum splits into four disjoint sums, over sets with:

- no coincidences: $d\mathbf{x}_i, d\mathbf{x}_j, d\mathbf{x}_k, d\mathbf{x}_l$ all distinct,
- one coincidence, but no 3-chain: $d\mathbf{x}_i = d\mathbf{x}_k$ only or $d\mathbf{x}_j = d\mathbf{x}_l$ only,
- one coincidence, forming a 3-chain: $d\mathbf{x}_j = d\mathbf{x}_k$ only or $d\mathbf{x}_i = d\mathbf{x}_l$ only,
- two coincidences: $d\mathbf{x}_i = d\mathbf{x}_k$ and $d\mathbf{x}_j = d\mathbf{x}_l$.

Thus the integral expression for $\langle C_2^2 \rangle$ becomes

$$\begin{aligned}
\langle C_2^2 \rangle = \int_A d\mathbf{x} \int_{J^+(\mathbf{x})} d\mathbf{x}' \int_{\substack{A \\ \mathbf{y} \neq \mathbf{x}, \mathbf{x}'}} d\mathbf{y} \int_{\substack{J^+(\mathbf{y}) \\ \mathbf{y}' \neq \mathbf{x}, \mathbf{x}'}} d\mathbf{y}' + 2 \int_A d\mathbf{x} \int_{J^+(\mathbf{x})} d\mathbf{x}' \int_{\substack{J^+(\mathbf{x}) \\ \mathbf{y}' \neq \mathbf{x}'}} d\mathbf{y}' \\
+ 2 \int_A d\mathbf{x} \int_{J^+(\mathbf{x})} d\mathbf{x}' \int_{J^+(\mathbf{x}')} d\mathbf{y}' + \int_A d\mathbf{x} \int_{J^+(\mathbf{x})} d\mathbf{x}'.
\end{aligned}$$

The last two terms are immediately recognizable as $2\langle C_3 \rangle$ and $\langle C_2 \rangle$, respectively; the first term is just $\langle C_2 \rangle^2$ since the forbidden coincidences have measure zero; only

the second term is unfamiliar. But it is easily computed using the intermediate results in the proof of Theorem III.2:

$$2\int_A d\mathbf{x}\int_{J^+(\mathbf{x})} d\mathbf{x}'\int_{\substack{J^+(\mathbf{x})\\ \mathbf{y}'\neq\mathbf{x}'}} d\mathbf{y}' = 2\int_A d\mathbf{x}\,(\mathrm{vol}[J^+(\mathbf{x})])^2$$
$$= \langle C_3\rangle \frac{8\Gamma(3\omega)}{\Gamma(d+2)\Gamma(\omega)}.$$

Plugging in these results we find

$$\mathrm{Var}(C_2) = 2\langle C_3\rangle\left[\frac{4\Gamma(3\omega)}{\Gamma(d+2)\Gamma(\omega)}+1\right]+\langle C_2\rangle.$$

Thus the variance of the measured quantity $C_2/(\mathrm{vol}[A])^2$ goes as $(\mathrm{vol}[A])^{-1}$ (from $(\mathrm{vol}[A])^{-4}\left[(\mathrm{vol}[A])^3+(\mathrm{vol}[A])^2\right]$ or more precisely, from $\Delta(C_2/N^2)\approx\Delta C_2/N^2 - 2C_2\Delta N/N^3 \sim \left((\mathrm{vol}[A])^3+(\mathrm{vol}[A])^2\right)^{1/2}(\mathrm{vol}[A])^{-2}-2(\mathrm{vol}[A])^2(\mathrm{vol}[A])^{1/2}(\mathrm{vol}[A])^{-3}$ $\sim (\mathrm{vol}[A])^{-1/2}$). So for large volumes, *i.e.*, for large $N(A)$, the approximation to the dimension obtained this way should be very good. Note that this result is not peculiar to C_2; it is clear that in the corresponding calculation for C_k one also finds that the variance of $C_k/(\mathrm{vol}[A])^k$ goes as $(\mathrm{vol}[A])^{-1}$.

Flat space: numerical results

Let us apply this procedure, then, to causal sets obtained by sprinkling points in Minkowski space and verify that it reproduces the dimension of the manifold. Specifically, we sprinkle points uniformly in an Alexandroff neighborhood of Minkowski space, compute the relations among them, extract the resulting causal set and then using only the information in the causal set compute a Hausdorff dimension: For each interval $[x,y]$ in the causal set we count the number of elements z such that $z\in[x,y]$ and $z\neq x,y$; this is $N([x,y])$. We also count the number of relations among these elements; this is $C_2([x,y])$. Finally we determine the value of d such that

$$f(d) = \frac{C_2([x,y])}{(N([x,y]))^2};$$

this is the Hausdorff dimension of the interval $|x, y|$.

This algorithm is implemented by the Pascal program listed in Appendix B. Let us first apply it to the 200 element causal set shown in Figure III.2. This causal set has a total of 10385 relations, leading to a value of $d \approx 0.95$ if we use the information that it embeds faithfully in an Alexandroff neighborhood. Figure III.5 contains the results interval by interval: for each a dot is plotted with horizontal coordinate $N(|x, y|)$ and vertical coordinate the Hausdorff dimension. There is a wide variation in the Hausdorff dimension of the smaller neighborhoods, but, as expected, the variance decreases rapidly with increasing volume. To illustrate this further Figure III.6 shows the results from a causal set with 500 elements, still in an Alexandroff neighborhood of two dimensional Minkowski space: the spatial Hausdorff dimension is clearly converging to one. (In this graph and all those following, rather than plotting a dot for each interval, for each volume a vertical line centered at the average Hausdorff dimension and extending one standard deviation above and below is plotted; approximately 68% of the intervals fall into this range.)

Moving to higher dimensions, Figures III.7 and III.8 show the results for 500 points sprinkled uniformly in Alexandroff neighborhoods in $2 + 1$ and $3 + 1$ dimensional Minkowski space. These causal sets display qualitatively the same behavior as did the two dimensional examples, but the accuracy of the approximated dimension is decreasing with increasing dimension. This is due to the fact that $f(d)$ decreases rapidly so that there are fewer large intervals with which to make accurate estimates in higher dimensions. Figures III.9 and III.10 are the same two cases, but with 1000 element causal sets instead. It is clear that again the Hausdorff dimension is converging to the correct value as the volume of the intervals increases and, moreover, that increasing the number of elements has increased the number of large volume intervals.

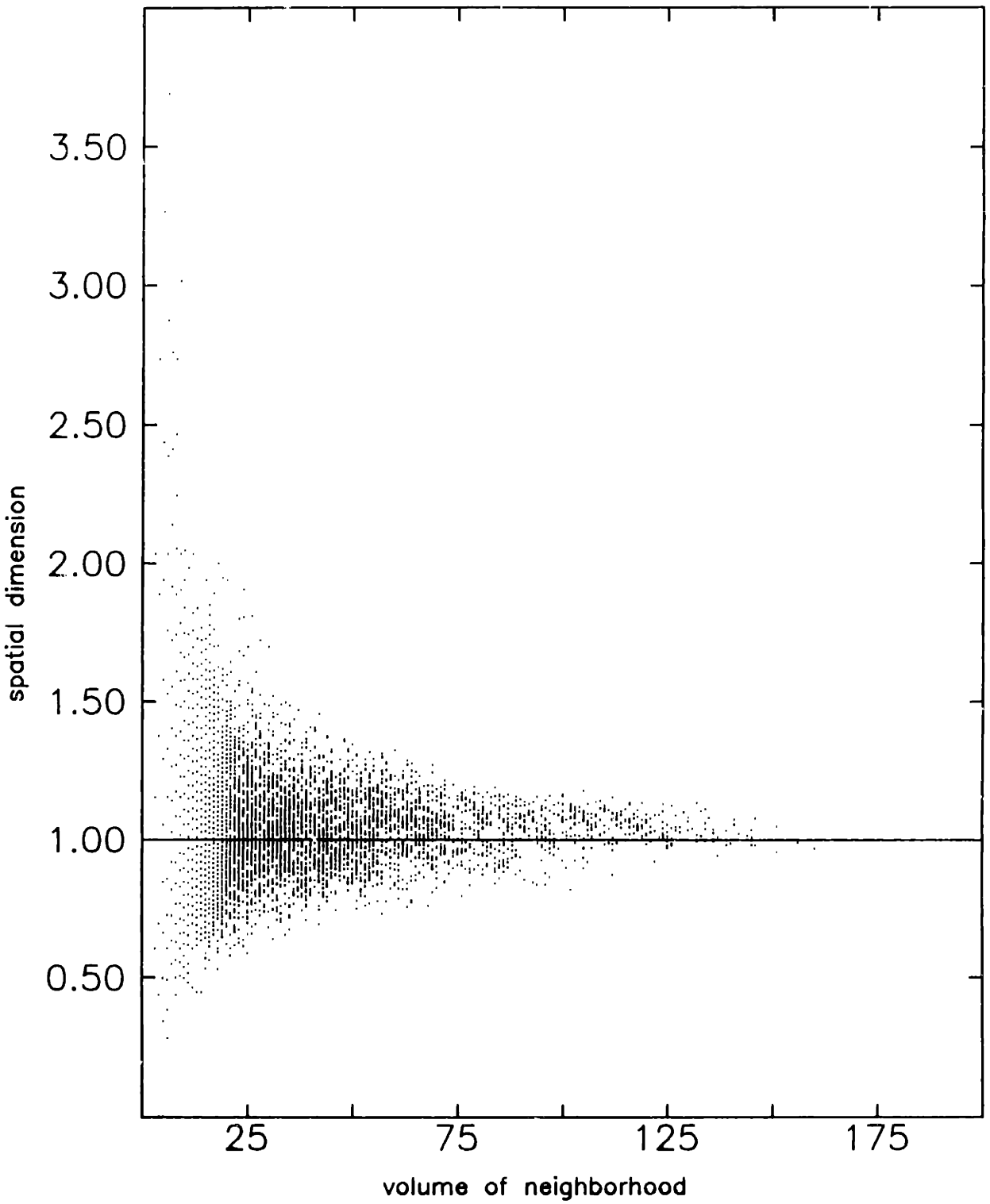

Figure III.5: The spatial Hausdorff dimension of each interval in the 200 element causal set of Figure III.2 is plotted against its volume. Note the large variation at small volumes and the convergence to dimension 1 as the volume of the interval increases.

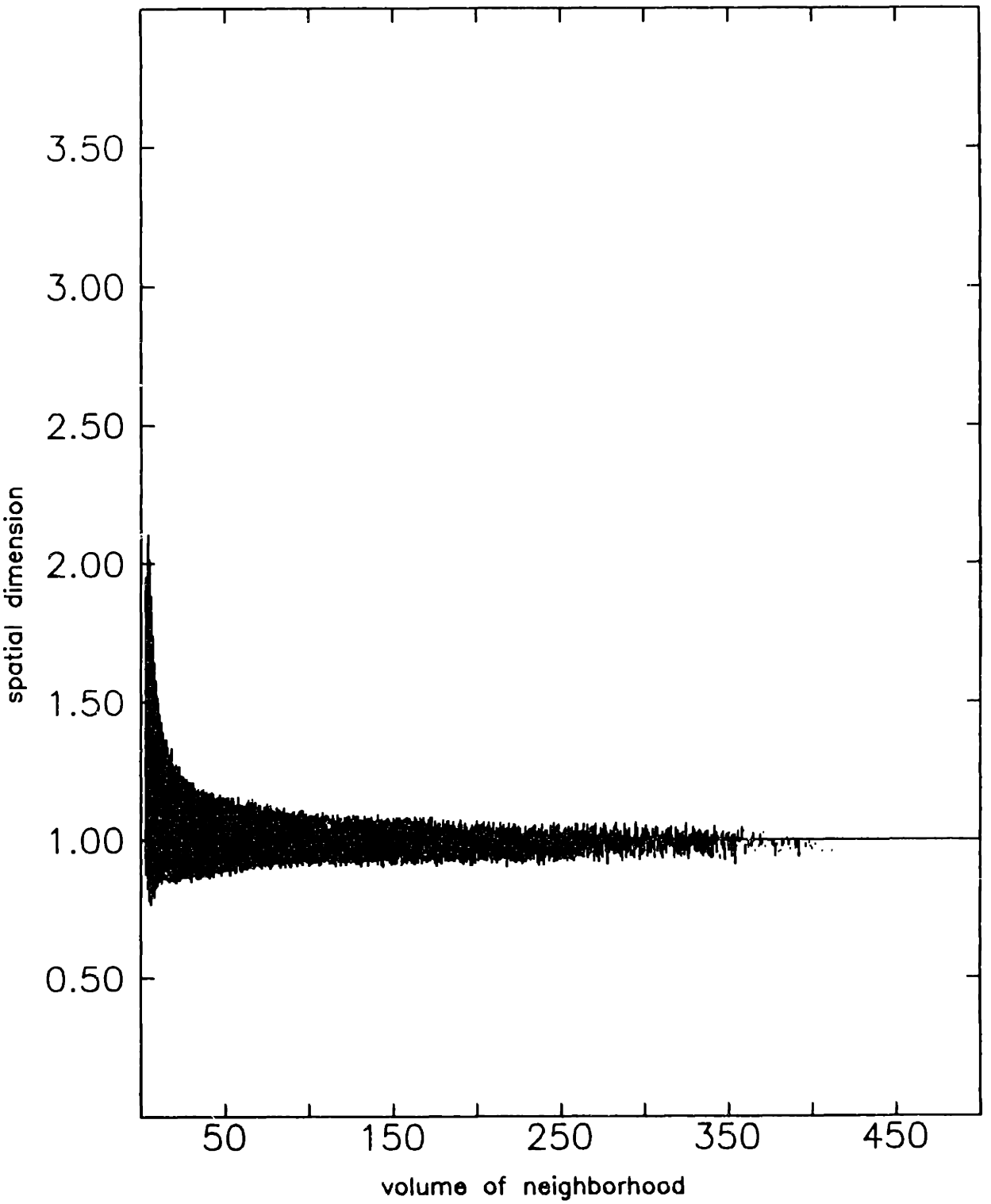

Figure III.6: The spatial Hausdorff dimension is plotted as a function of volume for a 500 element causal set in $1 + 1$ dimensional Minkowski space. The results for all intervals of each volume are averaged and plotted with error bars of one standard deviation above and below. We see that the estimated dimension continues to improve as the volume increases.

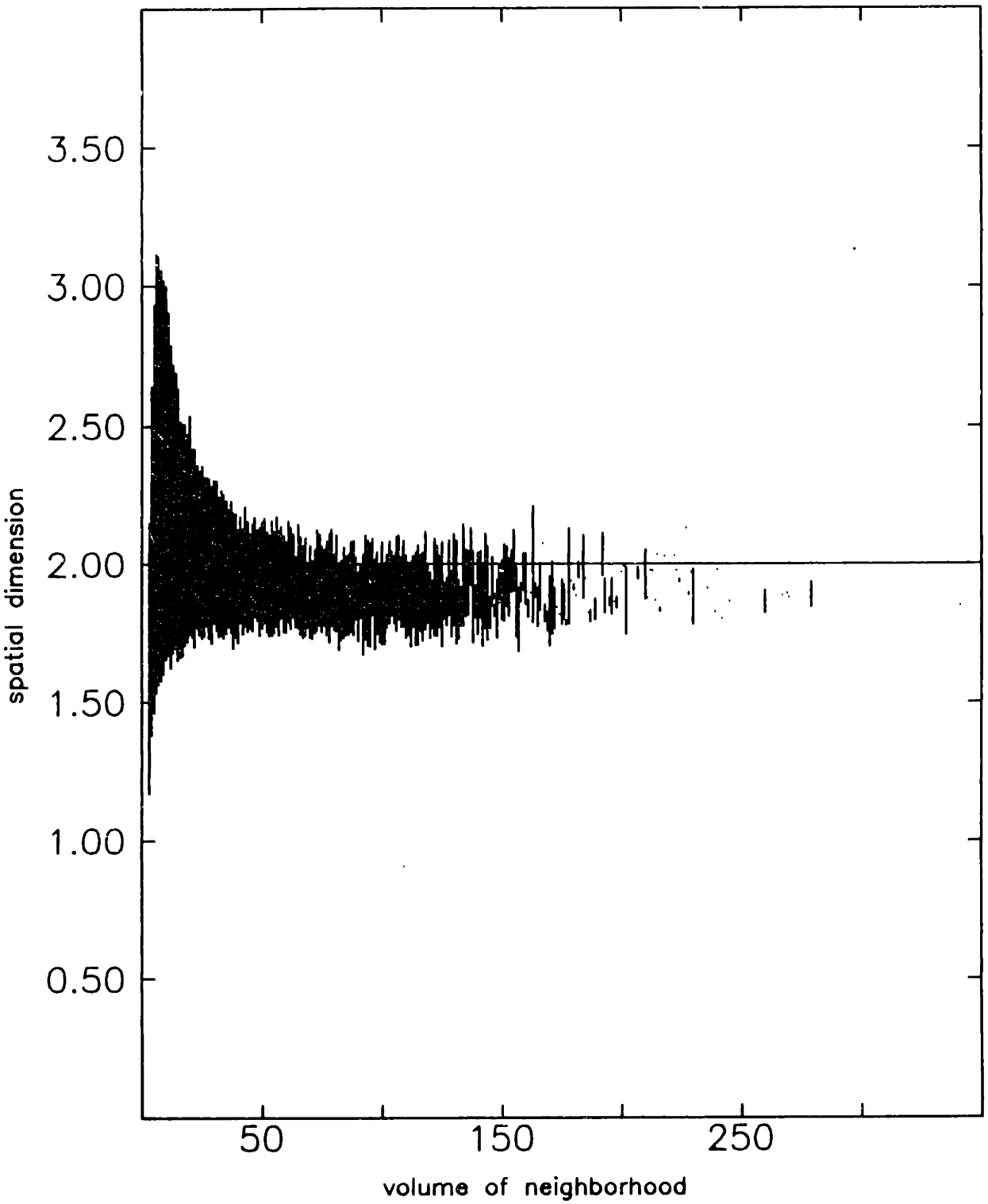

Figure III.7: The spatial Hausdorff dimension is plotted as a function of volume for a 500 element causal set in $2 + 1$ dimensional Minkowski space. Although the results are converging correctly as the volume increases, they are not as good as in Figure III.6.

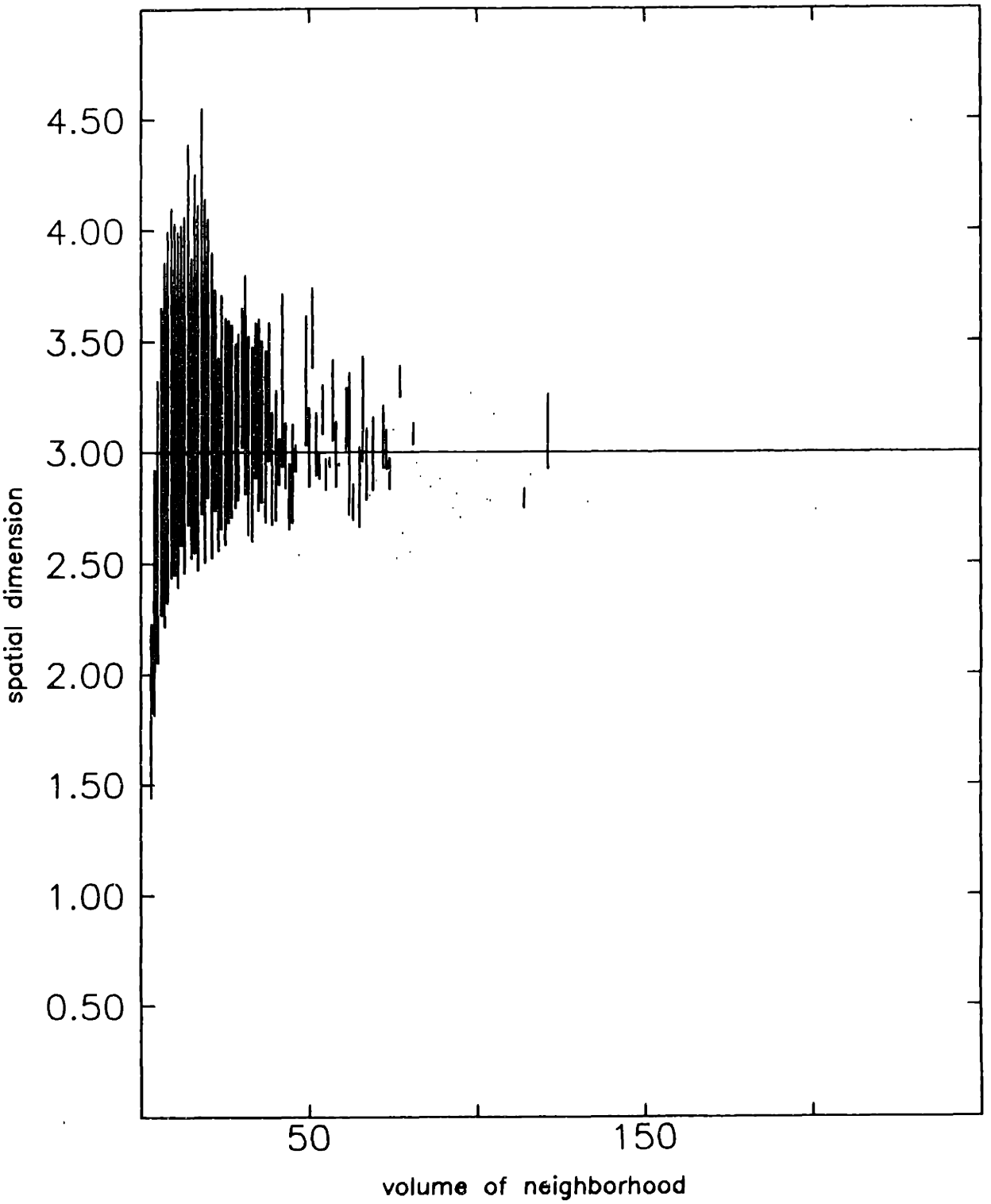

Figure III.8: The spatial Hausdorff dimension is plotted as a function of volume for a 500 element causal set in $3 + 1$ dimensional Minkowski space. Again the results have deteriorated; there are simply not enough large intervals to produce good estimates.

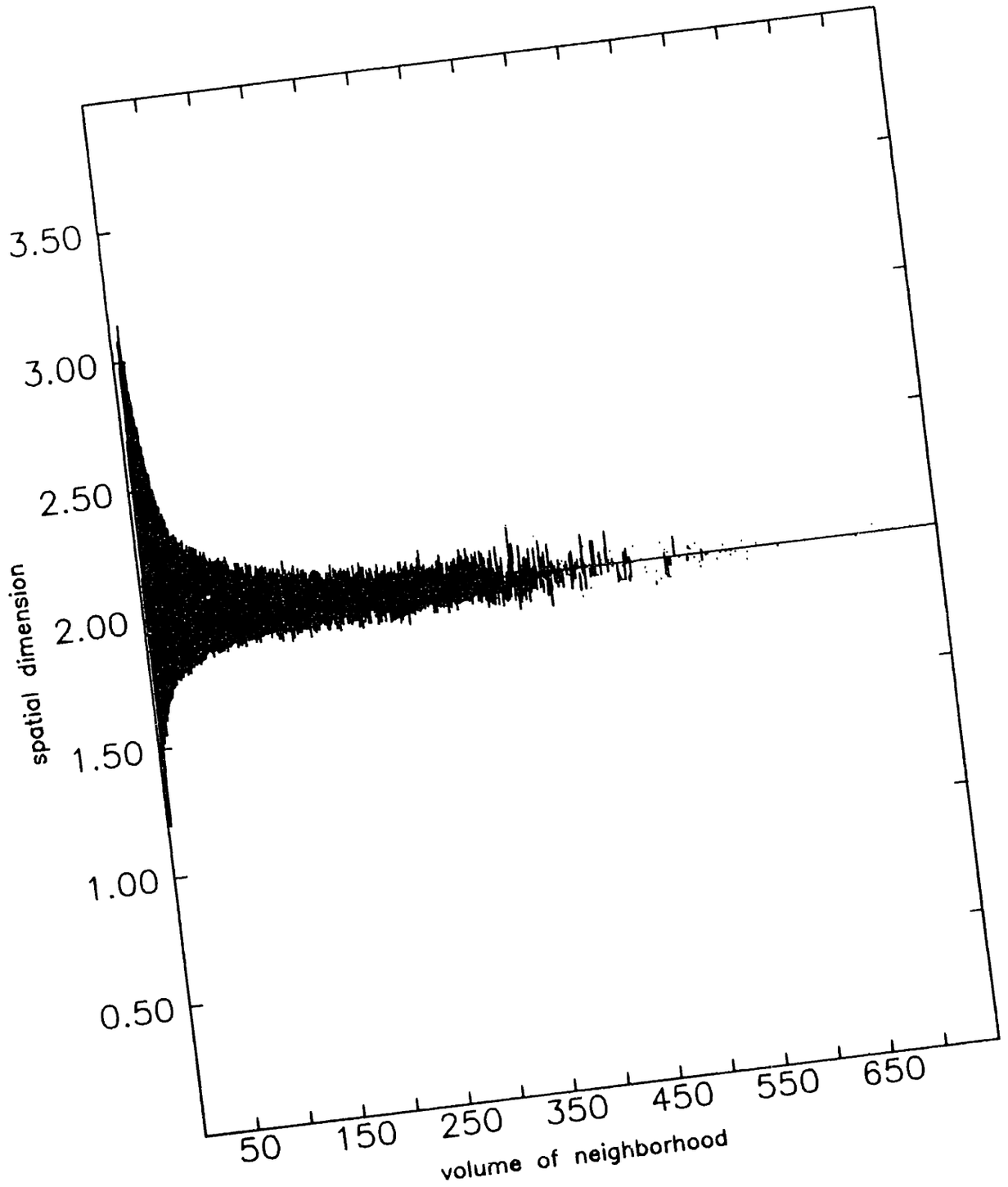

Figure III.9: The spatial Hausdorff dimension is plotted as a function of volume for a 1000 element causal set in $2+1$ dimensional Minkowski space. Increasing the size of the causai set has improved the convergence of the results, as expected. Compare with Figure III.7.

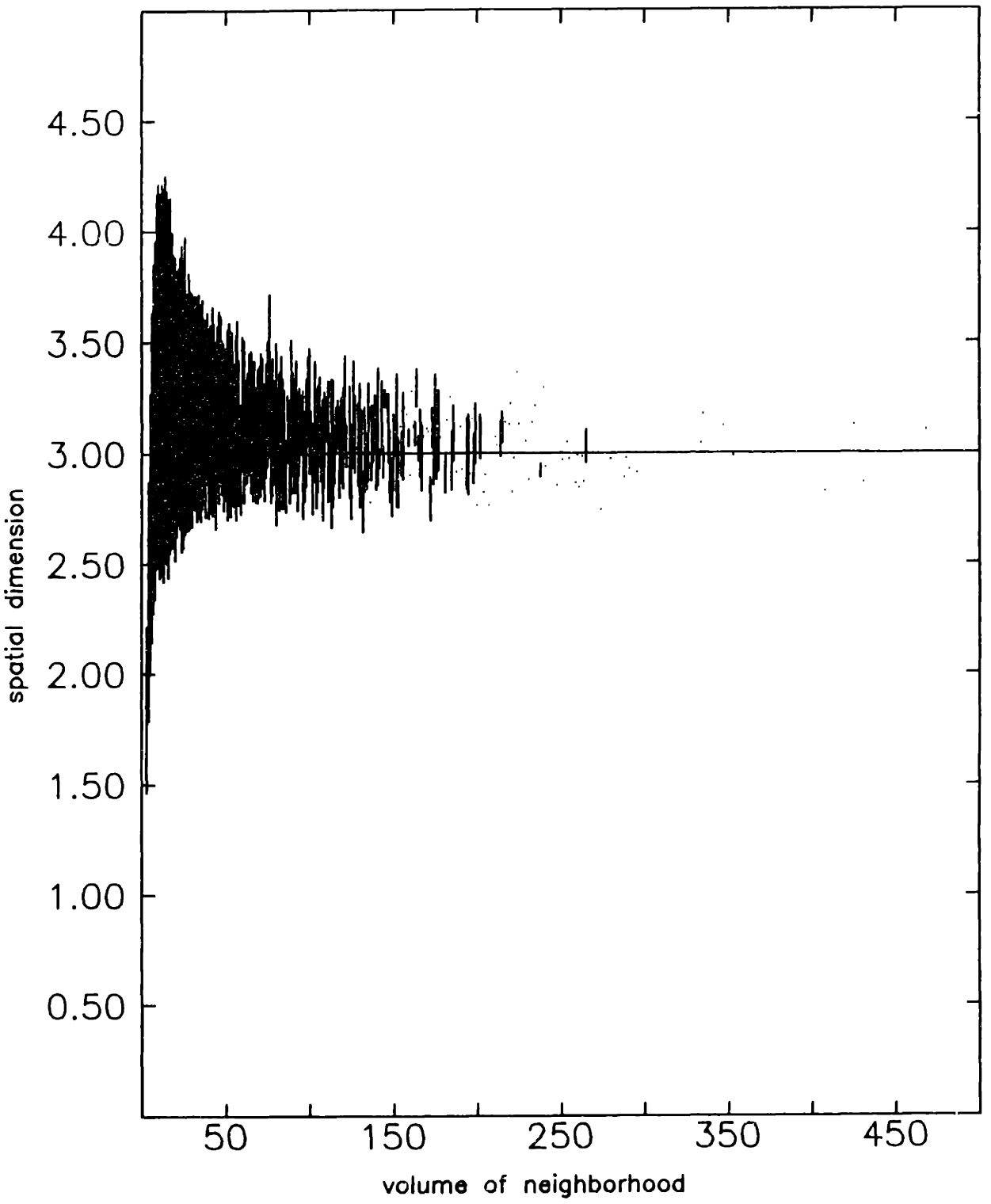

Figure III.10: The spatial Hausdorff dimension is plotted as a function of volume for a 1000 element causal set in $3 + 1$ dimensional Minkowski space. Again the results have improved over the smaller causal set of Figure III.8, but are not as good as the results for the same size causal set in lower dimensions.

It is easy to apply this procedure to another class of flat spacetimes: Kaluza-Klein type spacetimes obtained by making periodic identifications in spatial directions in Minkowski space. For example, consider the cylindrical spacetime formed by taking the strip $0 \leq x \leq c$, $0 \leq t \leq T$ from two dimensional Minkowski space and indentifying the timelike edges. Small Alexandroff neighborhoods, *i.e.*, those with height no more than c, in this manifold are identical to those in Minkowski space. Larger neighborhoods, however, wrap around the cylinder and are no longer simply connected, although they are still flat. Thus we expect that at small scales the manifold should appear to be a two dimensional Minkowski space; at intermediate scales the cylindrical character should be identifiable; and at large scales, $T \gg c$, the manifold should appear to have only one, timelike, dimension.

The Pascal program listed in Appendix B implements the Hausdorff dimension algorithm for this case also (the parameter *compact* is the number of spatial dimensions to be periodically identified). Figure III.11 shows the results for sprinkling 1000 points in a cylinder with circumference $c = 1$ and height $T = 10$ (not in Planck units!). The approximated dimension clearly decreases as the volume of the intervals increases. Figure III.12 is a closeup of the small intervals: the dimensions of the intervals with volumes no more than 50 (= 1000/20, the volume of a maximal simply connected Alexandroff neighborhood) are indistinguishable from the results for two dimensional Minkowski space (see Figure III.6); after 50 the dimensions begin to decrease. Thus we have an effective coarse-graining of the manifold: at small scales the Hausdorff dimension is two, while at large scales the Hausdorff dimension decreases and the internal dimension is seen less and less clearly. This is a slightly different sort of coarse graining than discussed in the Introduction; here the small scale structure is being washed out at the larger scale while sprinkling fewer points would have the same effect by simply missing the small scale.

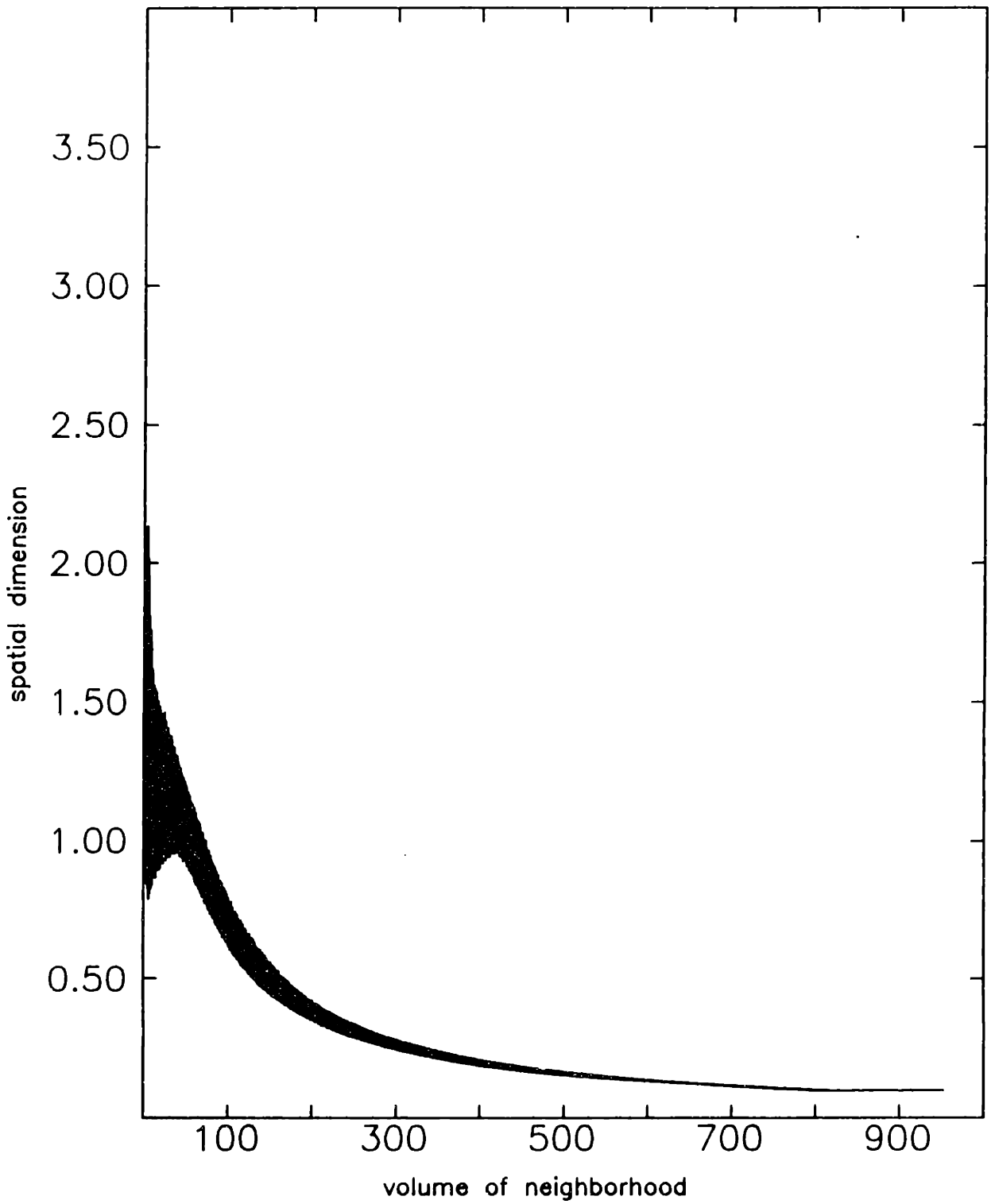

Figure III.11: The spatial Hausdorff dimension is plotted as a function of volume for a 1000 element causal set in a cylinder with height/circumference = 10 of a flat $1 + 1$ dimensional Kaluza-Klein spacetime. Small neighborhoods are isometric to neighborhoods of $1 + 1$ dimensional Minkowski space so they have spatial Hausdorff dimensions near 1. Larger neighborhoods see the cylinder as more and more like a $0 + 1$ dimensional flat spacetime so as the volume increases the spatial Hausdorff dimension decreases.

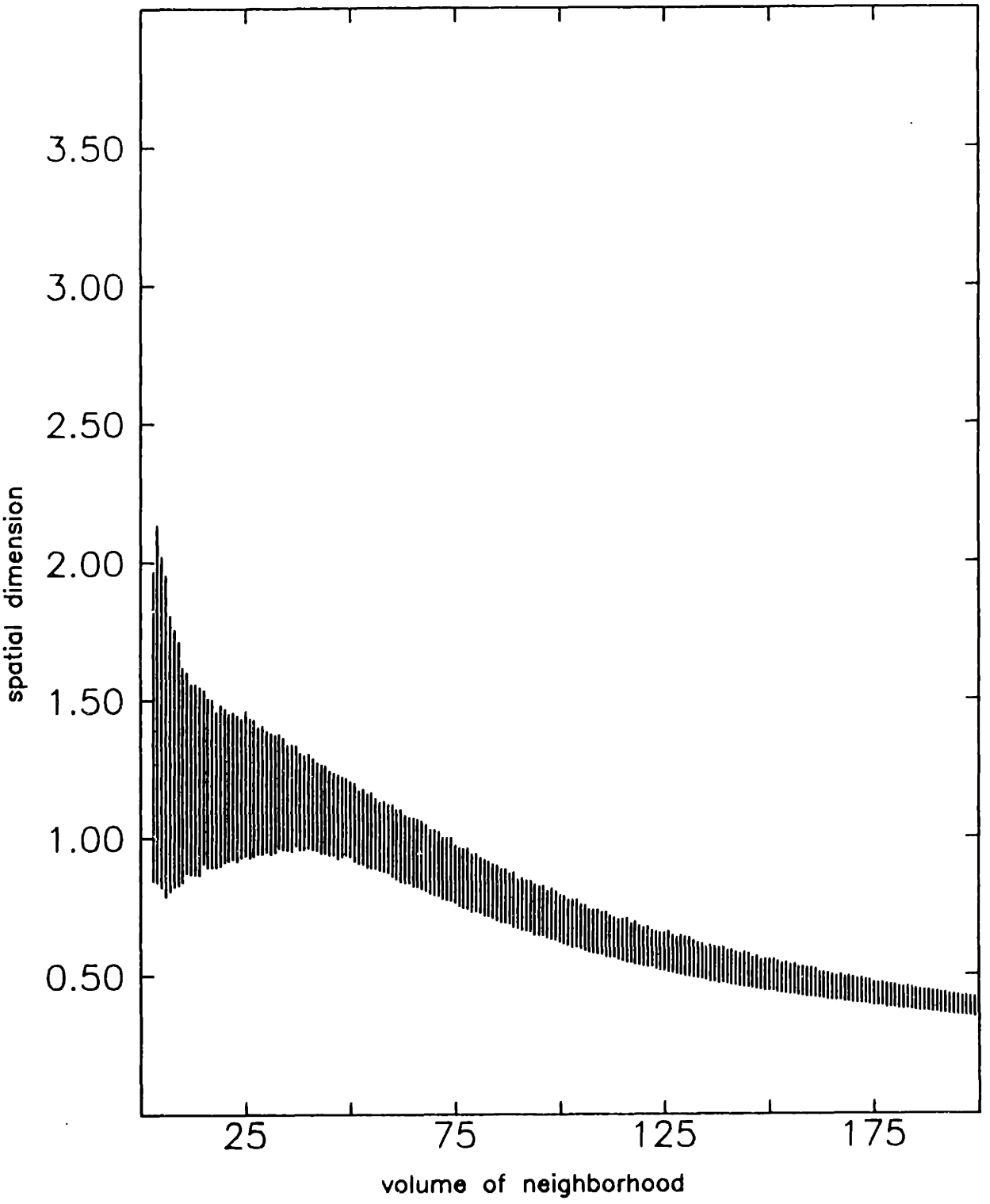

Figure III.12: The portion of the previous graph for volumes up to 200 may be compared with the results for $1 + 1$ dimensional Minkowski space shown in Figure III.6. Up to a volume of 50 the results are indistinguishable; beyond 50 the neighborhoods in the Kaluza-Klein space time are not simply connected and the effective dimension decreases.

It is worth noting that this situation also provides our first example of geometry captured by a faithfully embedded causal set. Although we would naïvely expect the spatial dimension to be decreasing to zero as the volume of the intervals increases, in Figure III.11 it appears to be asymptoting to some small but distinctly nonzero value. This is in fact correct. For a cylinder C with circumference c and height T, the volume is simply cT and we can easily compute the expected number of relations:

$$\begin{aligned}\langle C_2 \rangle &= \int_C d\mathbf{x}\, \mathrm{vol}[J^+(x)] \\ &= \int_0^c dx \left\{ \int_0^{T-c/2} dt \left[Tc - \left(\frac{c^2}{4} + ct \right) \right] + \int_{T-c/2}^{T} dt [T-t]^2 \right\} \\ &= \frac{T^2 c^2}{2} - \frac{Tc^3}{4} - \frac{c^4}{24}.\end{aligned}$$

Thus

$$f(d) = \frac{\langle C_2 \rangle}{c^2 T^2} = \frac{1}{2} - \frac{c}{4T} - \frac{c^2}{24T^2}.$$

For the case $c = 1$, $T = 10$ this formula gives $f(d) \approx 0.4746$, or $d \approx 0.083$. There were 474838 total relations for the casual set of Figures III.11 and III.12, giving a Hausdorff dimension of 0.101 which is in reasonably good agreement with the result of this formula. So using the information that the causal set is faithfully embedded in a cylinder, we can determine all the topology and geometry: the small intervals show that the dimension is two, then using the formulas for the volume and the number of relations we can solve for the circumference and height.

(Anti) de Sitter space: dimension

Given any causal set we can follow the procedure discussed in the two previous sections and compute a Hausdorff dimension for each interval assuming, as we do so, that the causal set can be faithfully embedded in some Minkowski space. The results, typically, will be non-integral. We might find, as we did for the causal sets

arising from uniform distributions of points in Minkowski space, that the dimensions, nevertheless, converge toward some integral value. More likely, they will not, varying in some simple manner as did those calculated for the cylindrical spacetime just considered, or in some more complicated and (so far) uninterpretable manner. Although we could choose to view each interval as approximated by some not necessarily integer dimensional Minkowski space, should the causal set be faithfully embeddable in some curved Lorentzian manifold, this would not help to determine the true dimension of that manifold nor its geometry. So let us consider causal sets arising from uniform distributions of points in curved manifolds.

The simplest situation is constant curvature, *i.e.*, de Sitter or anti-de Sitter space. In $d+1$ dimensions the Riemann tensor, Ricci tensor and scalar curvature are then

$$R_{\alpha\beta\gamma\delta} = K(g_{\alpha\gamma}g_{\beta\delta} - g_{\alpha\delta}g_{\beta\gamma})$$

$$R_{\beta\delta} = dKg_{\beta\delta}$$

$$R = d(d+1)K$$

where the Gaussian curvature K is a constant, positive for de Sitter space and negative for anti-de Sitter space. In fact, since the Einstein tensor

$$R_{\beta\delta} - \frac{1}{2}Rg_{\beta\delta} = -\frac{1}{2}d(d-1)Kg_{\beta\delta},$$

these spaces are solutions to the vaccuum Einstein equation with cosmological constant $\Lambda = \frac{1}{2}d(d-1)K$. The metric satisfying these conditions is conformally flat and may be written in the form [Eisenhart 1925, Petrov 1969]:

$$ds^2 = \frac{1}{\sigma^2}\left[-dt^2 + (dx^1)^2 + \cdots + (dx^d)^2\right]$$

where

$$\sigma = 1 + \frac{K}{4}\left[-t^2 + (x^1)^2 + \cdots + (x^d)^2\right].$$

Given the metric we can proceed as we did in Minkowski space, computing the volume moments of the Poisson distribution.

Lemma III.3: In a $d+1$ dimensional Lorentzian manifold with this metric, the volume of an Alexandroff neighborhood A conformal to one of height T in Minkowski space is

$$\mathrm{vol}[A] = \frac{V_{d-1}}{2^d} \sum_{i=0}^{\infty} \left(\frac{K}{4}\right)^i \frac{T^{d+2i+1}}{d+2i+1},$$

where again V_{d-1} is the volume bounded by a unit S^{d-1}.

Proof: The determinant of this metric is

$$\det \mathbf{g} = \det \frac{1}{\sigma^2}\eta = -\sigma^{-2(d+1)}$$

so

$$\begin{aligned}\mathrm{vol}[A] &= \int_A \sigma^{-(d+1)}\, d\mathbf{x} \\ &= \frac{1}{2}\int_0^T dv \int_0^v du \left(1 - \frac{K}{4}uv\right)^{-(d+1)} A_{d-1} r^{d-1}\end{aligned}$$

since $\sigma = 1 - \frac{K}{4}uv$ in the coordinate system used in the proof of Theorem III.2 (again A_{d-1} is the area of a unit S^{d-1}). Now,

$$\begin{aligned}\left(1 - \frac{K}{4}uv\right)^{-(d+1)} &= \sum_{i=0}^{\infty} \left(-\frac{K}{4}uv\right)^i \binom{-(d+1)}{i} \\ &= \sum_{i=0}^{\infty} \left(\frac{K}{4}uv\right)^i \binom{d+i}{i},\end{aligned}$$

which converges for $|\frac{K}{4}uv| < 1$, *i.e.*, for the whole domain over which this coordinate system is defined. Writing r as $(v-u)/2$ and using the binomial expansion gives

$$\begin{aligned}\mathrm{vol}[A] = \frac{A_{d-1}}{2^d} \sum_{i=0}^{\infty}\sum_{j=0}^{d-1} \binom{d+i}{i}\binom{d-1}{j}\left(\frac{K}{4}\right)^i (-1)^{d-1-j} \times \\ \times \int_0^T dv \int_0^v du\, v^{i+j} u^{d-1-j+i} \\ = \frac{A_{d-1}}{2^d} \sum_{i=0}^{\infty} \binom{d+i}{i}\left(\frac{K}{4}\right)^i \frac{T^{d+2i+1}}{d+2i+1} \sum_{j=0}^{d-1} (-1)^{d-j-1}\binom{d-1}{j}\frac{1}{i+d-j}.\end{aligned}$$

The sum over j is the same as the one which occurred in the proof of Theorem III.2, with $l\omega$ replaced by i, so we again simplify using Vandermonde's Theorem to get:

$$\begin{aligned}\mathrm{vol}[A] &= \frac{A_{d-1}}{2^d}\sum_{i=0}^{\infty}\binom{d+i}{i}\left(\frac{K}{4}\right)^i \frac{T^{d+2i+1}}{d+2i+1}\frac{1}{d+i}\binom{d+i-1}{d-1}^{-1} \\ &= \frac{V_{d-1}}{2^d}\sum_{i=0}^{\infty}\left(\frac{K}{4}\right)^i \frac{T^{d+2i+1}}{d+2i+1}. \quad \blacksquare\end{aligned}$$

Notice that we may extract the flat space result from this formula by setting $K = 0$, in which case only the $i = 0$ term in the sum contributes.

Next we compute the expected number of k–chains in this Alexandroff neighborhood. Define the random variables C_k just as in flat space. Then we have:

Theorem III.4:

$$\langle C_k\rangle = \left(\frac{V_{d-1}}{2^d}\right)^k \sum_{i_1,\ldots,i_k}^{\infty}\left(\frac{K}{4}\right)^{i_1+\cdots+i_k} T^{k(d+1)+2(i_1+\cdots+i_k)} G_d(i_1,\ldots,i_k),$$

where

$$G_d(i_1,\ldots,i_k) := \prod_{j=1}^{k}\frac{1}{j(d+1)+2(i_1+\cdots+i_j)}\times \\ \times\frac{\Gamma(d+i_j+1)}{\Gamma(i_j+1)}\frac{\Gamma\left(\frac{(j-1)(d+1)}{2}+i_1+\cdots+i_j+1\right)}{\Gamma\left(\frac{(j+1)(d+1)}{2}+i_1+\cdots+i_j\right)}.$$

Proof: The proof is again by induction. Lemma III.3 contains the result for $k = 1$. For $k = l + 1$,

$$\langle C_{l+1}\rangle = \int_A \sigma^{-(d+1)}\,d\mathbf{x}_1\int_{J^-(\mathbf{x}_1)}\sigma^{-(d+1)}\,d\mathbf{x}_2\ldots\int_{J^-(\mathbf{x}_l)}\sigma^{-(d+1)}\,d\mathbf{x}_{l+1},$$

where we are using the Alexandroff neighborhoods generated by the past lightcones $J^-(\mathbf{x}_j)\cap A$ for convenience (and denoting them simply by $J^-(\mathbf{x}_j)$). Then the

induction hypothesis gives

$$\begin{aligned}\langle C_{l+1}\rangle &= \int_A \sigma^{-(d+1)}\, d\mathbf{x} \langle C_l|_{J^-(\mathbf{x})\cap A}\rangle \\ &= \frac{1}{2}\int_0^T dv \int_0^v du\, \sigma^{-(d+1)} A_{d-1} r^{d-1} \langle C_l|_{J^-(\mathbf{x})\cap A}\rangle.\end{aligned}$$

The coordinate height of the Alexandroff neighborhood $J^-(\mathbf{x}) \cap A$ is $\sqrt{t^2 - r^2} = \sqrt{uv}$ so expanding σ and r in binomial series as in the preceding proof gives

$$\begin{aligned}\langle C_{l+1}\rangle = \frac{1}{2} A_{d-1} \int_0^T dv \int_0^v du \sum_{i_{l+1}=0}^{\infty} \left(\frac{K}{4}uv\right)^{i_{l+1}} \binom{d+i_{l+1}}{i_{l+1}} \times \\ \times \frac{1}{2^{d-1}} \sum_{j=0}^{d-1} \binom{d-1}{j} v^j u^{d-1-j} (-1)^{d-1-j} \times \\ \times \left(\frac{V_{d-1}}{2^d}\right)^l \sum_{i_1,\ldots,i_l}^{\infty} \left(\frac{K}{4}\right)^{i_1+\cdots+i_l} (uv)^{\frac{l(d+1)}{2}+(i_1+\cdots+i_l)} G_d(i_1,\ldots,i_l) \\ = \frac{A_{d-1}}{2^d} \left(\frac{V_{d-1}}{2^d}\right)^l \sum_{i_1,\ldots,i_{l+1}}^{\infty} \left(\frac{K}{4}\right)^{i_1+\cdots+i_{l+1}} \binom{d+i_{l+1}}{i_{l+1}} \times \\ \times G_d(i_1,\ldots,i_l) \frac{T^{(l+1)(d+1)+2(i_1+\cdots+i_{l+1})}}{(l+1)(d+1)+2(i_1+\cdots+i_{l+1})} \times \\ \times \sum_{j=0}^{d-1} \binom{d-1}{j} (-1)^{d-1-j} \frac{1}{\frac{l(d+1)}{2}+i_1+\cdots+i_{l+1}+d-j}.\end{aligned}$$

The sum over j is the same one we have seen twice before, so again we simplify using Vandermonde's Theorem:

$$\begin{aligned}\langle C_{l+1}\rangle = \frac{A_{d-1}}{2^d} \left(\frac{V_{d-1}}{2^d}\right)^l \sum_{i_1,\ldots,i_{l+1}}^{\infty} \left(\frac{K}{4}\right)^{i_1+\cdots+i_{l+1}} \binom{d+i_{l+1}}{i_{l+1}} \times \\ \times G_d(i_1,\ldots,i_l) \frac{T^{(l+1)(d+1)+2(i_1+\cdots+i_{l+1})}}{(l+1)(d+1)+2(i_1+\cdots+i_{l+1})} \times \\ \times \frac{1}{\frac{l(d+1)}{2}+i_1+\cdots+i_{l+1}+d} \binom{\frac{l(d+1)}{2}+i_1+\cdots+i_{l+1}+d-1}{d-1}^{-1} \\ = \left(\frac{V_{d-1}}{2^d}\right)^{l+1} \sum_{i_1,\ldots,i_{l+1}}^{\infty} \left(\frac{K}{4}\right)^{i_1+\cdots+i_{l+1}} \frac{T^{(l+1)(d+1)+2(i_1+\cdots+i_{l+1})}}{(l+1)(d+1)+2(i_1+\cdots+i_{l+1})} \times \\ \times \binom{d+i_{l+1}}{i_{l+1}} \binom{\frac{l(d+1)}{2}+i_1+\cdots+i_{l+1}+d}{d}^{-1} G_d(i_1,\ldots,i_l).\end{aligned}$$

Thus

$$G_d(i_1,\ldots,i_{l+1}) = \frac{G_d(i_1,\ldots,i_l)}{(l+1)(d+1)+2(i_1+\cdots+i_{l+1})}\times$$
$$\times \binom{d+i_{l+1}}{i_{l+1}}\binom{\frac{l(d+1)}{2}+i_1+\cdots+i_{l+1}+d}{d}^{-1}$$
$$= \frac{G_d(i_1,\ldots,i_l)}{(l+1)(d+1)+2(i_1+\cdots+i_{l+1})}\times$$
$$\times \frac{\Gamma(d+i_{l+1}+1)}{\Gamma(i_{l+1}+1)}\frac{\Gamma\left(\frac{l(d+1)}{2}+i_1+\cdots+i_{l+1}+1\right)}{\Gamma\left(\frac{(l+2)(d+1)}{2}+i_1+\cdots+i_{l+1}\right)}.$$

Solving this simple recursion relation gives $G_d(i_1,\ldots,i_k)$. ∎

With these results we can, given a causal set faithfully embedded in an Alexandroff neighborhood of (anti) de Sitter space, approximate the dimension of the manifold. Letting $C_1(A) := N(A)$ we have the formulae $\langle C_k(A)\rangle = f_k(d,K;T)$ where the functions $f_k(d,K;T)$ are given in Theorem III.4 for each positive integer k (although for $k \gg \mathrm{vol}[A]$, $\langle C_k(A)\rangle \ll 1$). Since there are three unknown parameters, the simplest procedure is to count the number of elements in an interval C_1, the number of relations C_2, the number of 3-chains C_3 and then solve the system of equations

$$C_1 = f_1(d,K;T)$$

$$C_2 = f_2(d,K;T)$$

$$C_3 = f_3(d,K;T)$$

for d, K and T. The resulting dimension is analogous to the Hausdorff dimension we computed in Minkowski space; we will retain the terminology. The Gaussian curvature K and the height of the Alexandroff neighborhood T are also determined by this procedure; thus we are extracting geometry as well as topology from the causal set. Again we can verify the effectiveness of this procedure by computer simulations: applying it to causal sets constructed to be faithfully embeddable in constant curvature Lorentzian manifolds.

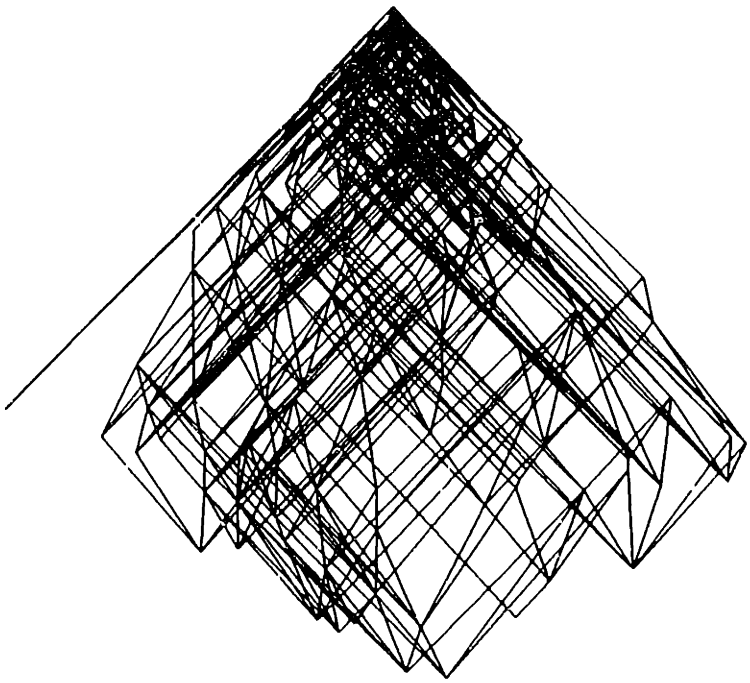

Figure III.13: The Hasse diagram for a 200 element causal set embedded in an Alexandroff neighborhood of two dimensional de Sitter space with $KT^2 = 3.9$.

(Anti) de Sitter space: uniform distributions

The most straightforward way to obtain causal sets faithfully embeddable in a curved manifold would be to define a coordinate system $\mathbf{x}$ for (some patch of) the manifold, choose points $\mathbf{x}$ uniformly distributed with respect to the volume form (in this patch) and then determine the causal relations among these points. This is exactly what we did earlier to find causal sets faithfully embeddable in flat spacetimes. With curvature present, however, both the second and the third steps are considerably less trivial. Fortunately, in the case of constant curvature, we can bypass most of the difficulties. Since (anti) de Sitter manifolds are conformally flat, the causal relationship of two points is the same as that of their images under the conformal transformation to flat space (although their proper separation is not). Thus we need only distribute points in flat space according to the conformal factor. As we found in the proof of Lemma III.3 the conformal factor appears in the volume form as $\sigma^{-(d+1)}$. So we can apply the rejection method [Knuth 1969,

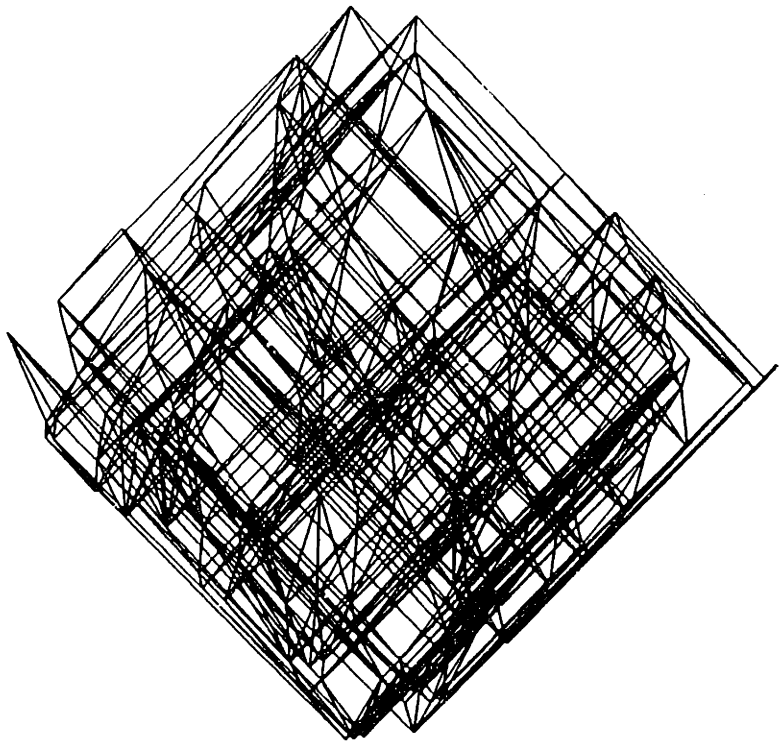

Figure III.14: The Hasse diagram for a 200 element causal set embedded in an Alexandroff neighborhood of two dimensional anti-de Sitter space with $KT^2 = -3.9$.

Press, Flannery, Teukolsky and Vetterling 1986]: Let M be the maximum value that $\sigma^{-(d+1)}$ achieves in the Alexandroff neighborhood A of the previous section, $(1 - KT^2/4)^{-(d+1)}$ if $K > 0$ and 1 if $K \leq 0$. If we distribute points uniformly in the region $A \times [0, M]$ and use their projections $\mathbf{x}$ into A when their last coordinate is less than $\sigma^{-(d+1)}$ evaluated at $\mathbf{x}$, the points will clearly be distributed uniformly with respect to the conformal factor.

This algorithm is implemented by procedure *ccsprinkle* in the Pascal program listed in Appendix A. The causal relations among the resulting points can be calculated using their (flat) coordinates just as in the earlier programs. A causal set faithfully embeddable in an Alexandroff neighborhood in a two dimensional de Sitter space with $KT^2 = 3.9$ is shown in Figure III.13, while a causal set faithfully embeddable in an Alexandroff neighborhood in a two dimensional anti-de Sitter

space with $KT^2 = -3.9$ is shown in Figures III.14. Each of these causal sets has 200 elements and may be compared with the one embedded faithfully in flat space in Figure III.1 or III.2.

(Anti) de Sitter space: numerical results

After producing a causal set faithfully embeddable in some (anti) de Sitter space, the Pascal program listed in Appendix C implements the procedure discussed in the paragraph following Theorem III.4. That is, for each interval in the causal set it counts the number of elements, relations and 3–chains and then attempts to solve the system of equations obtained from Theorem III.4 for d, K and T. These equations are highly nonlinear; solving them numerically is a nontrivial problem. The Newton Raphson method [Press, Flannery, Teukolsky and Vetterling 1986] used in the program converges for most of the large intervals. For example, in the case $N = 400$, $d = 1 + 1$ and $KT^2 = 1.0$, Figure III.15 contains histograms for both the converging and nonconverging neighborhoods (the one which peaks more sharply at small volumes is for the nonconverging neighborhoods). Figure III.16 shows the fraction of all neighborhoods at each volume which converge; here it is clear that the best results should come from the medium to large volume neighborhoods.

The next three figures are for such a causal set faithfully embedded in an Alexandroff neighborhood of $1 + 1$ dimensional de Sitter space with $KT^2 = 1.0$. For 400 elements this means that $K \approx 1.438 \times 10^{-3}$ and $T \approx 2.637 \times 10^{1}$. In each case the true values are indicated by the continuous curve. Just as in Minkowski space we see in Figure III.17 that the Hausdorff dimension converges toward the correct value as the size of the interval increases. In Figure III.18 the curvature behaves similarly (although the variance is still large enough even for the biggest intervals that it is not clearly converging to a nonzero value) and we can see from

Figure III.19 that the conformal height T is being computed correctly also.

Increasing the curvature to $KT^2 = 3.5$ (for $N = 400$ this means that $K \approx 1.134 \times 10^{-2}$ and $T \approx 1.757 \times 10^{1}$) we obtain the graphs for the Hausdorff dimension and curvature shown in Figures III.20 and III.21, respectively, which indicate that the results are still good for $d = 1 + 1$. Note that the curvature here is clearly converging to a nonzero value.

For anti-de Sitter space KT^2 is negative and results for this case, still in $1 + 1$ dimensions, are shown in Figures III.22 to III.25. The first two figures are for the case $KT^2 = -1.0$ which, for $N = 400$, means that $K \approx -1.116 \times 10^{-3}$ and $T \approx 2.994 \times 10^{1}$. Again both the dimension and the curvature appear to be converging to the correct values. To see that the negative curvature is indeed being computed correctly, the next two figures show the results for $N = 400$ and $KT^2 = -3.5$ (hence $K \approx -3.190 \times 10^{-3}$ and $T \approx 3.313 \times 10^{1}$). For these cases the method also appears to be providing good estimates of dimension and curvature from large intervals; the curvature is clearly converging to a nonzero value.

As before, in the Minkowski case, we expect the results to deteriorate with increasing dimension. In fact, as soon as we reach $2+1$ dimensional de Sitter space we face a major problem. For $N = 400$, 800 and even 1000, with $KT^2 = 1.0$, for most of the neighborhoods the Newton Raphson algorithm converges to $d \approx 4.6 + 1$ and negative curvature. That this is not due to a flaw in the algorithm can be checked by computing the predicted numbers of relations and 3–chains and verifying that the algorithm converges to the correct values of the dimension and curvature. If these numbers are perturbed by more than about 5%, however, a solution near $4.6 + 1$ with negative curvature is found. In fact, a similar, though less severe, phenomenon is already present in the $1 + 1$ dimensional cases just considered. Notice

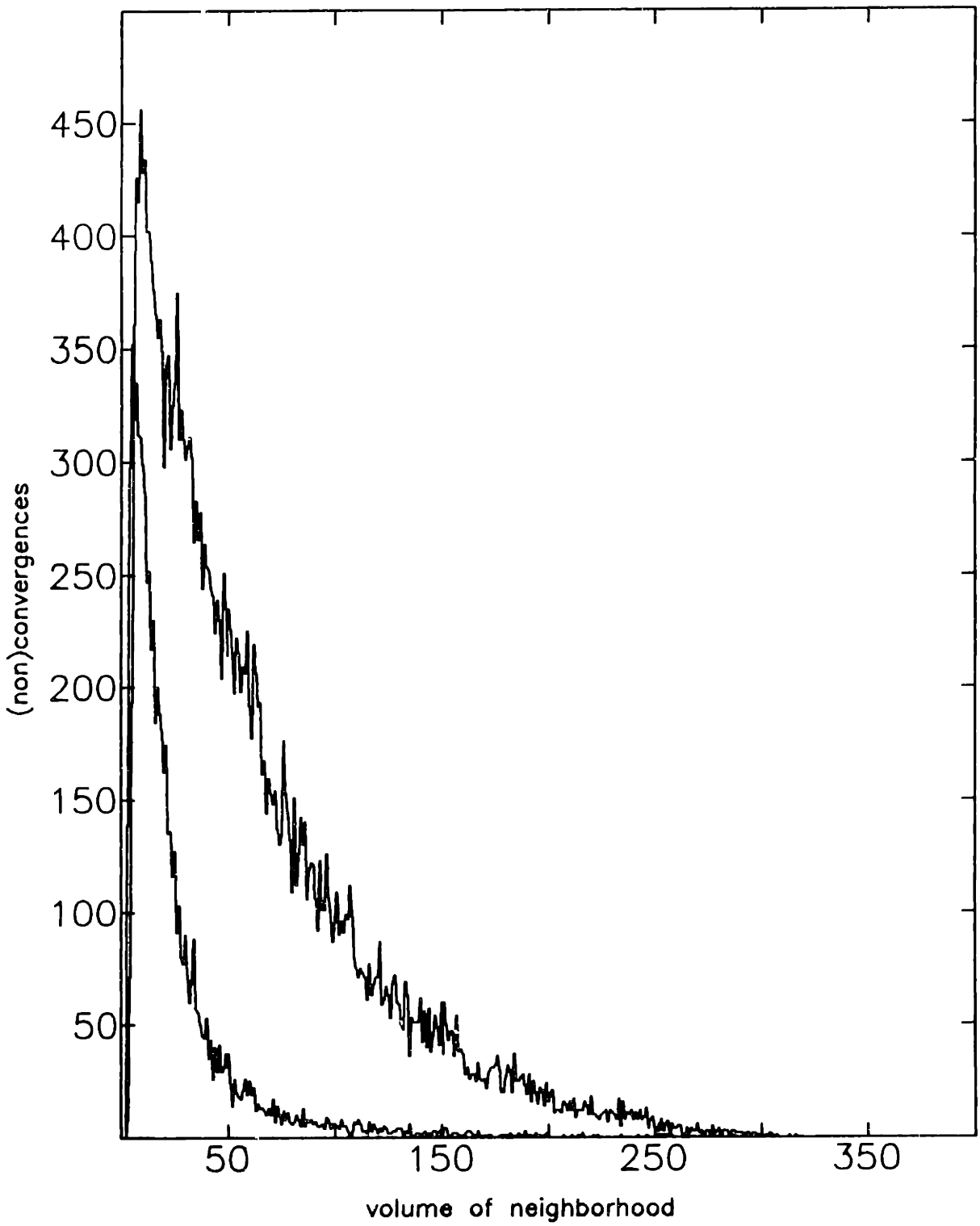

Figure III.15: When the Newton Raphson method is used to try to solve for d, K and T in each interval of a causal set, the method does not converge in every interval. For the case $N = 400$, $d = 1 + 1$ and $KT^2 = 1.0$ the upper curve plots the number of intervals in which the method converges while the lower plots the number in which it fails.

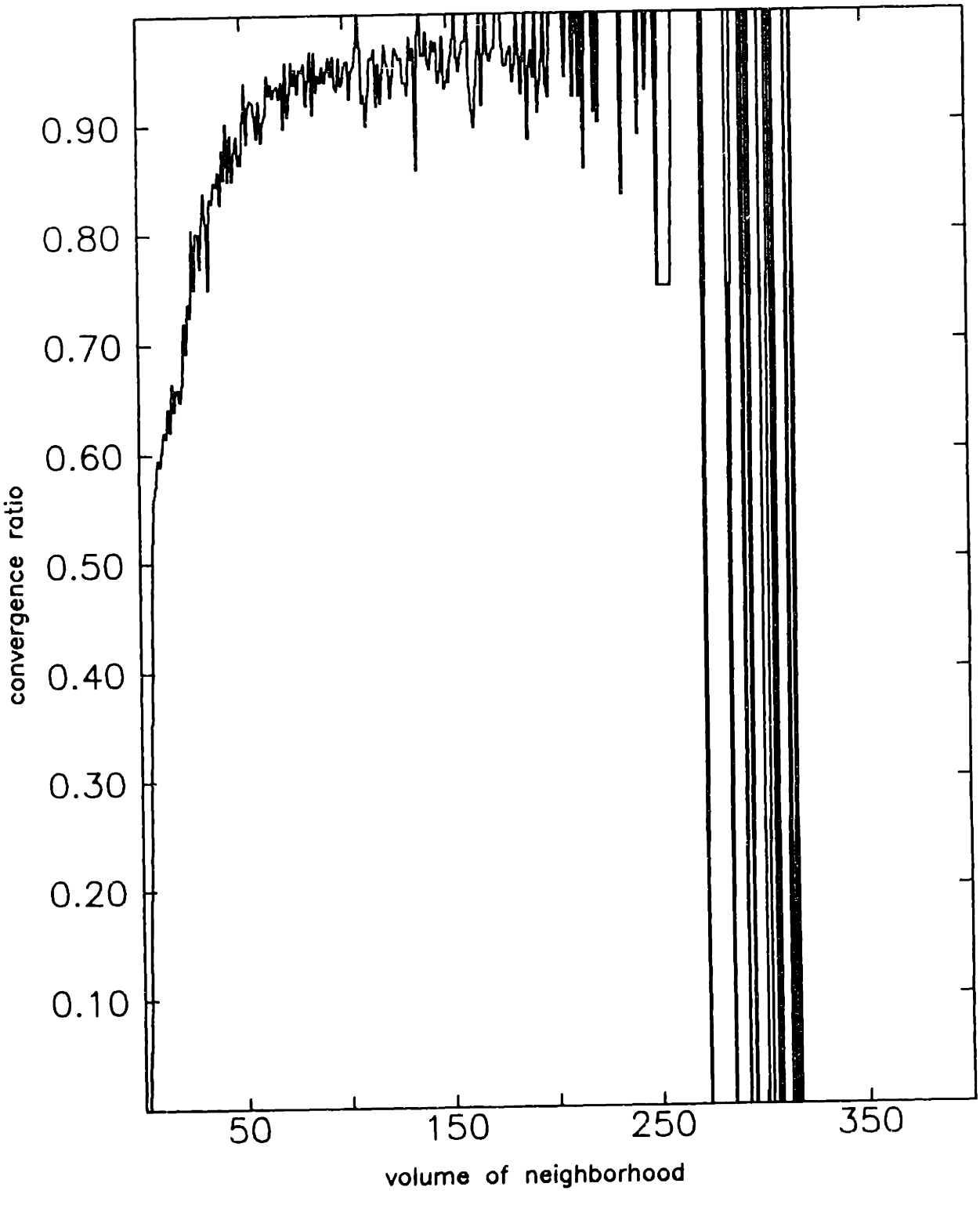

Figure III.16: The same data as in Figure III.15, here plotted as the fraction of all intervals of a given volume in which the method converges. Clearly the best statistics will be obtained from the medium to large neighborhoods.

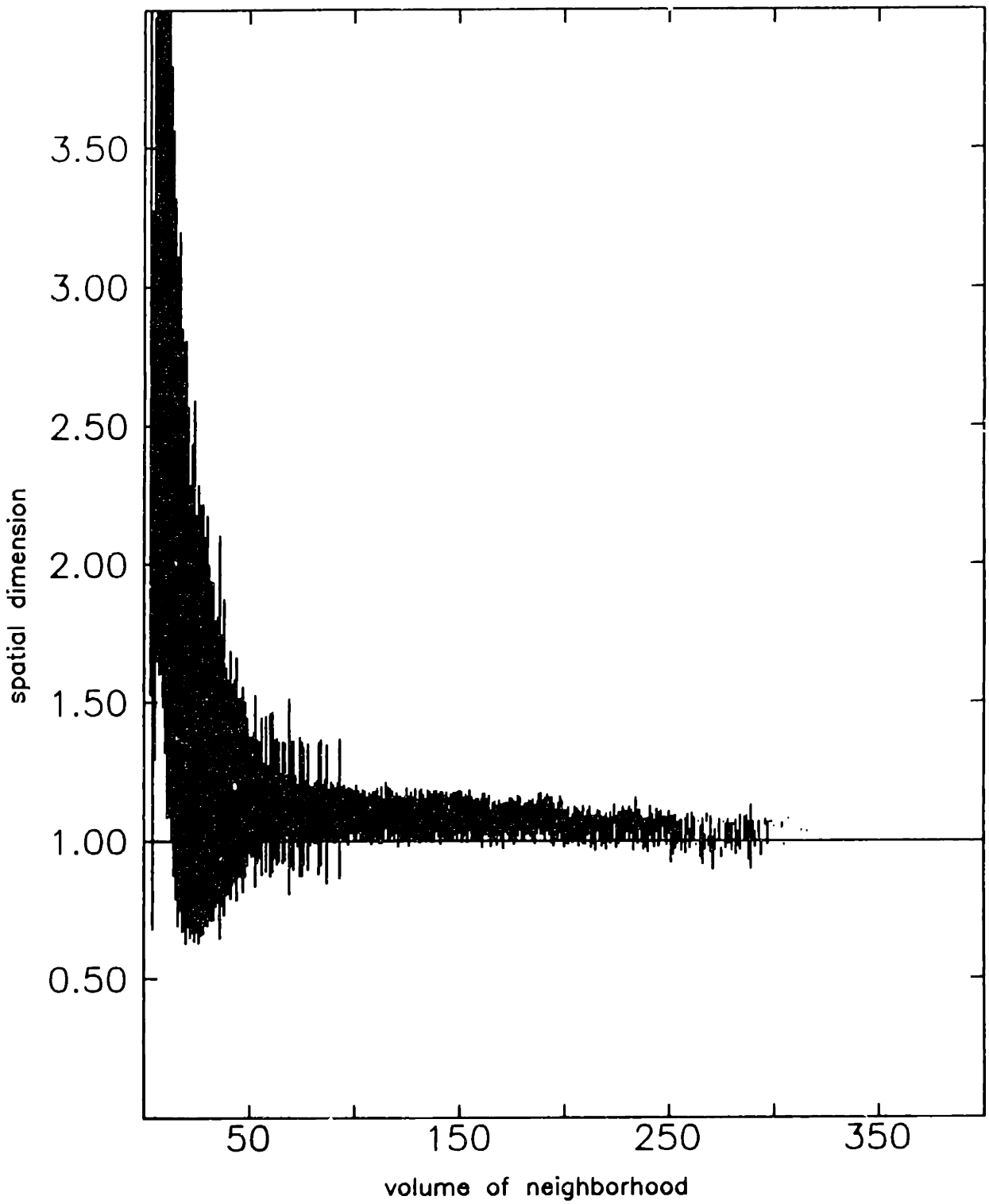

Figure III.17: The spatial Hausdorff dimension is plotted as a function of volume for a 400 element causal set in a Alexandroff neighborhood of $1+1$ dimensional de Sitter space with $KT^2 = 1.0$. Just as in the flat case we see that the esimated dimension appears to be converging to the correct value, large intervals providing a better estimate than smaller ones.

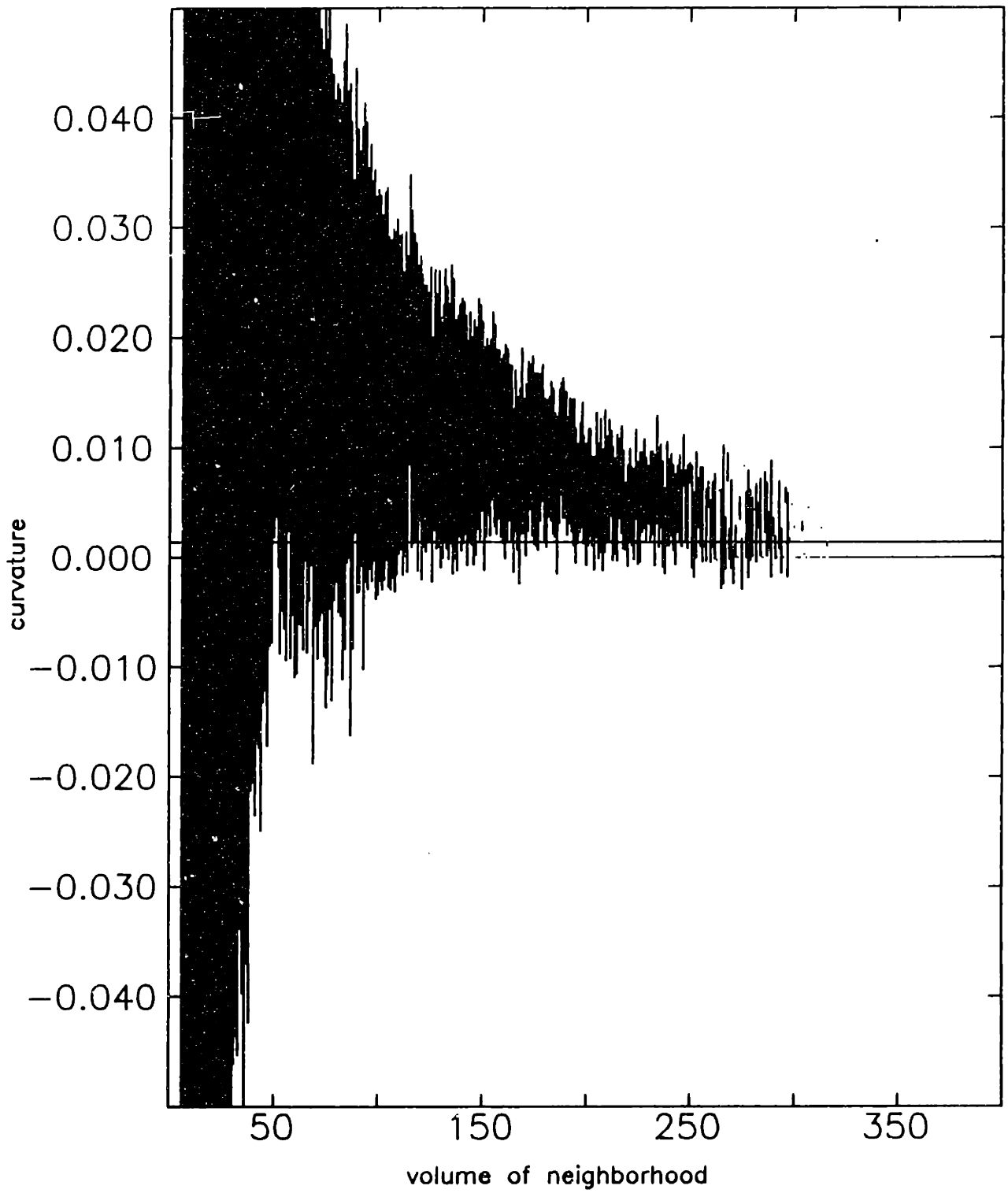

Figure III.18: Here the estimated curvature for each interval in the same causal set as in Figure III.17 is plotted as a function of volume. The correct value of $K \approx 1.438 \times 10^{-3}$ is indicated by the solid line; the results appear to be converging to it.

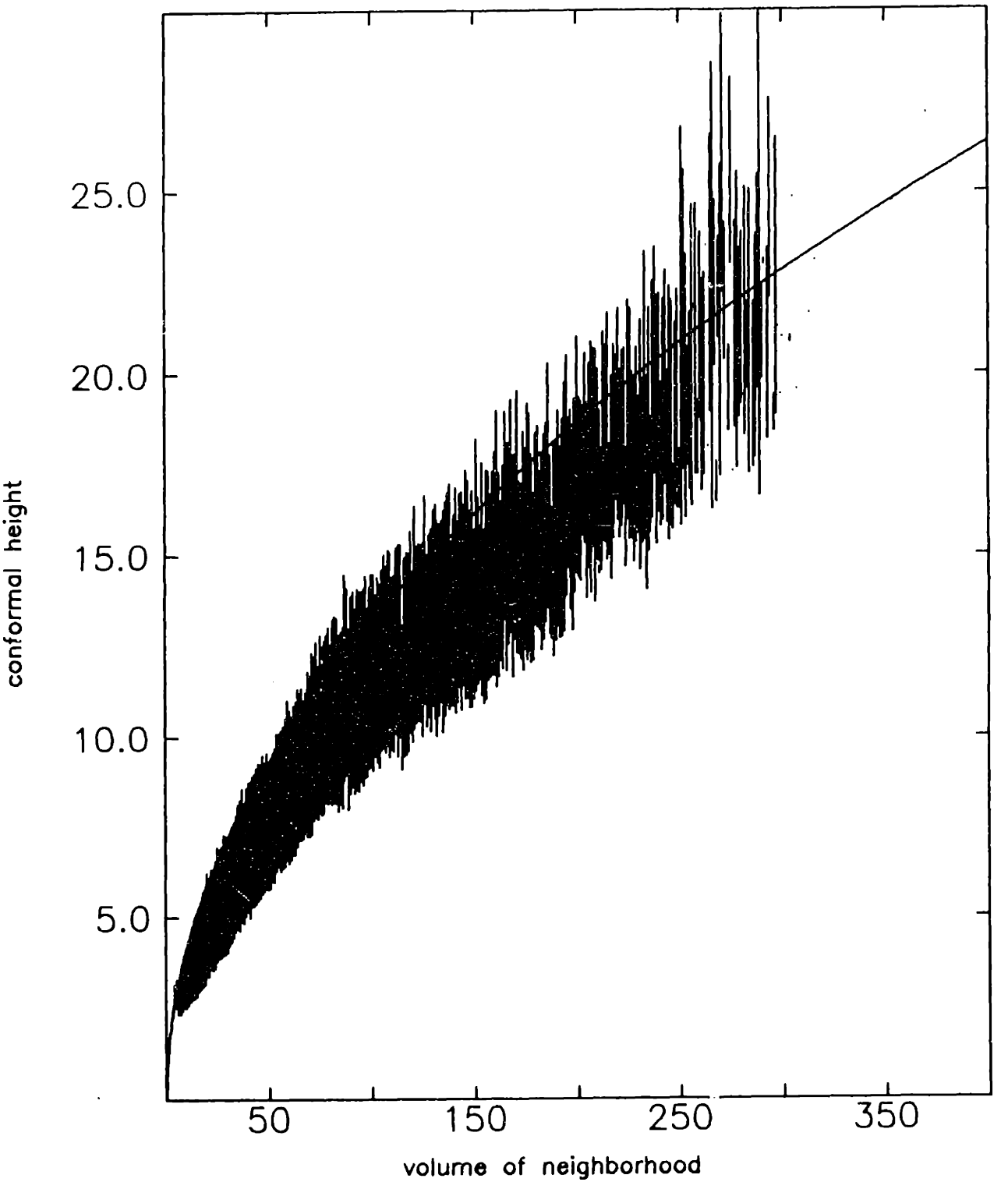

Figure III.19: The conformal heights estimated in the same computation as the dimensions and curvatures shown in Figures III.17 and III.18, plotted as a function of volume. The correct values are again indicated by the solid curve.

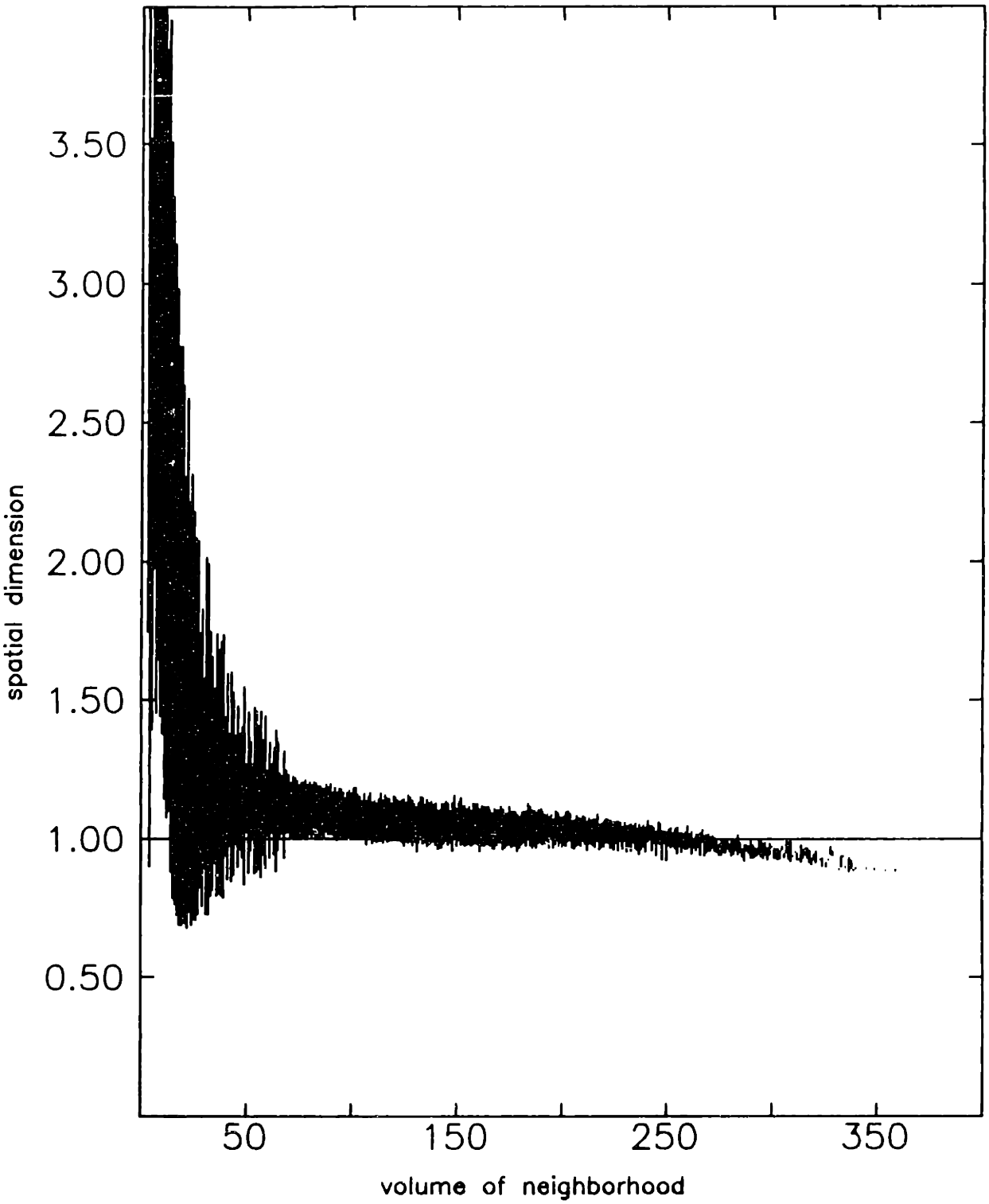

Figure III.20: The spatial Hausdorff dimension is plotted as a function of volume for a 400 element causal set in a Alexandroff neighborhood of $1+1$ dimensional de Sitter space with $KT^2 = 3.5$. Increasing the curvature does not appear to harm convergence; compare with Figure III.17.

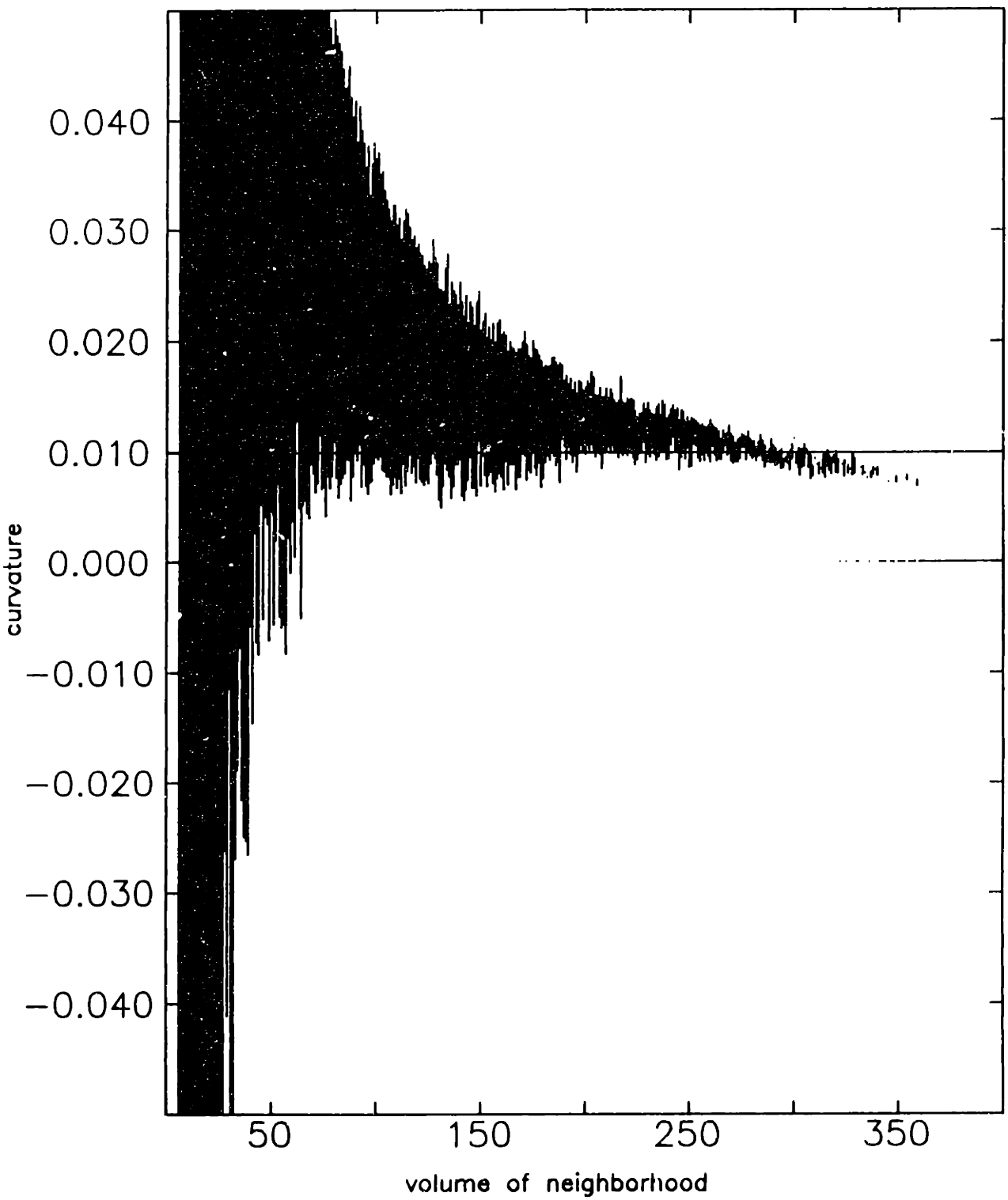

Figure III.21: Here the estimated curvature for each interval in the same causal set as in Figure III.20 is plotted as a function of volume. The correct value of $K \approx 1.134 \times 10^{-2}$ is indicated by the solid line; it is clearer than in the case of Figure III.18 that the results are converging to it rather than to zero.

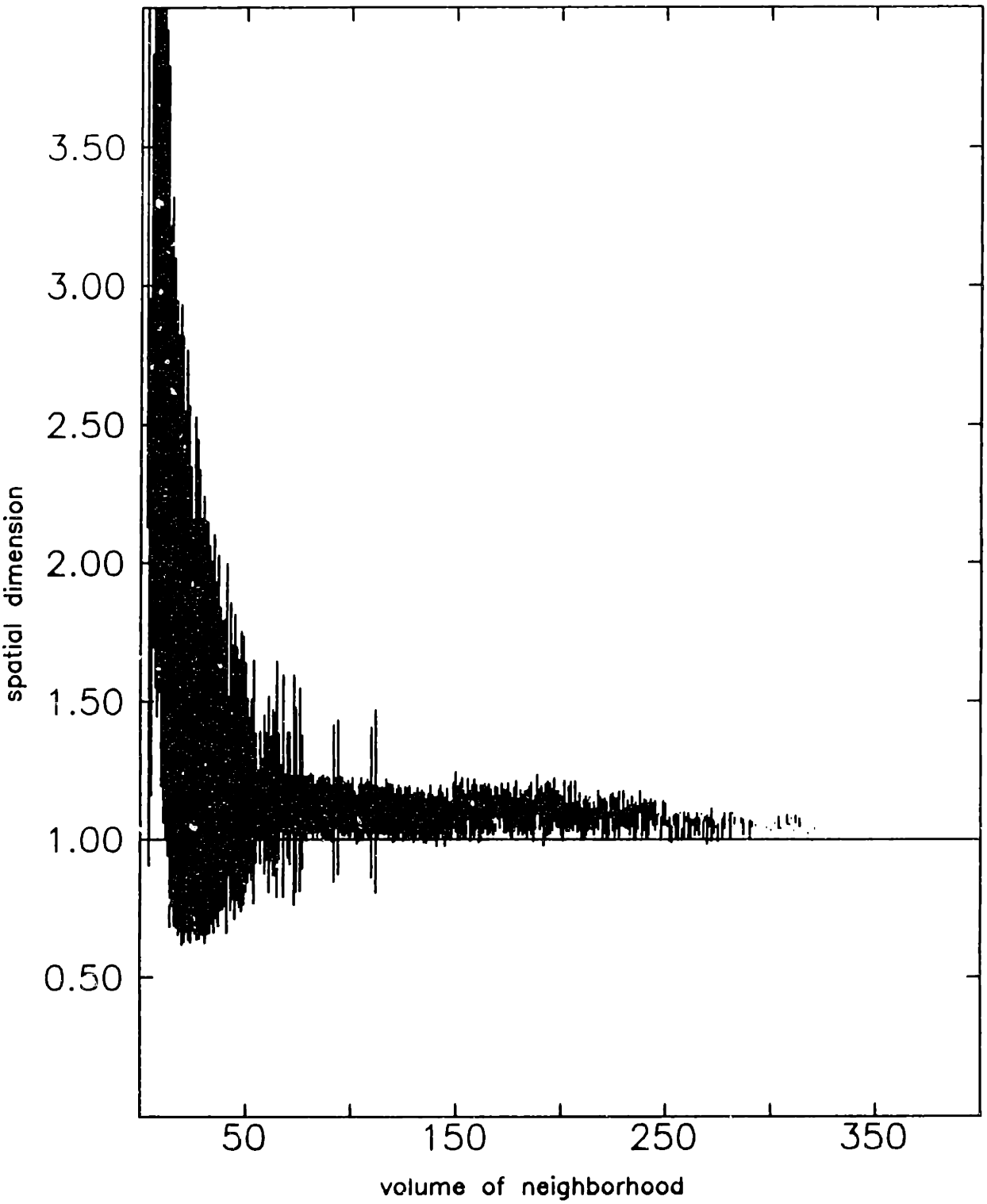

Figure III.22: The spatial Hausdorff dimension is plotted as a function of volume for a 400 element causal set in a Alexandroff neighborhood of $1+1$ dimensional anti-de Sitter space with $KT^2 = -1.0$. Just as in the previous cases we see that the esimated dimension appears to be converging to the correct value, large intervals providing a better estimate than smaller ones.

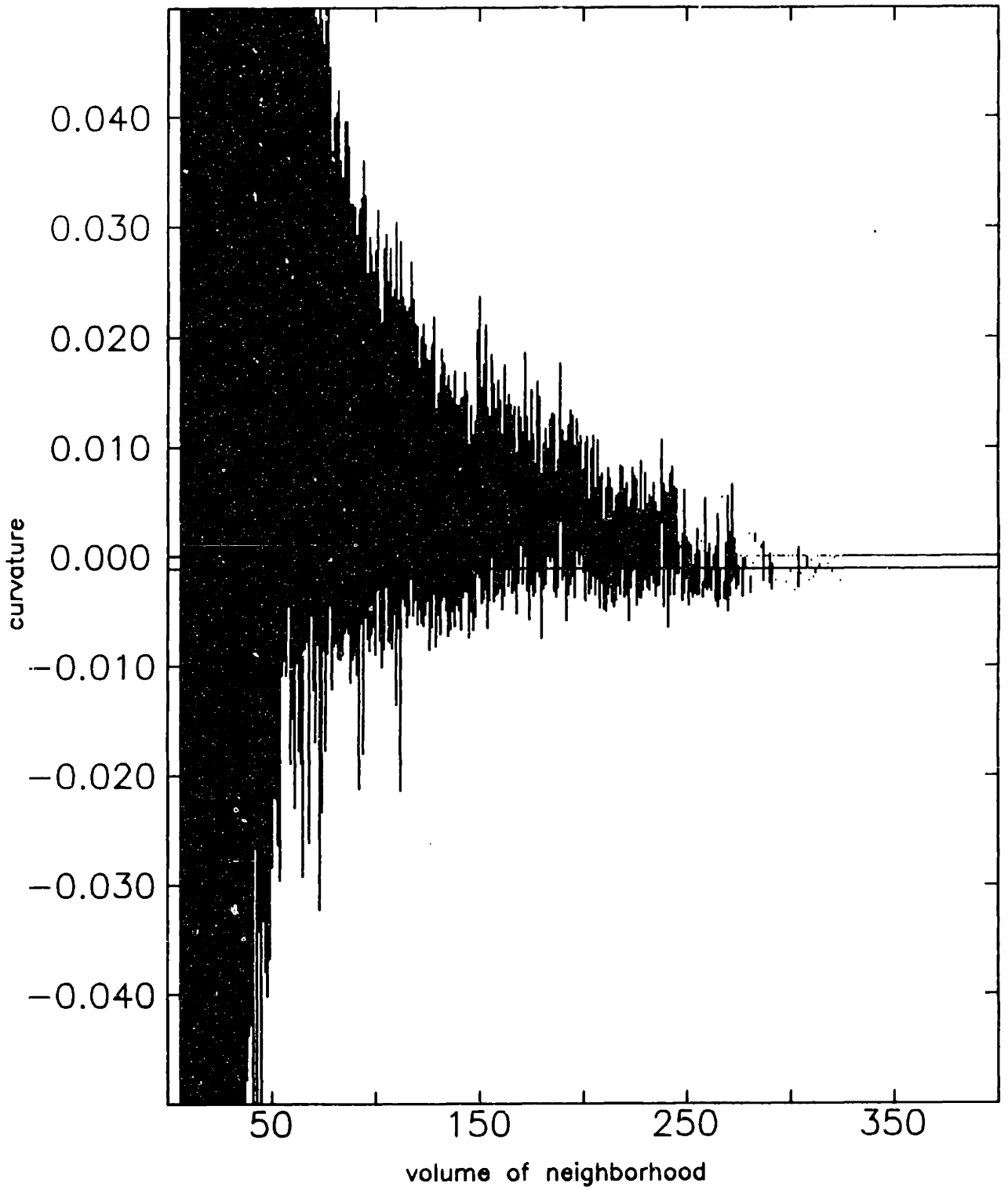

Figure III.23: Here the estimated curvature for each interval in the same causal set as in Figure III.22 is plotted as a function of volume. The correct value of the curvature $K \approx -1.116 \times 10^{-3}$ is indicated by the solid line; the results appear to be converging to this value.

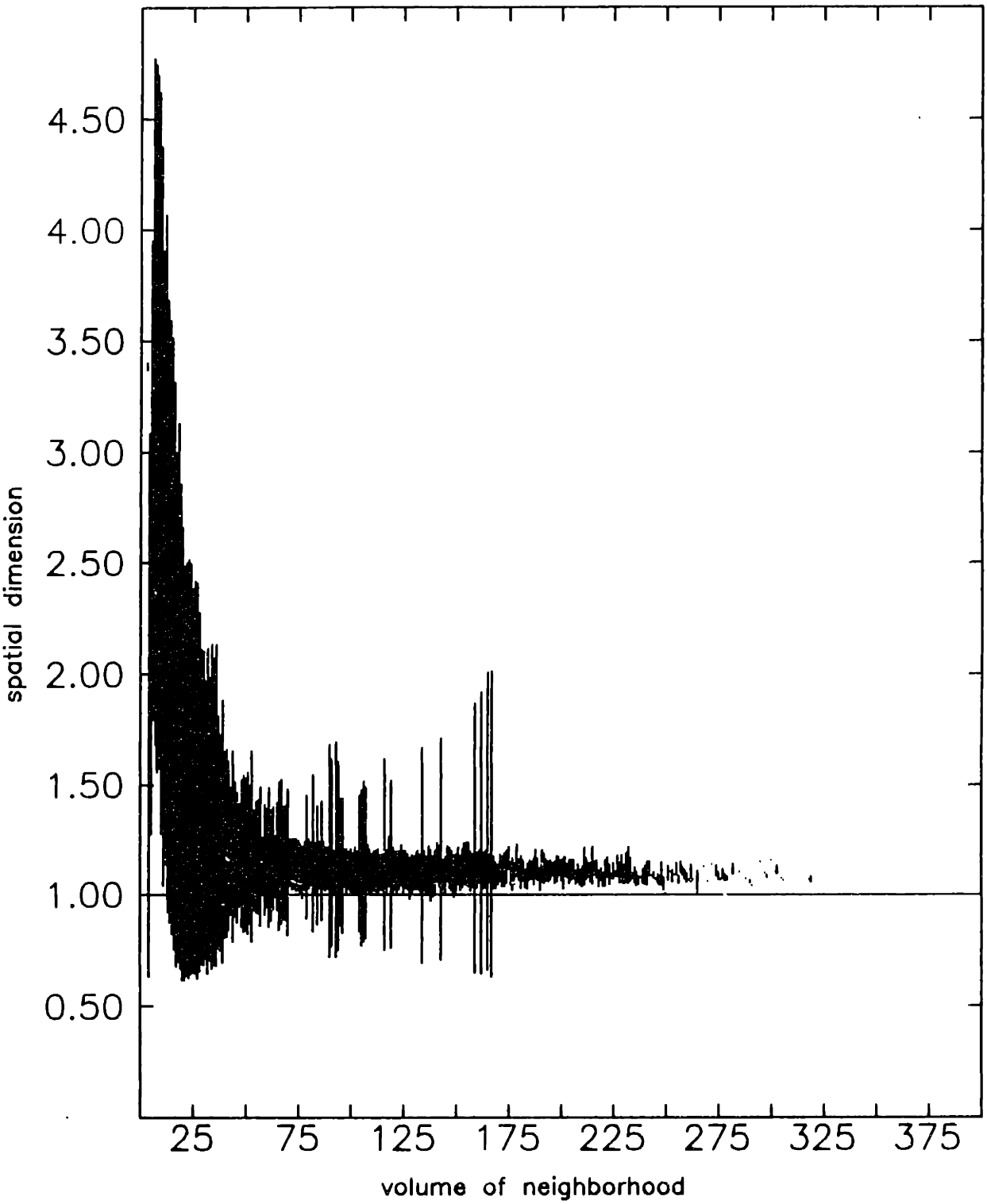

Figure III.24: The spatial Hausdorff dimension is plotted as a function of volume for a 400 element causal set in a Alexandroff neighborhood of $1 + 1$ dimensional anti-de Sitter space with $KT^2 = -3.5$. Increasing the curvature does not appear to harm convergence; compare with Figure III.22.

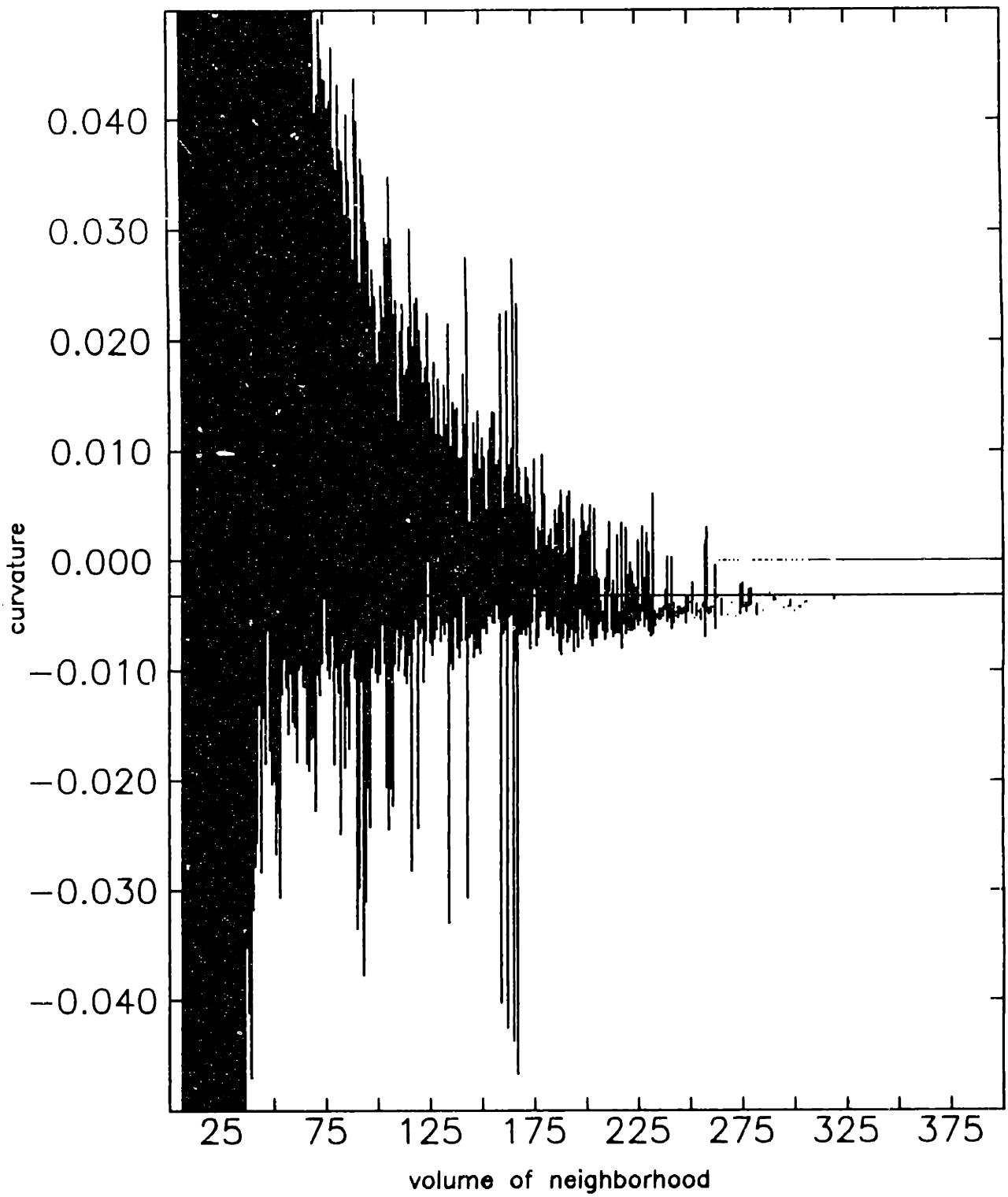

Figure III.25: Here the estimated curvature for each interval in the same causal set as in Figure III.24 is plotted as a function of volume. The correct value of the curvature $K \approx -3.190 \times 10^{-3}$ is indicated by the solid line; it is clearer than in the case of Figures III.18 and III.23 that the results are converging to it rather than to zero.

in the dimension plots for anti-de Sitter space, Figures III.22 and especially III.24, the isolated interval volumes with large variations occurring in the range where the variation has decreased to a few tenths for the majority of the volumes. These are caused by the presence of significant numbers of intervals at these volumes for which the Newton Raphson algorithm converges to the 'wrong' value. The scatter plot in Figure III.26 shows this clearly for the $KT^2 = -3.5$ case of Figures III.24 and III.25. Moreover, this is not a difficulty associated only with negative curvature. Figure III.27 shows the analagous results for the $KT^2 = 3.5$ case of Figures III.20 and III.21.

There is apparently some duality here, manifesting itself in nonuniqueness of solutions to our system of equations, which should be investigated. Algebraically, the difficulty is that the expressions for the number of elements, relations and 3-chains, although independent, form a system of equations which is almost singular, *i.e.*, dependent. This indicates that one might consider using other causal set parameters: the number of links, for example, in addition to, or instead of, these three. For our immediate purposes, however, this indicates that we must go to considerably larger N in order to reduce the statistical fluctuations sufficiently to converge to the correct value. A straightforward calculation of the variances in this case (parallel to the flat case computation) would determine the necessary order for N. As the runs described here use on the order of 10 hours of CPU time on a VAX 3200 already, additional computer facilities seem to be required to obtain good results. This is discussed further in the Conclusion. Nevertheless, it is clear that in principle the procedure is working and that we can indeed extract numerically both topological information (the dimension) and geometrical information (the curvature) from these causal sets.

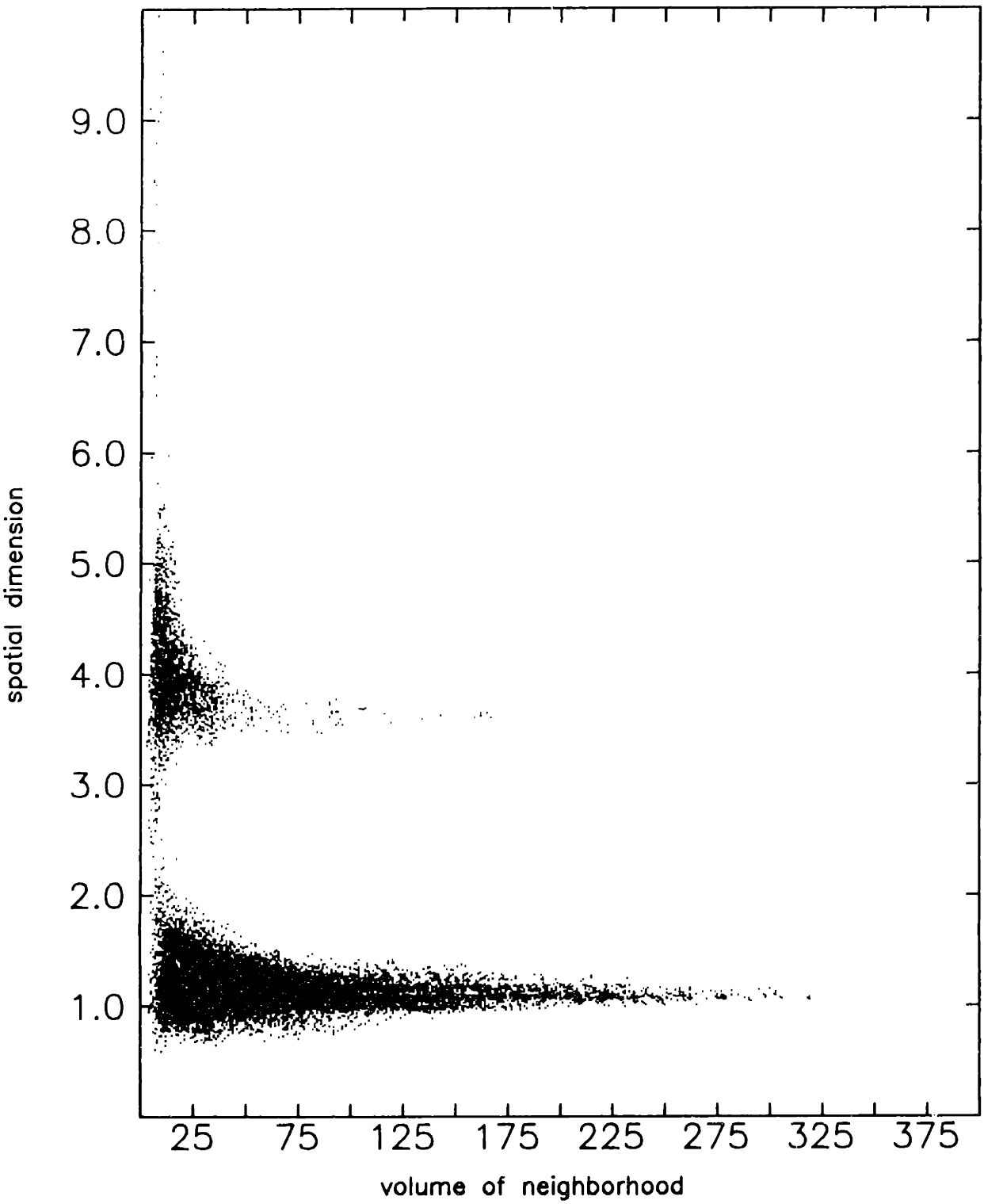

Figure III.26: As in Figure III.5, the computed dimension for each interval is plotted against its volume as a single point. Notice that although the majority of the results cluster near 1, there is an appreciable number at about 3.6. The presence of these intervals creates the isolated large variations in Figure III.24.

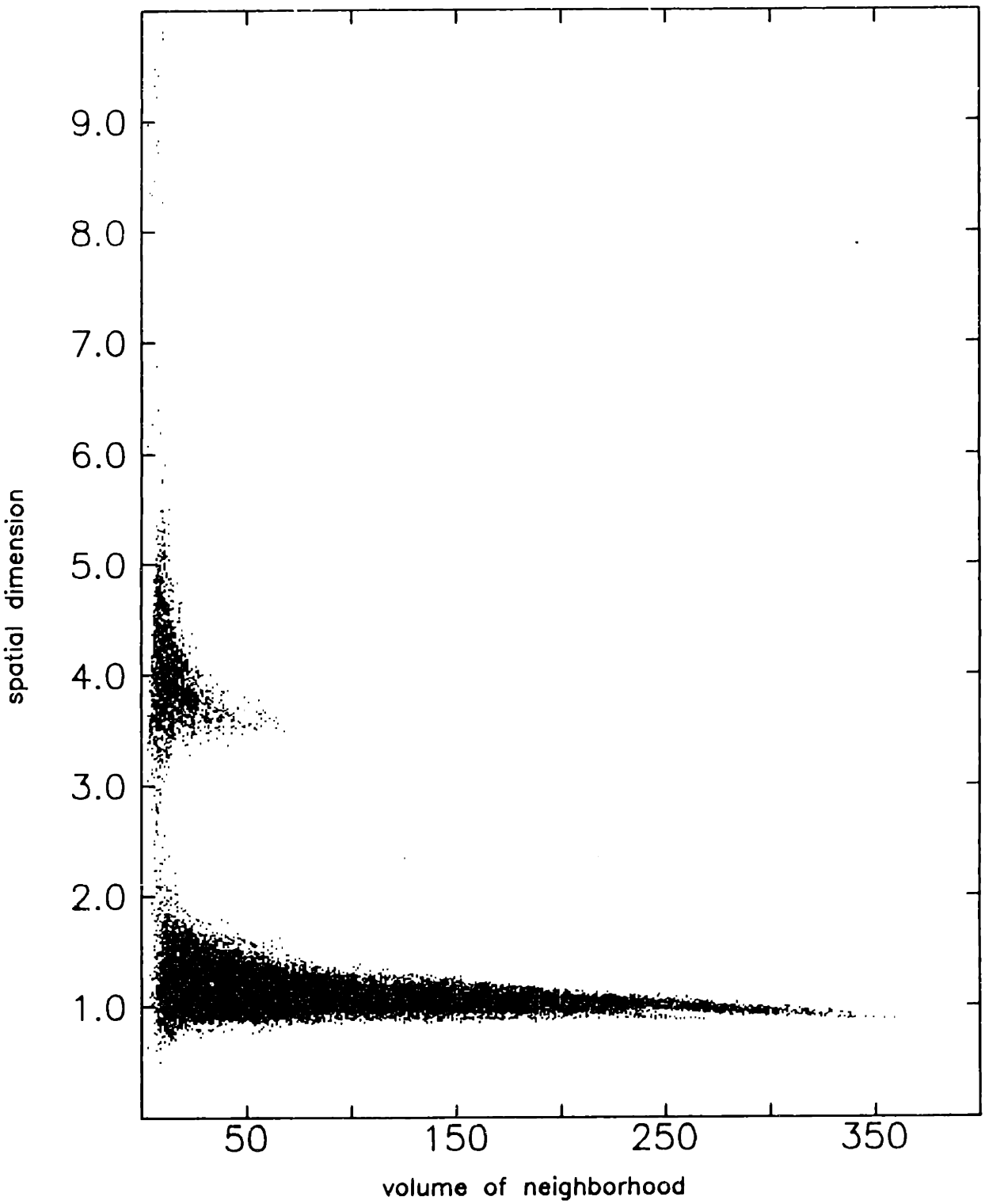

Figure III.27: For the causal set of Figures III.20 and III.21, $KT^2 = 3.5$, the computed dimension for each interval is plotted against its volume as a single point. Again, although the majority of the results cluster near 1, there is an appreciable number at about 3.6 or 3.7. The presence of these intervals is particularly evident in the volume range 50–100 in Figure III.20.

IV. Conclusion

In the three preceding chapters we defined what is meant by causal sets and investigated two notions of dimension associated with them. This Conclusion summarizes the results, notes their possible implications for a quantum dynamics of causal sets and suggests directions for further work.

Summary of results

Dimension is a topological property of the Lorentzian manifolds of general relativity; since any theory of quantum gravity should agree with general relativity in the classical regime, and with the *Hauptvermutung* that faithful embeddings of causal sets into Lorentian manifolds determine the manifold with metric up to "approximate isometry" in mind, it is in terms of embeddings into these manifolds that we have defined the dimensions of a causal set.

The first notion of dimension, relevant on small scales at which a Lorentzian manifold is approximately flat, is the Minkowski dimension—defined to be the dimension of the minimal Minkowski space into which a causal set can be embedded. We found that this dimension is closely related to the combinatorial dimension of a poset: identical in dimension 2 and with the same irreducible configurations for

dimensions 2 and 3. We also showed that irreducible causal sets existed for arbitrarily large Minkowski dimension, and that there were irreducible causal sets with sizes which grew no faster than the volume as a function of the dimension, thus providing an effective local characterization of the dimension.

The second notion of dimension is relevant on larger scales where we can take advantage of the requirement that the embedding be faithful, *i.e.*, that the images of the causal set elements be uniformly distributed in the manifold. After taking the Poisson process to model this distribution we found that expectation values of causal set paramenters, in particular the number of chains of a given length, depend on the dimension of the manifold in which the Poisson process is occurring. The Hausdorff dimension is defined to be the dimension extracted from this dependence for intervals of a causal set. For the physically interesting (and mathematically simple!) cases of Minkowski, de Sitter and anti-de Sitter space we obtained explicit formulae for $\langle C_k \rangle$ in terms of the dimension, curvature and height of an Alexandroff neighborhood. Numerical simulations confirmed these results and showed that the Hausdorff dimension could be effectively computed. Moreover, we verified that as expected, geometrical as well as topological quantities could be determined when the embedding is faithful: the scalar curvature of these constant curvature manifolds and the circumference and height of cylinders obtained by periodic identifications of Minkowski space.

Directions for further work

From a mathematical point of view these results can be taken as evidence supporting the *Hauptvermutung* that a faithful embedding of a causal set into a Lorentzian manifold determines the manifold with metric up to "approximate isometry," but are not really steps in the direction of proving it. This is clearly an outstanding

problem. A simplified version of this conjecture can be stated precisely, however, and it is reasonably clear how a proof should proceed. That is, an embedding (not necessarily faithful) of a causal set into a Lorentzian manifold is an approximation (not necessarily a good one!) to the causal structure of the manifold and thus, as we know from the theorems of Hawking and Malament described in the Introduction, should approximately determine at least the topology of the manifold. "Approximately" here should be taken to mean that the manifold, as a topological space, is the limit of an inverse system of finite topological spaces (as in [Sorkin 1987]) associated with causal sets which embed in the manifold. Working through the details of a proof of this statement may shed a little light on the general conjecture.

Several more mathematical questions arise in connection with the Minkowski dimension of causal sets. It is hard to imagine that there are causal sets which cannot be embedded in some Minkowski space of sufficiently large dimension. Nevertheless, despite efforts by several people, there is no proof to the contrary. As noted at the end of the first section on combinatorial dimension the largest number of dimensions which could possibly be necessary is one less than the number of elements in the causal set. Since the intersections of past lightcones with a spacelike hypersurface are spheres, this problem is equivalent to the question of whether every acyclic directed graph is a containment graph for some set of spheres in a Euclidean space of dimension no more than one less than the number of spheres. There ought to be a geometrical combinatorics argument verifying that this is the case. This problem might also be solved as an immediate consequence of a proof of another outstanding conjecture about the Minkowski dimension: that the Minkowski dimension of a causal set is never larger than its combinatorial dimension. Since determining the combinatorial dimension of a causal set is an NP-complete problem [Garey and Johnson 1979], such a result would have implications for the computability of the

Minkowski dimension as well. Finally, one would also obtain an existence proof and an upper bound if a One-point Removal Theorem were proved for Minkowski dimension.

More concretely, the Minkowski dimension of additional causal sets should be computed explicitly. One approach to doing so is an application of simulated annealing [Kirkpatrick, Gelatt and Vecchi 1983]: for a given causal set P, define an energy $E := \sum_{i>j} E_{ij}$ associated to each map of P into $d+1$ dimensional Minkowski space, where E_{ij} vanishes if the images of $i, j \in P$ have the correct causal relation. A map with vanishing energy is an embedding, and implies an upper bound on the Minkowski dimension of P. In addition, once phrased in this manner, there are immediate connections with statistical mechanics. Work along these lines is in progress.

Further numerical work could be done for the Hausdorff dimension as well. Running simulations with larger numbers of points N would provide better statistics, especially for larger dimensional spacetimes. Specifically, it would be nice to see a flat five dimensional Kaluza-Klein manifold with one compactified dimension. More significantly, in the case of constant curvature, larger N simulations are necessary to reduce statistical fluctuations sufficiently to extract the correct results even in dimension 3. Other sets of causal set parameters might also be considered, to decrease the near singularity of the system of equations being solved. It is worth noting in this context that the algorithms are eminently parallelizable: the matrix multiplications required to compute the numbers of k-chains can be done by computing vector dot products in parallel; moreover, the Newton Raphson solution for the dimension and curvature can be done for each interval independently, and therefore in parallel.

The obvious extension of the analytic results on the Hausdorff dimension is to more general manifolds. The case of Minkowski space demonstrates that the dimension can really be extracted from causal set parameters, while the cases of constant curvature space show that geometrical quantities can be extracted as well. For a general manifold the expectation values $\langle C_k \rangle$ in an Alexandroff neighborhood should be calculable by working in Riemann normal coordinates [Eisenhart 1925, Petrov 1969] to find their dependence on the metric and its derivatives at a point of origin in the neighborhood. In particular we would expect still to be able to extract a Hausdorff dimension and also the scalar curvature; this might have relevance for the quantum dynamics of causal sets—the topic which we discuss, briefly, in the last section.

Quantum dynamics of causal sets

Recall that we envision the causal set program as an approach to quantum gravity. The Lorentzian manifold of general relativity is then only a large scale approximation arising as the classical limit from the condition of constructive interference among the quantum amplitudes of contributing causal sets. This means that a quantum amplitude should be defined for every causal set in such a way that, in situations which admit a classical general relativistic continuum solution, the causal sets which can be faithfully embedded (possibly after coarse graining) in the continuum geometry should dominate the sum over histories, in the sense that they have stationary phase. If we suppose that the amplitude of such a causal set is multiplicative, *i.e.*, it is approximately the product of the amplitudes of any subcausal sets into which the given causal set can be (macroscopically) partitioned, then the action (which is proportional to the logarithm of the amplitude) has the form in the continuum approximation of an integral over the manifold of a (local) scalar density.

In general relativity, of course, the action is $\int R\, dV$. Although there are several proposals for the amplitude of a causal set which are possibly more natural from the point of view that causal sets are the fundamental structure (see [Bombelli 1987]), the results of the line of investigation we have followed in the preceding chapters suggest an action which corresponds to this general relativistic action. That is, to each element of the causal set associate a scalar curvature (computed for intervals as in the case of the constant curvature manifolds we considered in the last chapter, or more generally, as proposed at the end of the previous section) in a way which best fits the curvatures for the intervals used and then sum the curvatures over the elements of the causal set. This should, in fact, be an approximation to the Einstein-Hilbert action. Of course, there is no guarantee that with this choice of action the causal sets faithfully embeddable in Lorentzian manifolds really dominate a sum over histories. Nevertheless, this is a concrete proposal for the action and its consequences can be investigated.

In fact, this action, as well as others one might define, can be investigated numerically. For an action which is effectively computable, we would like to evaluate $\sum f(P) \exp(\frac{i}{\hbar} S[P])$, where the sum is over all contributing causal sets P, to find the amplitude for some quantity (operator) $f(P)$. If large causal sets contribute to this sum it is impractical to compute it exactly (since as $N \to \infty$ the number of posets with N elements is asymptotically proportional to $2^{N^2/4+3N/2} e^N N^{-N-1}$ [Kleitman and Rothschild 1975]), but we might hope to do some sort of Monte Carlo simulation (possibly by defining real amplitudes—Euclideanizing) by summing only over a random selection of causal sets. Alternatively, we might also determine the "classical" solutions by identifying the critical points (insofar as a discrete system has critical points) of the action (perhaps by simulated annealing) and then evaluate the quantity $f(P)$ for those causal sets. In particular, if $f(P)$ were the Hausdorff

dimension of the causal set, this would give an expectation value for the dimension of spacetime. Thus the causal set program, with the notion of the dimension of causal sets, may provide the opportunity to explain some of the phenomenology we discussed in the Introduction as possibly derivable consequences of a quantum theory of gravity.

Appendix A

The Pascal program listed here produces causal sets faithfully embedded in two dimensional Minkowski or (anti) de Sitter space, uses the chi-square test described in Chapter III to test the uniformity of the distribution of points and then draws the Hasse diagram for the causal set. The function *random* is a modification of the subroutine `RAN3` listed in [Press, Flannery, Teukolsky and Vetterling 1986] which is an implemention of an algorithm suggested by Knuth in [Knuth 1969]. The procedure *topsort* is a modification of the *Quicksort* procedure given in [Graham 1980] which is again an implementation of an algorithm described by Knuth in [Knuth 1973b].

```
program csdraw(output);
   const
      dim = 2;
      N = 200;
      B = 7;
      KT2 = 3.9;
   type
      matrix = array[1..N,1..N] of integer;
      pmatrix = array[1..N,1..dim] of real;
   var
      randlist : array[1..55] of real;
      randnexti,randnextj : integer;
      x : pmatrix;
      relations,links : integer := 0;
      z : matrix;
      bins : array[0..B-1,0..B-1] of integer;
      i : integer;
      xoffset,yoffset : real;
      rnd : real;
      seed : integer := 1959;

   function random(var initialize : boolean) : real;
      const
         big = 4.0e6;
         seed = 1959028.0;
      var
         i,imod,j : integer;
         a,b : real;
      begin
         if initialize then
            begin
               a := seed;
               if a>=0 then
                  a := a - big*trunc(a/big)
               else
                  a := big - abs(a) + big*trunc(abs(a)/big);
               randlist[55] := a;
               b := 1;
               for i:=1 to 54 do
                  begin
                     imod := 21*i mod 55;
                     randlist[imod] := b;
                     b := a - b;
                     if b<0 then
                        b := b + big;
                     a := randlist[imod]
                  end;
               for j:=1 to 4 do
                  for i:=1 to 55 do
                     begin
                        randlist[i] := randlist[i] - randlist[1 + ((i+30) mod 55)];
                        if randlist[i]<0 then
                           randlist[i] := randlist[i] + big
                     end;
               randnexti := 0;
               randnextj := 31;
```

```
            initialize := false
         end;
      randnexti := randnexti + 1;
      if randnexti=56 then
         randnexti := 1;
      randnextj := randnextj + 1;
      if randnextj=56 then
         randnextj := 1;
      a := randlist[randnexti] - randlist[randnextj];
      if a<0 then
         a := a + big;
      randlist[randnexti] := a;
      random := a/big
   end; { random }

{procedure random(var seed : integer; var rnd : real);
fortran;}

procedure sprinkle;

   var
      initialize : boolean;
      i,l,ubin,vbin : integer;
      hold : real;

   begin
      bins := zero;
      initialize := true;
      for i:=1 to N do
         begin
            for l:=1 to dim do
               begin
                  {random(seed,rnd);
                  x[i,l] := rnd}
                  x[i,l] := random(initialize)
               end;
            ubin := trunc(x[i,1]*B);
            vbin := trunc(x[i,2]*B);
            bins[ubin,vbin] := bins[ubin,vbin] + 1;
            hold := x[i,2];
            x[i,2] := hold + x[i,1];
            x[i,1] := x[i,1] - hold
         end
   end; { sprinkle }

procedure ccsprinkle;

   var
      i,l : integer;
      r2,norm,sigma : real;
      initialize : boolean;

   begin
      norm := 1;
      if KT2>0 then
         norm := (norm - KT2/4.0)**(-dim);
      initialize := true;
      i := 1;
      repeat
         r2 := 0;
         for l:=1 to dim do
```

```
            begin
               x[i,1] := random(initialize);
               if 1<dim then
                   r2 := r2 + (x[i,1]-0.5)**2
            end;
         if (r2<x[i,dim]**2) and (r2<(1-x[i,dim])**2) then
            begin
               sigma := 1 + KT2*(r2-x[i,dim]**2)/4.0;
               sigma := sigma**(-dim);
               if no..1*random(initialize)<=sigma then
                  i := i + 1
            end
      until i=N+1
   end; { ccsprinkle }

procedure chisquare;
   var
      ubin,vbin,Ysmall,Ybig,k,dof : integer;
      Y : array[0..N] of integer;
      remaining,counted,fraction,expect,chi2 : real;
   begin
      Y := zero;
      for ubin:=0 to B-1 do
         for vbin:=0 to B-1 do
            Y[bins[ubin,vbin]] := Y[bins[ubin,vbin]] + 1;
      for k:=0 to N do
         writeln(k,Y[k]);
      remaining := B*B;
      counted := 0;
      fraction := 1/remaining;
      expect := remaining*((1-fraction)**N);
      Ysmall := 0;
      k := 0;
      dof := 0;
      while (expect<5) or (counted<5) do
         begin
            Ysmall := Ysmall + Y[k];
            remaining := remaining - expect;
            counted := counted + expect;
            expect := expect*(N-k)*fraction/((k+1)*(1-fraction));
            k := k + 1
         end;
      writeln(k-1,Ysmall,counted);
      if k>0 then
         begin
            chi2 := ((Ysmall - counted)**2)/counted;
            dof := dof + 1
         end
      else
         chi2 := 0;
      while (expect>5) and (remaining-expect>5) do
         begin
            writeln(k,Y[k],expect);
            chi2 := chi2 + ((Y[k] - expect)**2)/expect;
            dof := dof + 1;
            remaining := remaining - expect;
            expect := expect*(N-k)*fraction/((k+1)*(1-fraction));
            k := k + 1
```

```
         end;
      write(k);
      Ybig := 0;
      repeat
         Ybig := Ybig + Y[k];
         expect := expect*(N-k)*fraction/((k+1)*(1-fraction));
         k := k + 1
      until k=N+1;
      writeln(Ybig,remaining);
      chi2 := chi2 + ((Ybig - remaining)**2)/remaining;
      writeln('chi2 with ',dof,' degrees of freedom = ',chi2)
   end; { chisquare }

procedure drawstart;
fortran;

procedure rescale(xoffset,yoffset : real);
fortran;

procedure postdraw;
fortran;

procedure topsort;
   var
      i,j,l,first,last,middle,top : integer;
      stack : array[1..N] of integer;
      cutoff,hold : real;
   begin
      stack[1] := 1;
      stack[2] := N;
      top := 2;
      repeat
         last := stack[top];
         top := top - 1;
         first := stack[top];
         top := top - 1;
         i := first;
         repeat
            j := last;
            middle := (first + last) div 2;
            cutoff := x[middle,dim];
            repeat
               while x[i,dim] < cutoff do
                  i := i + 1;
               while x[j,dim] > cutoff do
                  j := j - 1;
               if i <= j then
                  begin
                     for l:=1 to dim do
                        begin
                           hold := x[i,l];
                           x[i,l] := x[j,l];
                           x[j,l] := hold
                        end;
                     i := i + 1;
                     j := j - 1
                  end
            until i > j;
            if first < j then
```

```
            begin
               top := top + 1;
               stack[top] := first;
               top := top + 1;
               stack[top] := j
            end;
         first := i
      until first >= last
   until top = 0
end; { topsort }

procedure incidence;
   var
      i,j,l : integer;
      s2 : real;
   begin
      z := zero;
      for i:=1 to N-1 do
         for j:=i+1 to N do
            begin
               s2 := -(x[j,dim] - x[i,dim])**2;
               for l:=1 to dim-1 do
                  s2 := s2 + (x[j,l] - x[i,l])**2;
               if s2 < 0 then
                  begin
                     relations := relations + 1;
                     z[i,j] := 1
                  end
            end
end; { incidence }

procedure volume;
   var
      i,j,k : integer;
   begin
      for i:=1 to N-2 do
         for j:=i+2 to N do
            for k:=i+1 to j-1 do
               if z[k,j] = 1 then
                  z[j,i] := z[j,i] + z[i,k]
end; { volume }

procedure flink(x0,y0,x1,y1 : real);
fortran;

procedure adjacency;
   var
      i,j : integer;
   begin
      for i:=1 to N-1 do
         for j:=i+1 to N do
            if (z[i,j] = 1) and (z[j,i] = 0) then
               begin
                  flink(x[i,1],x[i,2],x[j,1],x[j,2]);
                  links := links + 1
               end
end; { adjacency }
```

```
begin { csdraw }
   drawstart;
   writeln('sprinkling points ...');
   sprinkle;
   {ccsprinkle;}
   chisquare;
   rescale(-0.600,-9.000);
   writeln('sorting points ...');
   topsort;
   write('ordering points ...');
   incidence;
   writeln(' relations =',relations:4);
   writeln('computing volumes ...');
   volume;
   write('finding links ...');
   adjacency;
   writeln(' links =',links:4);
   postdraw
end. { csdraw }
```

Appendix B

The Pascal program listed here produces causal sets faithfully embedded in *dim* dimensional Minkowski space or in a cylindrical spacetime obtained from Minkowski space by making periodic identifications in *compact* number of spatial dimensions Having produced the causal set it computes the number of elements and relations in each interval $|x, y|$ and inverts the formula

$$f(d) = \frac{C_2\left(|x,y|\right)}{\left(N\left(|x,y|\right)\right)^2};$$

to find the Hausdorff dimension of the interval. The results are output to a graphics program which produces the plots shown in Chapter III.

```
program reldim(input,output);
   const
      dim = 3;
      N = 500;
      compact = 1;
      H = 10;
   type
      matrix = array[1..N,1..N] of integer;
   var
      randlist : array[1..55] of real;
      randnexti,randnextj : integer;
      x : array[1..N,1..dim] of real;
      totalrelations : integer := 0;
      totaldimension : real;
      z,zT : matrix;
      rd : array[1..N,1..N] of real;
      F : array[0..100] of real;
   function random(var initialize : boolean) : real;
      const
         big = 4.0e6;
         seed = 1959028.0;
      var
         i,imod,j : integer;
         a,b : real;
      begin
         if initialize then
            begin
               a := seed;
               if a>=0 then
                  a := a - big*trunc(a/big)
               else
                  a := big - abs(a) + big*trunc(abs(a)/big);
               randlist[55] := a;
               b := 1;
               for i:=1 to 54 do
                  begin
                     imod := 21*i mod 55;
                     randlist[imod] := b;
                     b := a - b;
                     if b<0 then
                        b := b + big;
                     a := randlist[imod]
                  end;
               for j:=1 to 4 do
                  for i:=1 to 55 do
                     begin
                        randlist[i] := randlist[i] - randlist[1 + ((i+30) mod 55)];
                        if randlist[i]<0 then
                           randlist[i] := randlist[i] + big
                     end;
               randnexti := 0;
               randnextj := 31;
               initialize := false
            end;
         randnexti := randnexti + 1;
```

```
      if randnexti=56 then
         randnexti := 1;
      randnextj := randnextj + 1;
      if randnextj=56 then
         randnextj := 1;
      a := randlist[randnexti] - randlist[randnextj];
      if a<0 then
         a := a + big;
      randlist[randnexti] := a;
      random := a/big
   end; { random }

function Finverse(x : real) : real;
   const
      phi = 0.618033988;
   var
      left,right,guess : integer;
   begin
      left := 0;
      right := 100;
      repeat
         guess := trunc(left + phi*(right - left));
         if F[guess]<x then
            right := guess
         else
            left := guess
      until right = left + 1;
      Finverse := (right - (x - F[right])/(F[left] - F[right]))/10
   end; { Finverse }

procedure sprinkle;
   var
      i,l : integer;
      r2 : real;
      initialize : boolean;
   begin
      initialize := true;
      i := 1;
      repeat
         r2 := 0;
         for l:=1 to dim do
            begin
               x[i,l] := random(initialize);
               if l<dim then
                  r2 := r2 + (x[i,l]-0.5)**2
            end;
         if compact > 0 then
            begin
               for l:=compact+1 to dim do
                  x[i,l] := H*x[i,l];
               i := i + 1
            end
         else
            if (r2<x[i,dim]**2) and (r2<(1-x[i,dim])**2) then
               i := i + 1
      until i=N+1
   end; { sprinkle }
```

```
procedure topsort;
   var
      i,j,l,first,last,middle,top : integer;
      stack : array[1..N] of integer;
      cutoff,hold : real;
   begin
      stack[1] := 1;
      stack[2] := N;
      top := 2;
      repeat
         last := stack[top];
         top := top - 1;
         first := stack[top];
         top := top - 1;
         i := first;
         repeat
            j := last;
            middle := (first + last) div 2;
            cutoff := x[middle,dim];
            repeat
               while x[i,dim] < cutoff do
                  i := i + 1;
               while x[j,dim] > cutoff do
                  j := j - 1;
               if i <= j then
                  begin
                     for l:=1 to dim do
                        begin
                           hold := x[i,l];
                           x[i,l] := x[j,l];
                           x[j,l] := hold
                        end;
                     i := i + 1;
                     j := j - 1
                  end
            until i > j;
            if first < j then
               begin
                  top := top + 1;
                  stack[top] := first;
                  top := top + 1;
                  stack[top] := j
               end;
            first := i
         until first >= last
      until top = 0
   end; { topsort }

procedure incidence;
   var
      i,j,l : integer;
      s2,min,max : real;
   begin
      for i:=1 to N-1 do
         for j:=i+1 to N do
```

```
            begin
               s2 := -(x[j,dim] - x[i,dim])**2;
               for l:=1 to compact do
                  begin
                     min := (x[j,l] - x[i,l])**2;
                     max := (x[j,l] - x[i,l] + 1)**2;
                     if min > max then
                        min := max;
                     max := (x[j,l] - x[i,l] - 1)**2;
                     if min > max then
                        min := max;
                     s2 := s2 + min
                  end;
                  for l:=compact+1 to dim-1 do
                     s2 := s2 + (x[j,l] - x[i,l])**2;
                  if s2 < 0 then
                     begin
                        z[i,j] := 1;
                        zT[j,1] := 1;
                        totalrelations := totalrelations + 1
                     end
            end
   end; { incidence }

procedure volume;
   var
      i,j,k : integer;
   begin
      for i:=1 to N-2 do
         for j:=i+2 to N do
            for k:=i+1 to j-1 do
               if zT[j,k] = 1 then
                  zT[i,j] := zT[i,j] + z[i,k]
   end; { volume }

procedure relation;
   var
      i,j,k : integer;
   begin
      for i:=1 to N-2 do
         for j:=i+2 to N do
            if z[i,j]=1 then
               for k:=i+1 to j-1 do
                  if z[i,k]*zT[j,k]=1 then
                     rd[i,j] := rd[i,j] + zT[k,j]
   end; { relation }

procedure readtable;
   var
      infile : text;
      i : integer;
   begin
      open(infile,'dimcoef.dat',old);
      reset(infile);
      for i:=1 to 100 do
         readln(infile,F[i])
   end; { readtable }
```

```
procedure scatterstart;
fortran;

procedure scatter(i,x : integer; y : real);
fortran;

procedure scatterstop;
fortran;

procedure dimension;
   var
      i,j,k,npts : integer;
   begin
      readtable;
      scatterstart;
      npts := 0;
      for i:=1 to N-2 do
         for j:=i+2 to N do
            if rd[i,j]>0 then
               begin
                  npts := npts + 1;
                  rd[i,j] := Finverse(rd[i,j]/(zT[i,j]**2));
                  scatter(1,zT[i,j],rd[i,j])
               end;
      for i:=0 to N do
         scatter(4,i,dim-1);
      scatterstop;
      totaldimension := Finverse(totalrelations/(N*N))
   end; { dimension }

begin { reldim }
   writeln('sprinkling points ...');
   sprinkle;
   writeln('sorting points ...');
   topsort;
   writeln('ordering points ...');
   incidence;
   writeln('computing volumes ... totalvolume ',N);
   volume;
   writeln('computing relations ... totalrelations ',totalrelations);
   relation;
   write('computing dimensions ... totaldimension ');
   dimension;
   writeln(totaldimension)
end. { reldim }
```

Appendix C

The Pascal program listed here produces causal sets faithfully embedded in an Alexandroff neighborhood of *dim* dimensional (anti) de Sitter space parameterized by *KT2*. Having produced the causal set it computes the number of elements C_1, relations C_2 and 3-chains C_3 in each interval and then solves the system of equations

$$C_1 = f_1(d, K; T)$$

$$C_2 = f_2(d, K; T)$$

$$C_3 = f_3(d, K; T)$$

for d, K and T. (The function *Gammaln* used by procedure *Gcoef* to compute the coefficients $G_d(i_1, \ldots, i_k)$ in the functions $f_k(d, K; T)$ is a slight modification of the subroutine `gammln` listed in [Press, Flannery, Teukolsky and Vetterling 1986].) The results are output to a graphics program which produces the plots shown in Chapter III.

```
program ccNR(input,output);
   const
      dim = 3;
      N = 400;
      KT2 = 1.0;
      mintabled = 0;
      maxtabled = 100;
      degree = 10;
      pi = 3.141592654;
      maxiterations = 100;
   type
      matrix = array[1..N,1..N] of integer;
   var
      randlist : array[1..55] of real;
      randnexti,randnextj : integer;
      x : array[1..N,1..dim] of real;
      totalrelations : integer := 0;
      total3chains : integer := 0;
      totaldimension : real;
      z,zT : matrix;
      F : array[0..100] of real;
       : array[mintabled..maxtabled,0..degree] of double;
      G2 : array[mintabled..maxtabled,0..degree,0..degree] of double;
      G3 : array[mintabled..maxtabled,0..degree,0..degree,0..degree] of double;
      C1,C2,C3 : integer;
      Kold,Told,dold : double;
      Knew,Tnew,dnew : double;
      iterations : integer;
      i,j,number : integer;
      restart : boolean;
      totaliterations : integer := 0;
      convergences : integer := 0;
      convergencefailures : integer := 0;
   function random(var initialize : boolean) : real;
      const
         big = 4.0e6;
         seed = 1959028.0;
      var
         i,imod,j : integer;
         a,b : real;
      begin
         if initialize then
            begin
               a := seed;
               if a>=0 then
                  a := a - big*trunc(a/big)
               else
                  a := big - abs(a) + big*trunc(abs(a)/big);
               randlist[55] := a;
               b := 1;
               for i:=1 to 54 do
                  begin
                     imod := 21*i mod 55;
                     randlist[imod] := b;
                     b := a - b;
```

```
                if b<0 then
                   b := b + big;
                a := randlist[imod]
             end;
          for j:=1 to 4 do
             for i:=1 to 55 do
                begin
                   randlist[i] := randlist[i] - randlist[1 + ((i+30) mod 55)];
                   if randlist[i]<0 then
                      randlist[i] := randlist[i] + big
                end;
          randnexti := 0;
          randnextj := 31;
          initialize := false
       end;
    randnexti := randnexti + 1;
    if randnexti=56 then
       randnexti := 1;
    randnextj := randnextj + 1;
    if randnextj=56 then
       randnextj := 1;
    a := randlist[randnexti] - randlist[randnextj];
    if a<0 then
       a := a + big;
    randlist[randnexti] := a;
    random := a/big
 end; { random }

function Finverse(x : real) : real;
 const
    phi = 0.618033988;
 var
    left,right,guess : integer;
 begin
    left := 0;
    right := 100;
    repeat
       guess := trunc(left + phi*(right - left));
       if F[guess]<x then
          right := guess
       else
          left := guess
    until right = left + 1;
    Finverse := (right - (x - F[right])/(F[left] - F[right]))/10
 end; { Finverse }

function Gammaln(x : double) : double;
 const
    roottwopi = 2.50662827465;
 var
    z,temp,sum : double;
    i : integer;
    coef : array[1..6] of double;
    small : boolean;
    hold : double;
```

```
   begin
      coef[1] :=  76.18009173;
      coef[2] := -86.50532033;
      coef[3] :=  24.01409822;
      coef[4] := -1.231739516;
      coef[5] :=  0.120858003e-2;
      coef[6] := -0.536382e-5;
      small := false;
      if x<1 then
         begin
            small := true;
            x := 1 - x
         end;
      z := x - 1;
      temp := z + 5.5;
      temp := (z + 0.5)*ln(temp) - temp;
      sum := 1;
      for i:=1 to 6 do
         begin
            z := z + 1;
         end;sum := sum + coef[i]/z

      hold := temp + ln(roottwopi*sum);
      Gammaln := hold;
      if small then
         Gammaln := ln(pi) - hold - ln(sin(pi*x));
   end; { Gammaln }

procedure readtable;
   var
      infile : text;
      i : integer;
   begin
      open(infile,'dimcoef.dat',old);
      reset(infile);
      for i:=1 to 100 do
         readln(infile,F[i])
   end; { readtable }

procedure Gcoef;
   var
      tabled,i1,i2,i3 : integer;
      d,fact,expo : double;
   begin
      for tabled:=mintabled to maxtabled do
         begin
            d := tabled/10.0;
            for i1:=0 to degree do
               begin
                  G1[tabled,i1] := 1/(d+2*i1+1);
                  for i2:=0 to degree-i1 do
                     begin
                        fact := G1[tabled,i1]/(2*(d+1)+2*(i1+i2));
                        expo := Gammaln(d+i2+1)+Gammaln((d+1)/2+i1+i2+1);
                        expo := expo-Gammaln(i2+1)-Gammaln(3*(d+1)/2+i1+i2);
                        G2[tabled,i1,i2] := fact*exp(expo);
```

```
                        for i3:=0 to degree-i1-i2 do
                           begin
                              fact := G2[tabled,i1,i2]/(3*(d+1)+2*(i1+i2+i3));
                              expo := Gammaln(d+i3+1)+Gammaln(d+2+i1+i2+i3);
                              expo := expo-Gammaln(i3+1)-Gammaln(2*(d+1)+i1+i2+i3);
                              G3[tabled,i1,i2,i3] := fact*exp(expo)
                           end
                     end
               end
         end
   end; { Gcoef }

procedure scatterstart;
fortran;

procedure scatter(i,x : integer; y : double);
fortran;

procedure scatterstop;
fortran;

procedure ccsprinkle;
   var
      i,l : integer;
      r2,norm,sigma : real;
      initialize : boolean;
   begin
      norm := 1;
      if KT2>0 then
         norm := (norm - KT2/4.0)**(-dim);
      initialize := true;
      i := 1;
      repeat
         r2 := 0;
         for l:=1 to dim do
            begin
               x[i,l] := random(initialize);
               if l<dim then
                   r2 := r2 + (x[i,l]-0.5)**2
            end;
         if (r2<x[i,dim]**2) and (r2<(1-x[i,dim])**2) then
            begin
               sigma := 1 + KT2*(r2-x[i,dim]**2)/4.0;
               sigma := sigma**(-dim);
               if norm*random(initialize)<=sigma then
                  i := i + 1
            end
      until i=N+1
   end; { ccsprinkle }

procedure topsort;
   var
      i,j,l,first,last,middle,top : integer;
      stack : array[1..N] of integer;
      cutoff,hold : real;
   begin
      stack[1] := 1;
      stack[2] := N;
      top := 2;
```

```
      repeat
         last := stack[top];
         top := top - 1;
         first := stack[top];
         top := top - 1;
         i := first;
         repeat
            j := last;
            middle := (first + last) div 2;
            cutoff := x[middle,dim];
            repeat
               while x[i,dim] < cutoff do
                  i := i + 1;
               while x[j,dim] > cutoff do
                  j := j - 1;
               if i <= j then
                  begin
                     for l:=1 to dim do
                        begin
                           hold := x[i,l];
                           x[i,l] := x[j,l];
                           x[j,l] := hold
                        end;
                     i := i + 1;
                     j := j - 1
                  end
            until i > j;
            if first < j then
               begin
                  top := top + 1;
                  stack[top] := first;
                  top := top + 1;
                  stack[top] := j
               end;
            first := i
         until first >= last
      until top = 0
   end; { topsort }

procedure incidence;
   var
      i,j,l : integer;
      s2 : real;
   begin
      for i:=1 to N-1 do
         for j:=i+1 to N do
            begin
               s2 := -(x[j,dim] - x[i,dim])**2;
               for l:=1 to dim-1 do
                  s2 := s2 + (x[j,l] - x[i,l])**2;
               if s2 < 0 then
                  begin
                     z[i,j] := 1;
                     zT[j,i] := 1;
                     totalrelations := totalrelations + 1
                  end
            end
   end; { incidence }
```

```
procedure volume;
   var
      i,j,k : integer;
   begin
      for i:=1 to N-2 do
         for j:=i+2 to N do
            begin
               for k:=i+1 to j-1 do
                  zT[i,j] := zT[i,j] + z[i,k]*zT[j,k];
               total3chains := total3chains + zT[i,j]
            end
   end; { volume }

procedure relation;
   var
      i,j,k : integer;
   begin
      for i:=1 to N-2 do
         for j:=i+2 to N do
            if zT[i,j]>=1 then
               for k:=i+1 to j-1 do
                  z[j,i] := z[j,i] + z[i,k]*zT[k,j]
   end; { relation }

procedure threechain;
   var
      i,j,k : integer;
   begin
      for i:=1 to N-1 do
         for j:=i+1 to N do
            begin
               zT[j,i] := 0;
               if z[j,i]>=1 then
                  for k:=i+1 to j-1 do
                     zT[j,i] := zT[j,i] + z[i,k]*z[j,k]
            end
   end; { threechain }

procedure NewtonRaphson;
   var
      s : double;
      tabled,i1,i2,i3 : integer;
      S1,S2,S3,S1_K,S2_K,S3_K,S1_d,S2_d,S3_d : double;
      f1,f2,f1_K,f2_K,f1_d,f2_d : double;
      denom,deltaK,deltad,E : double;
      outsiderange : integer;
      dtemp,Ktemp,p1,p2 : double;
   begin
      if restart then
         begin
            dold := Finverse(C2/(C1**2));
            Kold := 0.0001
         end;
      dnew := dold;
      Knew := Kold;
```

```
deltad := 0;
deltaK := 0;
iterations := 0;
repeat
   outsiderange := 0;
   repeat
      dtemp := dnew + deltad/(2**outsiderange);
      tabled := trunc(10.0*dtemp);
      outsiderange := outsiderange + 1
   until ((tabled<maxtabled) and (tabled>mintabled)) or (outsiderange=20);
   dnew := dtemp;
   outsiderange := 0;
   repeat
      Ktemp := Knew + deltaK/(2**outsiderange);
      outsiderange := outsiderange + 1
   until ((Ktemp<1) and (Ktemp>-1)) or (outsiderange=20);
   Knew := Ktemp;
   s := 10.0*dnew - tabled;
   if tabled>=maxtabled then
      begin
         tabled := maxtabled - 1;
         s := 1
      end;
   if tabled<mintabled then
      begin
         tabled := mintabled;
         s := 0
      end;
   if Knew>1 then
      Knew := 0.0001;
   if Knew<-1 then
      Knew := -0.0001;
   S1 := 0;
   S2 := 0;
   S3 := 0;
   S1_K := 0;
   S2_K := 0;
   S3_K := 0;
   S1_d := 0;
   S2_d := 0;
   S3_d := 0;
   for i1:=0 to degree do begin
      p1 := (1-s)*G1[tabled,i1]+s*G1[tabled+1,i1];
      p2 := (0.99-s)*G1[tabled,i1]+(0.01+s)*G1[tabled+1,i1]);
      S1 := S1 + (Knew**i1)*p1;
      S1_K := S1_K + i1*(Knew**(i1-1))*p1;
      S1_d := S1_d + (Knew**i1)*p2;
      for i2:=0 to degree-i1 do begin
         p1 := (1-s)*G2[tabled,i1,i2]+s*G2[tabled+1,i1,i2];
         p2 := (0.99-s)*G2[tabled,i1,i2]+(0.01+s)*G2[tabled+1,i1,i2];
         S2 := S2 + (Knew**(i1+i2))*p1;
         S2_K := S2_K + (i1+i2)*(Knew**(i1+i2-1))*p1;
         S2_d := S2_d + (Knew**(i1+i2))*p2;
         for i3:=0 to degree-i1-i2 do begin
            p1 := (1-s)*G3[tabled,i1,i2,i3]+s*G3[tabled+1,i1,i2,i3];
            p2 := (0.99-s)*G3[tabled,i1,i2,i3]+(0.01+s)*G3[tabled+1,i1,i2,i3];
            S3 := S3 + (Knew**(i1+i2+i3))*p1;
```

```
                S3_K := S3_K + (i1+i2+i3)*(Knew**(i1+i2+i3-1))*p1;
                S3_d := S3_d + (Knew**(i1+i2+i3))*p2
             end
          end
       end;
       S1_d := (S1_d - S1)*1000;
       S2_d := (S2_d - S2)*1000;
       S3_d := (S3_d - S3)*1000;
       f1 := C2*(S1**2) - (C1**2)*S2;
       f2 := C3*(S1**3) - (C1**3)*S3;
       f1_K := 2*C2*S1*S1_K - (C1**2)*S2_K;
       f2_K := 3*C3*(S1**2)*S1_K - (C1**3)*S3_K;
       f1_d := 2*C2*S1*S1_d - (C1**2)*S2_d;
       f2_d := 3*C3*(S1**2)*S1_d - (C1**3)*S3_d;
       denom := f1_d*f2_K - f1_K*f2_d;
       deltad := (-f1*f2_K + f1_K*f2)/denom;
       deltaK := (-f1_d*f2 + f1*f2_d)/denom;
       E := (f1**2) + (f2**2);
       iterations := iterations + 1;
    until (E<1.0e-6) or (iterations=maxiterations);
    if (iterations=maxiterations) and (E<1.0e-2) then
       iterations := iterations - 1;
    Tnew := S1
 end; { NewtonRaphson }

begin { ccNR }
 writeln('sprinkling points ... totalvolume ',N);
 ccsprinkle;
 writeln('sorting points ...');
 topsort;
 write('ordering points ... ');
 incidence;
 writeln('totalrelations ',totalrelations);
 write('computing volumes ... ');
 volume;
 writeln('total3chains ',total3chains);
 writeln('computing relations ... ');
 relation;
 writeln('computing threechains ... ');
 threechain;
 readtable;
 Gcoef;
 scatterstart;
 writeln('computing dimensions, curvatures ... ');
 for i:=1 to N-2 do begin
    restart := true;
    for j:=i+2 to N do
       if zT[j,i]>0 then begin
          C1 := zT[i,j];
          C2 := z[j,i];
          C3 := zT[j,i];
          NewtonRaphson;
          if iterations<maxiterations then begin
             restart := false;
             Kold := Knew;
             dold := dnew;
             totaliterations := totaliterations + iterations;
             convergences := convergences + 1;
```

```
                Tnew := dnew*exp(Gammaln(dnew/2))*C1/((pi**(dnew/2))*Tnew);
                Tnew := ((2**(dnew-1))*Tnew)**(1/(dnew+1));
                Knew := 4*Knew/(Tnew**2);
                scatter(1,zT[i,j],dnew);
                scatter(2,zT[i,j],Knew);
                scatter(3,zT[i,j],Tnew);
                scatter(7,zT[i,j],1.0)
             end
             else begin
                convergencefailures := convergencefailures + 1;
                scatter(8,zT[i,j],1.0)
             end
          end
    end;
    writeln(' convergences ',convergences);
    writeln(' convergencefailures ',convergencefailures);
    writeln(' average iterations ',totaliterations/convergences);
    C1 := N;
    C2 := totalrelations;
    C3 := total3chains;
    NewtonRaphson;
    writeln(' K = ',Knew,' T = ',Tnew,' KT2 = ',Knew*Tnew*Tnew,' d = ',dnew);
    Tnew := 0.0;
    dnew := dim - 1;
    for i:=0 to degree do
       Tnew := Tnew + ((KT2/4.0)**i)*G1[10*(dim - 1),i];
    Tnew := (2**(dnew-1))*dnew*exp(Gammaln(dnew/2))*N/((pi**(dnew/2))*Tnew);
    Tnew := Tnew**(1/(dnew+1));
    Knew := KT2/(Tnew**2);
    for i:=0 to N do begin
       scatter(4,i,dnew);
       scatter(5,i,Knew);
       scatter(6,i,Tnew*((i/N)**(1/dim)))
    end;
    scatterstop;
    writeln(' K = ',Knew,' T = ',Tnew,' KT2 = ',Knew*Tnew*Tnew,' d = ',dnew)
end. { ccNR }
```

Appendix D

This appendix contains a reprint of an earlier paper "On the stability of a non-supersymmetric ground state," *Class. Quantum Grav.* **3** (1986) 881–887 which describes the results of the previous project I worked on, under the guidance of Professor Daniel Z. Freedman at MIT.

Class. Quantum Grav. 3 (1986) 881-887. Printed in Great Britain

On the stability of a non-supersymmetric ground state

David A Meyer

Department of Mathematics, Massachusetts Institute of Technology, Cambridge, Massachusetts 02139, USA

Received 2 November 1985

Abstract. We consider the gauged $N=2$ (simple) supersymmetric seven-dimensional ($d=7$) supergravity theory with the scalar field potential having two critical points. Applying a modified Witten argument reduces the question of stability to deciding if a particular non-linear ordinary differential equation has a global solution. We show that it does and that therefore the non-supersymmetric ground state is stable against arbitrary spin-0, spin-1 and spin-2 fluctuations.

1. Introduction

The gauged $N=2$ (simple) supersymmetric seven-dimensional ($d=7$) supergravity theory has been constructed [1]; with a topological mass term the scalar field potential has two critical points as shown in figure 1. In [2] the stability of the local maximum against spin-0 and spin-2 fluctuations was investigated. The local maximum is a supersymmetric AdS ground state and it was shown to be stable both perturbatively and for arbitrarily large fluctuations which vanish asymptotically.

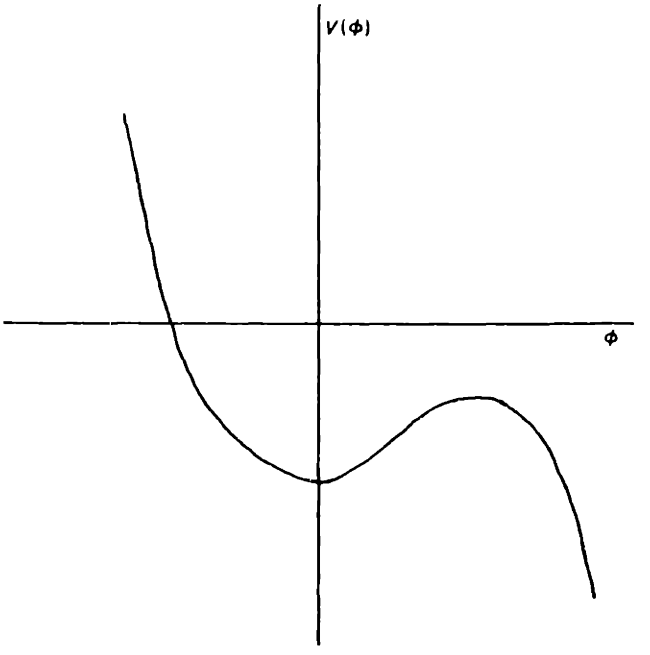

Figure 1. $V(\phi)$ has two critical points and is unbounded below. The case $g/h=4\sqrt{2}$ is shown.

0264-9381/86/050881+07$02.50

The local minimum is a non-supersymmetric state; Boucher [3] has shown how to investigate non-perturbative stability in such cases. In this paper we show that his approach can be used to establish the global stability of the local minimum of the scalar field potential, despite the fact that the potential is unbounded below.

The explicit form of the potential is

$$V(\phi) = -60m^2 + 10(m + 2h\sigma^4)^2 \tag{1.1}$$

where

$$m = -2h\sigma^4/5 - g\sigma^{-1}/5\sqrt{2} \tag{1.2}$$

$$\sigma = \exp(-\phi/\sqrt{5}). \tag{1.3}$$

The entire Lagrangian and transformation rules are given in references [1, 2]. For our purposes we set $A_{\mu i}' = 0$, which is consistent with its field equation. Then the bosonic part of the gauged Lagrangian is

$$L = -\tfrac{1}{2}R - \tfrac{1}{48}\sigma^{-4}(F_{\mu\nu\rho\sigma})^2 - \tfrac{1}{2}(\partial_\mu\phi)^2 - V(\phi) - \tfrac{1}{36}ih\epsilon^{\mu\nu\rho\sigma\kappa\lambda\tau}F_{\mu\nu\rho\sigma}A_{\kappa\lambda\tau} \tag{1.4}$$

and the transformation rules are (with bilinear fermion terms omitted)

$$\delta\psi_{\mu i} = D_\mu\varepsilon_i + (\sigma^{-2}/80\sqrt{2})(\Gamma_\mu{}^{\alpha\beta\gamma\delta} - \tfrac{8}{3}\delta_\mu^\alpha\Gamma^{\beta\gamma\delta})F_{\alpha\beta\gamma\delta}\varepsilon_i + m\Gamma_\mu\varepsilon_i \tag{1.5}$$

$$\delta\lambda_i = \tfrac{1}{2}\not{D}\varphi\varepsilon_i + (\sigma^{-2}/24\sqrt{10})\Gamma^{\mu\nu\rho\sigma}F_{\mu\nu\rho\sigma}\varepsilon_i - \sqrt{5}(m + 2h\sigma^4)\varepsilon_i. \tag{1.6}$$

The conventions are those of [1], namely

$$\{\Gamma_\mu, \Gamma_\nu\} = 2\delta_{\mu\nu} \tag{1.7}$$

$$\Gamma^{\mu_1\cdots\mu_n} = \Gamma^{[\mu_1}\cdots\Gamma^{\mu_n]} \tag{1.8}$$

$$F_{\mu_1\cdots\mu_n} = n!\partial_{[\mu_1}A_{\mu_2\cdots\mu_n]}. \tag{1.9}$$

2. Stability of the local maximum

Mezinescu, Townsend and van Nieuwenhuizen use the standard Witten argument [4] to show that the supersymmetric local maximum is stable for arbitrarily large spin-0 and spin-2 fluctuations. Since the proof for the local minimum is a modification of this argument we review their work and at the same time extend it to include fluctuations in $A_{\mu\nu\rho}$.

Define

$$E^{\mu\nu} = \bar{\varepsilon}^i\Gamma^{\mu\nu\rho}\hat{D}_\rho\varepsilon_i \tag{2.1}$$

with ε_i a commuting spinor and $\hat{D}_\rho\varepsilon_i \equiv \delta\psi_{\rho i}$ given by (1.5). Then

$$D_\nu E^{\mu\nu} = \hat{D}_\nu\bar{\varepsilon}^i\Gamma^{\mu\nu\rho}\hat{D}_\rho\varepsilon_i + \bar{\varepsilon}^i\Gamma^{\mu\nu\rho}\hat{D}_\nu\hat{D}_\rho\varepsilon_i. \tag{2.2}$$

After some algebra the second term on the RHS of (2.2) becomes

$$\bar{\varepsilon}^i\Gamma^{\mu\nu\rho}\hat{D}_\nu\hat{D}_\rho\varepsilon_i = -\tfrac{1}{2}(G^{\mu\lambda} - T^{\mu\lambda})\bar{\varepsilon}^i\Gamma_\lambda\varepsilon_i - \delta\bar{\lambda}^i\Gamma^\mu\delta\lambda_i + (3/2\sqrt{2})\bar{\varepsilon}^i\sigma^2\Gamma_{\nu\rho}J^{\mu\nu\rho}\varepsilon_i \tag{2.3}$$

where $J^{\mu\nu\rho}$ is the current due to $A_{\mu\nu\rho}$:

$$J^{\mu\nu\rho} \equiv \delta L/\delta A_{\mu\nu\rho} = D_\alpha(\tfrac{1}{6}\sigma^{-4}F^{\alpha\mu\nu\rho} + \tfrac{1}{18}ih\varepsilon^{\alpha\mu\nu\rho\beta\gamma\delta}4!A_{\beta\gamma\delta}) \equiv D_\alpha U^{\alpha\mu\nu\rho} \tag{2.4}$$

$T^{\mu\lambda}$ is the energy-momentum tensor from the matter part of the Lagrangian in (1.4) and $\delta\lambda_i$ is given by (1.6). Thus, using Gauss' theorem and equations (2.2) and (2.3), we have

$$\int_{\partial\Sigma} d\Sigma_{\mu\nu} E^{\mu\nu} = -2 \int_{\Sigma} d\Sigma_{\mu} [\hat{D}_{\nu} \bar{\varepsilon}^i \Gamma^{\mu\nu\rho} \hat{D}_{\rho} \varepsilon_i - \tfrac{1}{2}(G^{\mu\lambda} - T^{\mu\lambda}) \bar{\varepsilon}^i \Gamma_{\lambda} \varepsilon_i - \delta\bar{\lambda}^i \Gamma^{\mu} \delta\lambda_i + (3/2\sqrt{2}) \bar{\varepsilon}^i \sigma^2 \Gamma_{\nu\rho} J^{\mu\nu\rho} \varepsilon_i] \tag{2.5}$$

for a spacelike surface Σ and its boundary $\partial\Sigma$. For spinors ε_i which approach Killing spinors of the background at spatial infinity and for fluctuations about the background which vanish asymptotically the integral over $\partial\Sigma$ converges. Moreover, we restrict the class of fluctuations to those which, and insist that $\hat{D}_{\rho}\varepsilon_i$ does also, vanish sufficiently rapidly at spatial infinity that the integrals over Σ converge for all spacelike surfaces Σ.

Following Freedman and Gibbons [5], we consider (2.5) for exact Killing spinors of the background and keep only terms up to linear in the fluctuations. Then

$$\int_{\partial\Sigma} d\Sigma_{\mu\nu} E_L^{\mu\nu} = -2 \int_{\Sigma} d\Sigma_{\mu} [-\tfrac{1}{2}(G_L^{\mu\lambda} - T_L^{\mu\lambda}) \bar{\varepsilon}^i \Gamma_{\lambda} \varepsilon_i + (3/2\sqrt{2}) \bar{\varepsilon}^i \sigma_0^2 \Gamma_{\nu\rho} J_L^{\mu\nu\rho} \varepsilon_i] \tag{2.6}$$

where σ_0 is the background (local maximum) value of σ. Upon integration by parts the last term becomes (for $\partial\Sigma$ at spatial infinity)

$$\int_{\Sigma} d\Sigma_{\mu} \bar{\varepsilon}^i \sigma_0^2 \Gamma_{\nu\rho} D_{\alpha} U_L^{\alpha\mu\nu\rho} \varepsilon_i = -\int_{\Sigma} d\Sigma_{\mu} D_{\alpha} (\bar{\varepsilon}^i \sigma_0^2 \Gamma_{\nu\rho} \varepsilon_i) U_L^{\alpha\mu\nu\rho} \tag{2.7}$$

and

$$D_{\alpha} (\bar{\varepsilon}^i \sigma_0^2 \Gamma_{\nu\rho} \varepsilon_i) = 2 m_0 \sigma_0^2 \bar{\varepsilon}^i (g_{\alpha\nu} \Gamma_{\rho} - g_{\alpha\rho} \Gamma_{\nu}) \varepsilon_i. \tag{2.8}$$

However $U_L^{\alpha\mu\nu\rho}$ is totally antisymmetric, so this term vanishes.

Now we can rewrite (2.6) as

$$\int_{\partial\Sigma} d\Sigma_{\mu\nu} E_L^{\mu\nu} = \int_{\Sigma} d\Sigma_{\mu} (G_L^{\mu\lambda} - T_L^{\mu\lambda}) \bar{\varepsilon}^i \Gamma_{\lambda} \varepsilon_i = i \bar{\xi}^i \sigma^{AB} \xi_i M[K_{AB}] \tag{2.9}$$

where [4, 5], ξ_i are constant spinors parametrising the Killing spinors $\varepsilon_i(x)$, σ^{AB} are the generators of the spin representation of the isometry group of $(AdS)_7$, SO(6, 2), and $M[K_{AB}]$ are the corresponding Killing charges, defined by

$$M[K] = \int_{\Sigma} d\Sigma_{\mu} (G_L^{\mu\lambda} - T_L^{\mu\lambda}) K_{\lambda} \tag{2.10}$$

for a Killing vector K_{λ}. Finally we note that at spatial infinity $E_L^{\mu\nu}$ can be replaced by $E^{\mu\nu}$. Hence (2.5) becomes

$$\bar{\xi}^i \sigma^{AB} \xi_i M[K_{AB}] = 2i \int_{\Sigma} d\Sigma_{\mu} (\hat{D}_{\nu} \bar{\varepsilon}^i \Gamma^{\mu\nu\rho} \hat{D}_{\rho} \varepsilon_i - \delta\bar{\lambda}^i \Gamma^{\mu} \delta\lambda_i) \tag{2.11}$$

where we have used the equations of motion

$$G^{\mu\lambda} = T^{\mu\lambda} \qquad J^{\mu\nu\rho} = 0. \tag{2.12}$$

Choosing a frame such that the 0 direction is normal to Σ, and using a Majorana representation (in which the spinors are real and $C\Gamma_0 = -i$, where C is the charge conjugation matrix), we have

$$\bar{\xi}^i \sigma^{AB} \xi_i M[K_{AB}] = -2 \int_{\Sigma} d\Sigma_0 [(\Gamma^a \hat{D}_a \varepsilon^i)^T (\Gamma^b \hat{D}_b \varepsilon_i) + (\hat{D}^a \varepsilon^i)^T (D_a \varepsilon_i) + \delta\lambda^{iT} \delta\lambda_i] \tag{2.13}$$

where $a = 1, \ldots, 6$. Imposing a modified Witten condition

$$\Gamma^a \hat{D}_a \varepsilon_i = 0 \tag{2.14}$$

(whose solutions limit to Killing spinors at spatial infinity), and taking the trace over spinor indices on each side, we have

$$\xi'^{\mathrm{T}} \xi_i M[K_{07}] = 2 \int_\Sigma d\Sigma_0 [(\hat{D}_a \varepsilon')^{\mathrm{T}} (\hat{D}_a \varepsilon_i) + \delta\lambda'^{\mathrm{T}} \delta\lambda_i]. \tag{2.15}$$

Thus $E = M[K_{07}]$ is non-negative, and is zero iff $\hat{D}_\nu \varepsilon_i = 0 = \delta\lambda_i$, namely in the supersymmetric AdS background of the local maximum.

3. The modified Witten argument at the local minimum

For the local minimum, although (2.5) still holds (if the integrals converge) its interpretation changes. Using exact Killing spinors of the background and linearising, the first term on the RHS no longer vanishes and the integrals do not converge, because $\hat{D}_\rho$ does not approach the covariant derivative for the background. Hence we no longer obtain the Killing charges in (2.9). One can modify $\hat{D}_\rho$ and $\delta\lambda_i$, however, and still obtain an identity like (2.5) [3] which does produce the Killing charges.

Restricting our attention to fluctuations of the scalar and gravity fields, we proceed as before, using (1.5) and (1.6), but leave as functions to be determined the coefficients whose background values depend on the scalar field. That is, we define

$$\hat{D}_\mu = D_\mu + f\Gamma_\mu \tag{3.1}$$

$$\delta\lambda_i = (\tfrac{1}{2}\not{\partial}\phi + b)\varepsilon_i \tag{3.2}$$

and let

$$\hat{E}^{\mu\nu} = \bar{\varepsilon}^i \Gamma^{\mu\nu\rho} \hat{D}_\rho \varepsilon_i \tag{3.3}$$

as before. Using the modified $\hat{D}_\rho$ we find

$$\bar{\varepsilon}^i \Gamma^{\mu\nu\rho} \hat{D}_\nu \hat{D}_\rho \varepsilon_i = -\tfrac{1}{2} G^{\mu\lambda} \bar{\varepsilon}^i \Gamma_\lambda \varepsilon_i + 5\partial_\nu f \bar{\varepsilon}^i \Gamma^{\mu\nu} \varepsilon_i - 30 f^2 \bar{\varepsilon}^i \Gamma^\mu \varepsilon_i. \tag{3.4}$$

Also,

$$\delta\bar{\lambda}^i \Gamma^\mu \delta\lambda_i = \bar{\varepsilon}^i [-\tfrac{1}{4}(2\partial^\mu \phi \partial_\nu \phi \Gamma^\nu - \partial_\nu \phi \partial^\nu \phi \Gamma^\mu) + b\Gamma^{\mu\nu}\partial_\nu \phi + b^2 \Gamma^\mu] \varepsilon_i \tag{3.5}$$

and

$$T^{\mu\lambda} = -\partial^\mu \phi \partial^\lambda \phi + \tfrac{1}{2}(\partial_\rho \phi)^2 g^{\mu\lambda} + V(\phi) g^{\mu\lambda}. \tag{3.6}$$

So a little algebra shows that

$$\begin{aligned} \bar{\varepsilon}^i \Gamma^{\mu\nu\rho} \hat{D}_\nu \hat{D}_\rho \varepsilon_i = &-\tfrac{1}{2}(G^{\mu\lambda} - T^{\mu\lambda}) \bar{\varepsilon}^i \Gamma_\lambda \varepsilon_i - \delta\bar{\lambda}^i \Gamma^\mu \delta\lambda_i + (5\partial_\nu f + b\partial_\nu \phi) \bar{\varepsilon}^i \Gamma^{\mu\nu} \varepsilon_i \\ &+ (b^2 - 30f^2 - \tfrac{1}{2} V(\phi)) \bar{\varepsilon}^i \Gamma^\mu \varepsilon_i. \end{aligned} \tag{3.7}$$

Now recall from the previous section that $E^{\mu\nu}$ must satisfy two conditions. First, the linearisation procedure must generate the Killing charges so that we can indeed obtain the energy; and second, that energy must be zero in the background. (The background is stable if the energy is positive for fluctuations.)

To zeroth (background) order:

$$D_\nu E_0^{\mu\nu} = \hat{D}_\nu^{(0)} \bar{\varepsilon}^i \Gamma^{\mu\nu\rho} \hat{D}_\rho^{(0)} \varepsilon_i - b_0^2 \bar{\varepsilon}^i \Gamma^\mu \varepsilon_i + (b_0^2 - 30 f_0^2 - \tfrac{1}{2} V(\phi_0)) \bar{\varepsilon}^i \Gamma^\mu \varepsilon_i. \tag{3.8}$$

This vanishes identically if and only if

$$\hat{D}_\rho^{(0)}\varepsilon_i = 0 \tag{3.9}$$

and

$$30f_0^2 = -\tfrac{1}{2}V(\phi_0). \tag{3.10}$$

Note that together this is exactly the condition that $\hat{D}_\rho^{(0)}$ is the AdS covariant derivative for the background.

To linear order

$$D_\nu E_L^{\mu\nu} = -\tfrac{1}{2}(G_L^{\mu\lambda} - T_L^{\mu\lambda})\bar{\varepsilon}^i\Gamma_\lambda\varepsilon_i + 5(\partial_\nu f)_L\bar{\varepsilon}^i\Gamma^{\mu\nu}\varepsilon_i - (30f^2 + \tfrac{1}{2}V(\phi))_L\bar{\varepsilon}^i\Gamma^\mu\varepsilon_i \tag{3.11}$$

(where again the terms involving b cancel). This will give the Killing charges if the last two terms vanish, i.e. if

$$f_0' \equiv \mathrm{d}f/\mathrm{d}\phi|_{\phi_0} = 0. \tag{3.12}$$

Finally, we can obtain a positive energy theorem if we require the last two terms in (3.7) to vanish to all orders, i.e.

$$5\partial_\nu f + b\partial_\nu\phi = 0 \tag{3.13}$$

$$b^2 - 30f^2 - \tfrac{1}{2}V(\phi) = 0. \tag{3.14}$$

Applying the initial condition (3.10) we see that

$$b_0 = 0. \tag{3.15}$$

Moreover, (3.13) and (3.14) can be rewritten as

$$b = -5f' \tag{3.16}$$

$$25f'^2 - 30f^2 - \tfrac{1}{2}V(\phi) = 0. \tag{3.17}$$

Now the problem has been reduced to finding a solution to this last ordinary differential equation subject to the initial condition of (3.10).

4. A solution to the ODE exists

Actually we need only show that (3.17) *has* a solution with this initial condition. A reasonably trivial modification of the Peano existence theorem (see, e.g., [6]) shows that there is a solution in the neighbourhood of the initial condition. One must then consider the possibility that the solution is not global, i.e. it blows up at some finite value of ϕ.

Let $g = 1/f$. Then the equation becomes

$$25g'^2 - 30g^2 - \tfrac{1}{2}g^4V(\phi) = 0. \tag{4.1}$$

It is easy to see that non-trivial solutions to this equation have no zeros. For $f' > 0$ (namely $\phi > \phi_0$), $g' < 0$. In this instance (4.1) becomes

$$5g' = -g(30 + \tfrac{1}{2}g^2V(\phi))^{1/2}. \tag{4.2}$$

At $g = 0$ the right-hand side of (4.2) satisfies the appropriate continuity and Lipschitz conditions for the Picard–Lindelöf theorem, so a unique solution exists. However, $g(\phi) \equiv 0$ is clearly a solution, so there is no non-trivial solution with a zero. Similarly for $f' < 0$, $g' > 0$ and using the positive branch. Hence the solution to (3.17) does not blow up for finite values of ϕ.

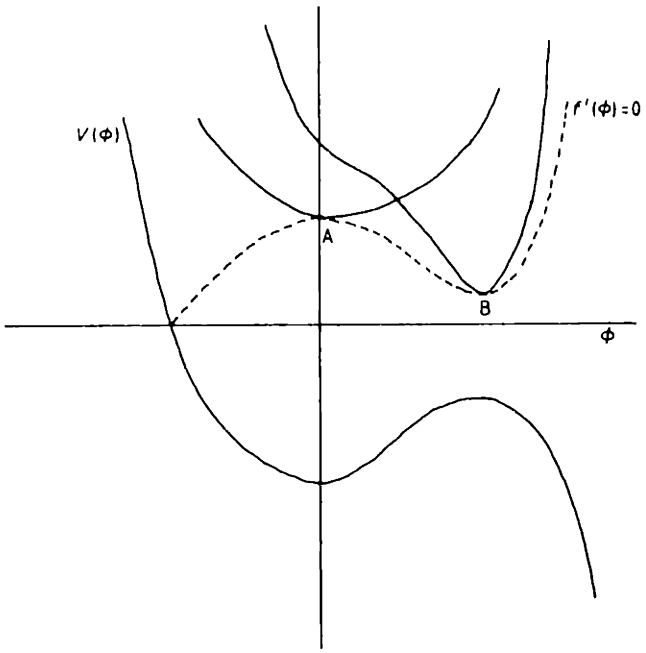

Figure 2. The solution to (3.17) with *IC* at A is bounded away from $f' = 0$ by the solution with *IC* at B.

The only remaining way in which (3.17) can fail to have a solution is for the solution curve to run into the $f'(\phi) = 0$ curve (equivalently $30f^2(\phi) = -V(\phi)/2$) as ϕ increases away from ϕ_0 (see figure 2). However, we know that the local maximum is stable. Hence (3.17) must have a solution with initial condition at B. In fact, we know that the solution is given by (1.5) with $A_{\mu\nu\rho} = 0$, i.e. $f = m$. That this is indeed a solution of (3.17) is easily verified. Uniqueness guarantees that the solution to (3.17) with initial condition at A never intersects the same-branch part of this curve and hence is bounded away from the $f'(\phi) = 0$ curve.

5. Conclusions

That a global solution to (3.17) exists demonstrates the stability of the local minimum against arbitrary spin-0 and spin-2 fluctuations. It is, in fact, unnecessary to actually solve (3.17) (thus defining $\hat{D}_\mu$ and $\delta\lambda_i$) since merely knowing that the solution exists guarantees that they will be defined and hence that the generalised positive energy theorem will go through.

Another observation to be made is that this argument trivially extends to include spin-1 fluctuations. (The inclusion of spin-1 fluctuations in the standard Witten argument at the local maximum could have been done similarly.) For then

$$G^{\mu\nu} - T^{\mu\lambda}(\phi) = T^{\mu\lambda}(A_{\alpha\beta\gamma}) \tag{5.1}$$

rather than 0. However, to zeroth and linear order this has no effect, and since $T^{\mu\lambda}(A_{\alpha\beta\gamma})$ satisfies the dominant energy condition (just as the energy-momentum tensor for the electromagnetic field does) we still obtain a positive energy theorem from (3.7). Notice that again here, to understand and apply the modified (or

unmodified) Witten argument, it is crucial to examine the relevant identity (3.7) to zeroth and linear orders to verify that it truly produces the energy, and then to all orders to show that the energy is positive.

Acknowledgments

I wish to express my thanks to Daniel Z Freedman who suggested this problem and with whom I had many useful discussions. I would also like to thank Ruben Rosales for his suggestions concerning § 4.

References

[1] Townsend P K and van Nieuwenhuizen P 1983 *Phys. Lett.* **125B** 41
[2] Mezinescu L, Townsend P K and van Nieuwenhuizen P 1984 *Phys. Lett.* **143B** 384
[3] Boucher W 1984 *Nucl. Phys.* B **242** 282
[4] Witten E 1981 *Commun. Math. Phys.* **80** 381
Nester J M 1981 *Phys. Lett.* **83A** 241
Gibbons G, Hull C and Warner N P 1983 *Nucl. Phys.* B **218** 173
Hull C M 1983 *Commun. Math. Phys.* **90** 545
[5] Freedman D Z and Gibbons G W 1984 *Nucl. Phys.* B **233** 24
[6] Hartman P 1964 *Ordinary Differential Equations* (New York: Wiley)

References

Abramowitz, M. and I. A. Stegun, eds. [1964], *Handbook of Mathematical Functions with Formulas, Graphs and Mathematical Tables*, National Bureau of Standards Applied Mathematics Series **55** (Washington, D.C.: U.S. Government Printing Office) table 26.8.

Appelquist, T., A. Chodos and P. G. O. Freund, eds. [1987], *Modern Kaluza-Klein Theories* (Wokingham: Addison-Wesley).

Ashtekar, A. [1988], *New Perspectives in Canonical Gravity* (Napoli: Bibliopolis).

Baclawski, K. and G.-C. Rota [1979], *An Introduction to Probability and Random Processes*, unpublished lecture notes.

Baker, K. A., P. C. Fishburn and F. S. Roberts [1971], "Partial orders of dimension 2," *Networks* **2** 11–28.

Besicovitch, A. S. [1934], "On rational approximation to real numbers," *J. Lond. Math. Soc.* **9** 126–131.

Besicovitch, A. S. [1935], "On the sum of digits of real numbers represented in the dyadic system (On sets of fractional dimensions II)," *Math. Annalen* **110** 321–330.

Besicovitch, A. S. and S. J. Taylor [1954], "On the complementary interval of a linear closed set of zero Lebesgue measure," *J. Lond. Math. Soc.* **29** 449–459.

Besicovitch, A. S. and H. D. Ursell [1937], "Sets of fractional dimensions (V): On dimensional numbers of some contiuous curves," *J. Lond. Math. Soc.* **12** 18–25.

Billingsley, P. [1965], *Ergodic Theory and Information* (New York: Wiley) section 14.

Birrell, N. D. and P. C. W. Davies [1982], *Quantum Fields in Curved Space* (Cambridge: Cambridge University Press).

Blackman, R. B. and J. W. Tukey [1959], *The Measurement of Power Spectra* (New York: Dover).

Bombelli, L. [1987], *Space-time as a Causal Set*, Ph.D. Thesis, Syracuse University.

Bombelli, L., J. Lee, D. Meyer and R. D. Sorkin [1987], "Space-time as a causal set," *Phys. Rev. Lett.* **59** 521–524.

Bombelli, L., J. Lee, D. Meyer and R. D. Sorkin [1988], reply to C. Moore in *Phys. Rev. Lett.* **60** 656.

Borel, A. and F. Hirzebruch [1959], "Characteristic classes and homogeneous spaces, II," *Amer. J. Math.* **LXXXI** 315–382(350).

Boulware, D., G. Horowitz and A. Strominger [1983], "Zero-energy theorem for scale-invariant gravity," *Phys. Rev. Lett.* **50** 1726–1729.

Bowick, M. J. and S. G. Rajeev [1987], "String theory as the Kähler geometry of loop space," *Phys. Rev. Lett.* **58** 535–538.

Breitenlohner, P. and D. Z. Freedman [1982], "Positive energy in anti-de Sitter backgrounds and gauged extended supergravity," *Phys. Lett.* **B115** 197–201 and "Stability in gauged extended supergravity," *Ann. of Phys.* **144** 249–281.

Christensen, S. [1984], ed., *Quantum Theory of Gravity: Essays in honor of the 60th birthday of Bryce S. DeWitt* (Bristol: Adam Hilgar).

Coish, H. R. [1959], "Elementary particles in a finite world-geometry," *Phys. Rev.* **114** 383–388.

Deser, S. and B. Zumino [1976], "Consistent supergravity," *Phys. Lett.* **62B** 335–337.

Diggle, P. J. [1983], *Statistical Analysis of Spatial Point Patterns* (London: Academic Press).

Dushnik, B. and E. W. Miller [1941], "Partially ordered sets," *Amer. J. Math.* **63** 600–610.

Eisenhart, L. P. [1925], *Riemannian Geometry* (Princeton: Princeton University Press) section 27.

Finkelstein, D. [1969], "Space-time code," *Phys. Rev.* **184**, 1261–1271.

Finkelstein, D. [1972], "Space-time code. II," *Phys. Rev.* **D5**, 320–328 and "Space-time code. III," *Phys. Rev.* **D5** 292–2937.

Finkelstein, D. [1974], "Space-time code. IV," *Phys. Rev.* **D9**, 2219–2231.

Finkelstein, D., G. Frye and L. Susskind [1974], "Space-time code. V," *Phys. Rev.* **D9** 2231–2236.

Fishburn, P. C. [1985], *Interval Orders and Interval Graphs: A study of partially ordered sets* (New York: Wiley).

Freund, P. G. O. and M. A. Rubin [1980], "Dynamics of dimensional reduction," *Phys. Lett.* **B97** 233–235.

Freund, P. G. O. and M. Olson [1987], "Non-Archimedean strings," *Phys. Lett.* **B199** 186–190.

Freund, P. G. O. and M. Olson [1988], "p-adic dynamical systems," *Nucl. Phys.* **B297** 86–102.

Freund, P. G. O. and E. Witten [1987], "Adelic string amplitudes," *Phys. Lett.* **B199** 191–194.

Freedman, D. Z., P. van Nieuwenhuizen and S. Ferrara [1976], "Progress toward a theory of supergravity," *Phys. Rev.* **D13** 3214–3218.

Garey, M. R. and D. S. Johnson, *Computers and Intractability: A guide to the theory of NP-completeness* (New York: W. H. Freeman).

Geroch, R. [1967], "Topology in general relativity," *J. Math. Phys.* **8** 782–786.

Geroch, R. [1972], "Einstein algebras," *Commun. Math. Phys.* **26** 271–275.

Graham, N. [1980], *Introduction to Pascal* (New York: West) chapter 10.

Green, M. B., J. H. Schwarz and E. Witten [1987], *Superstring Theory, Volume 1: Introduction* (Cambridge: Cambridge University Press) 1–27.

Harzheim, E. [1970], *"Ein Endlichkeitssatz über die Dimension teilweise geordneter Mengen," Math. Nachr.* **46** 183–188.

Hausdorff, F. [1919], *"Dimension und äusseres Mass, Math. Ann.* **79** 157–179.

Hawking, S. W. [1975], "Particle creation by black holes," *Commun. Math. Phys.* **43** 199–220.

Hawking, S. W. [1978], "Space-time foam," *Nucl. Phys.* **B144** 349–362.

Hawking, S. W. and G. F. R. Ellis [1973], *The Large Scale Structure of Space-time* (Cambridge: Cambridge University Press).

Hawking, S. W., A. R. King and P. J. McCarthy [1976], "A new topology for curved space-time which incorporates the causal, differential, and conformal structures," *J. Math. Phys.* **17** 174–181.

Hewitt, A., G. Burbidge and L. Z. Fang, eds. [1986], *Observational Cosmology: Proceedings of the 124th symposium of the International Astronomical Union held in Beijing, China, August 25–30, 1986* (Boston: Reidel 1987) chapter IV and references therein.

Hiraguchi T. [1951], "On the dimension of partially ordered sets," *Sci. Rep. Kanaza-*

wa Univ. **1** (1951) 77–94.

Hiraguchi T. [1955], "On the dimension of orders," *Sci. Rep. Kanazawa Univ.* **4** 1–20.

Horowitz, G. T., J. Lykkan, R. Rohm and A. Strominger [1986], "Purely cubic action for string field theory," *Phys. Rev. Lett.* **57** 283–286.

Horowitz, G. T. and D. M. Witt [1987], "Toward a string field theory independent of spacetime topology," *Phys. Lett.* **B199** 176–182.

Hurewicz, W. and H. Wallman [1941], *Dimension Theory* (Princeton: Princeton University Press).

Isham, C. J. [1984], "The contributions of Bryce DeWitt to quantum gravity," in *Quantum Theory of Gravity: Essays in honor of the 60th birthday of Bryce S. DeWitt*, ed. S. Christensen (Bristol: Adam Hilgar) 21–41.

Itzykson, C. [1984], "Fields on a random lattice," in *Progress in Gauge Field Theory: Proceedings of the NATO Advanced Study Institute held at Cargèse, Corsica, France, September 1-15, 1983*, NATO ASI Series **B115**, eds. 't Hooft, *et al.* (New York: Plenum) 337–371.

Itzykson, C. and J.-B. Zuber [1980], *Quantum Field Theory* (New York: McGraw Hill).

Jacob, M., ed. [1986], *Supersymmetry and Supergravity: A reprint volume of Physics Reports* (Amsterdam: North-Holland).

Kelly, D. [1977], "The 3-irreducible partially ordered sets," *Can. J. Math.* **XXIX** 367–383.

Kelly, D. and I. Rival [1975], "Certain partially ordered sets of dimension three," *J. Comb. Theory (Ser. A)* **18** 239-242.

Kelly, D. and G.-C. Rota [1973], "Some problems in combinatorial geometry," in *A Survey of Combinatorial Theory*, eds. J. N. Srivastava, *et al.* (New York: North Holland) 309–312.

Kelly, D. and W. T. Trotter, Jr. [1982], "Dimension theory for ordered sets," in *Ordered Sets: Proceedings of the NATO Advanced Study Institute held at Banff, Canada, August 28 to September 12, 1981*, NATO ASI Series **C83**, ed. I. Rival (Boston: Reidel) 171–211.

Kimble, R. J. [1973], *Extremal Problems in Dimension Theory for Partially Ordered Sets*, Ph.D. Thesis, M.I.T.

Kirkpatrick, S., C. D. Gelatt, Jr. and M. P. Vecchi [1983], "Optimization by simulated annealing," *Science* **220** 671–680.

Kleitman, D. J. and B. L. Rothschild [1975], "Asymptotic enumeration of partial orders on a finite set," *Trans. Am. Math. Soc.* **205** 205–220.

Knuth, D. E. [1969], *The Art of Computer Programming: Vol. 2/Seminumerical Algorithms* (Reading: Addison-Wesley) chapter 3.

Knuth, D. E. [1973a], *The Art of Computer Programming: Vol. 1/Fundamental Algorithms*, second edition (Reading: Addison-Wesley) section 1.2.6.

Knuth, D. E. [1973b], *The Art of Computer Programming: Vol. 3/Sorting and Searching* (Reading: Addison-Wesley) chapter 5.

Komm, H. [1948], "On the dimension of partially ordered sets," *Amer. J. Math.* **70** 507–520.

Kuratowski, K. [1930], *"Sur le problème des courbes gauches en topologie," Fund. Math.* **15** 271–283.

Lee, T. D. [1985], "Discrete mechanics," in *How Far Are We from the Gauge Forces*, ed. A. Zichichi (New York: Plenum) 15–92.

Lehto, M., H. B. Nielson and M. Ninomiya [1986], "Pregeometric quantum lattice: a general discussion," *Nucl. Phys.* **B272** 213-227.

Malament, D. B. [1977], "The class of continuous timelike curves determines the topology of spacetime," *J. Math. Phys.* **18** 1399–1404.

Mandelbrot, B. B. [1983], *The Fractal Geometry of Nature*," updated and augmented (New York: Freeman).

Meyer, D. [1986], "On the stability of a non-supersymmetric ground state," *Class. Quantum Grav.* **3** 881–887.

Milnor, J. [1963] "Spin structures on manifolds," *L'Enseignement Mathématique*, II^e *série* **IX** 198–203.

Moore, C. [1988], "Comment on 'Space-time as a causal set'," *Phys. Rev. Lett.* **60** 655.

Myrheim, J. [1978], "Statistical geometry," CERN preprint TH-2538.

Neyman, J. and E. L. Scott [1958], "Statistical approach to problems of cosmology" (with discussion), *J. Roy. Statist. Soc.* **B20** 1–43.

Paoli, M., W. T. Trotter, Jr. and J. W. Walker [1985], "Graphs and orders in Ramsey theory and in dimension theory," in *Graphs and Order: The Role of Graphs in the Theory of Ordered Sets and its Applications: Proceedings of the NATO Advanced Study Institute on Graphs and Order held at Banff, Canada, May 18–31, 1984*, NATO ASI Series **C147**, ed. I. Rival (Boston: Reidel) 351–394.

Peebles, P. J. E. [1974], "The nature of the distribution of galaxies," *Astron. Astrophys.* **32** 197–202.

Peebles, P. J. E. [1980], *The Large Scale Structure of the Universe* (Princeton: Princeton University Press).

Penrose, R. [1972a], *Techniques of Differential Topology in General Relativity* (Philadelphia: SIAM).

Penrose, R. [1972b], "On the nature of quantum geometry," in *Magic without Magic: John Archibald Wheeler: A collection of essays in honor of his sixtieth birthday*, ed. J. R. Klauder (San Francisco: W. H. Freeman) 333–359.

Penrose, R. [1975], "Twistor theory, its aims and achievements," in *Quantum Gravity: An Oxford symposium*, eds. C. J. Isham, R. Penrose and D. W. Sciama (Oxford: Clarendon Press) 268–407.

Percacci, R. [1986], *Geometry of Nonlinear Field Theories* (Singapore: World Scientific) chapter 4.

Petrov, A. Z. [1969], *Einstein Spaces*, transl. by R. F. Kelleher, transl. ed. by J. Woodrow (Oxford: Pergamon Press) chapter 1.

Press, W. H., B. P. Flannery, S. A. Teukolsky and W. T. Vetterling [1986], *Numerical Recipes: The art of scientific computing* (Cambridge: Cambridge University Press) chapter 7.

Raine, D. J. [1981], *The Isotropic Universe: An introduction to cosmology* (Bristol: Adam Hilgar) 8–28.

Riemann, G. F. B. [1854], *"Über die Hypothesen, welche der Geometrie zugrunde liegen,"* inaugural lecture at Göttingen, 10 june 1854, *Gött. Abh.* **13** (1867) 133; *Über die Hypothesen, welche der Geometrie zugrunde liegen: Neu herausgegeben und erläutert von H. Weyl* (Berlin: Verlag von Julius Springer 1919); quoted in translation in H. Weyl, *Space—Time—Matter* (New York: Dover 1952) 97.

Rival, I., ed. [1981], *Ordered Sets: Proceedings of the NATO Advanced Study Institute held at Banff, Canada, August 28 to September 12, 1981*, NATO ASI Series **C83** (Boston: Reidel).

Rival, I., ed. [1985], *Graphs and Order: The Role of Graphs in the Theory of Ordered Sets and its Applications: Proceedings of the NATO Advanced Study Institute on Graphs and Order held at Banff, Canada, May 18–31, 1984*, NATO ASI Series **C147** (Boston: Reidel).

Schild, A. [1949], "Discrete spacetime and integral Lorentz transformations," *Canad. J. Math.* **1** 29–47.

Singer, I. M. [1978], "Some remarks on the Gribov ambiguity," *Commun. Math. Phys.* **60** 7–12.

Sorkin, R. D. [1986a], "Topology change and monopole creation," *Phys. Rev.* **D33** 978–982 and "Non-time orientable Lorentzian cobordism allows for pair creation," *Int. J. Theor. Phys.* **25** 877–881.

Sorkin, R. D. [1986b], "Introduction to topological geons," in *Topological Properties and Global Structure of Space-time: Proceedings of the International School of Cosmology and Gravitation, Erice, 1985*, eds. P. G. Bergmann and V. de Sabbata, (New York: Plenum) 249–269.

Sorkin, R. D. [1987], "A finitary substitute for continuous topology," Institute for Advanced Study preprint IASSAS-HEP-87/39.

Stanley, R. P. [1986], *Enumerative Combinatorics: Volume I* (Monterey: Wadsworth & Brooks/Cole) chapter 3.

Steenrod, N. [1951], *The Topology of Fibre Bundles* (Princeton: Princeton University Press) part III.

Stelle, K. S. [1977], "Renormalization of higher-derivative quantum gravity," *Phys. Rev.* **D16** 953–969.

Szpilrajn, E. [1930], *"Sur l'extension de l'ordre partiel,"* *Fund. Math.* **16** 386–389.

Taketani M. [1936], "Dialectics of nature—on quantum mechanics," and other articles reprinted in *Supplement to Progress in Theoretical Physics* **50** (1971).

't Hooft, G. [1979], "Quantum gravity: a fundamental problem and some radical ideas," in M. Levy and S. Deser, eds., *Recent Developments in Gravitation: Proceedings of the 1978 Cargèse Summer Institute held in Cargèse, Corsica, July 10–29, 1978, and sponsored in part by NATO*, NATO ASI Series **B44** (New York: Plenum).

Tipler, F. J. [1977], "Singularities and causality violation," *Ann. of Phys.* **108** 1–36.

Trotter, W. T. [1974], "Irreducible posets with large height exist," *J. Comb. Theory (Ser. A)* **17** 337–344.

Trotter, W. T. [1975], "Inequalities in dimension theory for posets," *Proc. Amer. Math. Soc.* **47** 311–316.

Trotter, W. T. and J. I. Moore [1976], "Characterization problems for graphs, partially ordered sets, lattices, and families of sets," *Discrete Math.* **4** 361–368.

Trotter, W. T. and J. A. Ross [1982], "For $t \geq 3$, every t-dimensional partial order is a suborder of a $t + 1$-irreducible partial order," in *Proceedings of the 1981 Hungarian Conference on Combinatorics and Graph Theory held at Eger, Hungary.*

Utiyama, R. and B. S. DeWitt [1962], "Renormalization of a classical gravitational field interacting with quantized matter fields," *J. Math. Phys.* **3** 608–618.

Volovich, I. V. [1987], "p-adic string," *Class. Quant. Grav.* **4** L83–L87.

Weinberg, S. [1979], "Ultraviolet divergences in quantum theories of gravitation," in *General Relativity: The Einstein centenary survey*, eds. S. W. Hawking and W. Israel (Cambridge: Cambridge University Press) 790–831.

Wheeler, J. A. [1964], "Geometrodynamics and the issue of the final state," in *Relativity, Groups and Topology: Lectures delivered at Les Houches during the 1963 session of the Summer School of Theoretical Physics, University of Grenoble*, eds. B. DeWitt and C. DeWitt (New York: Gordon and Breach) 316–520.

Witten, E. [1986], "Non-commutative geometry and string field theory," *Nucl. Phys.* **B268** 253–294.

Yodzis, P. [1972], "Lorentz cobordism," *Commun. Math. Phys.* **26** 39–52.

Yodzis, P. [1973], "Lorentz cobordism. II," *Gen. Rel. Grav.* **4** 299–307.

Yodzis, P. [1975], "An algebraic approach to classical spacetime," *Proc. Roy. Irish Acad.* **A75** 37–47.